Blood Cells, Molecules and Diseases 70 (2018) 13–42

Contents lists available at ScienceDirect

Blood Cells, Molecules and Diseases

journal homepage: www.elsevier.com/locate/bcmd

Review

Structure and function of haemoglobins

David A. Gell

School of Medicine, University of Tasmania, TAS 7000, Australia

ARTICLE INFO

Keywords:
Haemoglobin
Myoglobin
Truncated haemoglobin
Flavohaemoglobin
Haem
Model porphyrins
Oxygen binding
Hexacoordinate haem
Nitric oxide
Cooperative oxygen binding
Allostery

ABSTRACT

Haemoglobin (Hb) is widely known as the iron-containing protein in blood that is essential for O_2 transport in mammals. Less widely recognised is that erythrocyte Hb belongs to a large family of Hb proteins with members distributed across all three domains of life—bacteria, archaea and eukaryotes. This review, aimed chiefly at researchers new to the field, attempts a broad overview of the diversity, and common features, in Hb structure and function. Topics include structural and functional classification of Hbs; principles of O_2 binding affinity and selectivity between O_2/NO/CO and other small ligands; hexacoordinate (containing bis-imidazole coordinated haem) Hbs; bacterial truncated Hbs; flavohaemoglobins; enzymatic reactions of Hbs with bioactive gases, particularly NO, and protection from nitrosative stress; and, sensor Hbs. A final section sketches the evolution of work on the structural basis for allosteric O_2 binding by mammalian RBC Hb, including the development of newer kinetic models. Where possible, reference to historical works is included, in order to provide context for current advances in Hb research.

1. Introduction and scope

This review attempts a broad overview of selected topics in Hb structure and function. It is necessarily superficial in all areas, but the hope is that there is some benefit in taking a broad view, and perhaps this can be a helpful for researchers new to the field. Throughout, I have tried to acknowledge authoritative work that has had enduring 'currency', regardless of publication date. Hb research is highly interdisciplinary and I have endeavoured to include some of the important contributions from bioinorganic chemistry, spectroscopy and structural biology that have shaped our current understanding of Hb proteins.

2. The Hb superfamily – evolutionary conservation and diversification of function

2.1. Hbs share a common three-dimensional structure and haem cofactor

All Hbs have a conserved core topology, comprising 6–8 α-helices (labelled A–H). The very first protein structures to be determined—those of myoglobin (Mb) from muscle of the sperm whale [1,2], and red blood cell (RBC) Hb from horse erythrocytes [3]—revealed the globin structural blueprint, and firmly established the enduring paradigm that structure underlies function. As the founding member of the Hb family, Mb provides the reference against which all other Hb sequences and structures are compared [4]. For example, in each of the > 200 non-redundant Hb structures in the protein data bank, position F8 refers to the amino acid residue that is structurally equivalent to the eighth residue in helix F of sperm whale Mb—this is the haem-coordinating histidine residue (HisF8), which is the only residue that is 100% conserved across the whole Hb superfamily [5,6]. Residues in non-helical segments are referenced in relation to adjacent helices; thus, CD1 refers to the first residue of the linker joining α-helices C and D, and HC3 refers to the third residue following helix H, on the carboxyl terminus.

Two different structural sub-classes of the globin fold are recognised (Table 1 and Fig. 1). The 3-on-3 fold is the canonical Hb fold, exemplified by Mb. The '3-on-3' designation refers to the α-helical 'sandwich' formed by the A-G-H and B-E-F helices [7]. The C and D helices are supporting structures, and are not always present. The second structural class is the truncated Hb (trHb) class—also called 2-on-2, 2-over-2, or 2/2 Hbs, based on the arrangement of the B–E and G–H helical pairs, [8]. In trHbs, the A, C, D, and F helices are much reduced or absent.

Whereas some Hbs function as monomers, other Hbs are assembled from multiple globin subunits. Examples of the latter include mammalian RBC Hb, which is a tetramer of two Hb α and two Hb β subunits [3], and earthworm Hb (erythrocruorin), which comprises 144 globin chains with four unique sequences together with an additional 36 non-globin subunits [9]. Within these oligomers it is the individual subunits that conform to the conserved globin fold. Allosteric function (see Section 7) and multisubunit organisation of Hbs have arisen a number of times in evolution to solve the problem of O_2 transport (see reviews

E-mail address: david.gell@utas.edu.au.

http://dx.doi.org/10.1016/j.bcmd.2017.10.006
Received 14 May 2017; Received in revised form 29 October 2017; Accepted 30 October 2017
Available online 31 October 2017

Table 1
Important amino acid residues in the haem pockets of Hbs from different Hb families.

Structural class	Family	Sub-family or other sub-grouping	B9	B10[1]	CD1	E7[1]	E11[1]	E14	F8[2]	FG5	G5[3]	G8[1]	H23[3]
3-on-3	Myoglobin-like PF00042	Plant & metazoan Hbs	LFIC	FLM	F	**H**LV**Q**	VILF	n.c.	H	IV	LF	FILV	–
		nsHb1/2	FL	F	F	**H**[¶]	V/Q	M	H[¶]	V	F	V/W	–
		FHb	F	**Y**	F	**Q**	L	ASG	H	IV	**Y**	V	**E**
		SDgb	F	**Y**	F	**Q**	L	AT	H	V	**Y**	V	**E**
	Sensor Hbs[4] PF11563	GCS	F	**Y**	ILF	LVKRSE	LMQF	WHY	H	LI	**Y**V	AG	–
		Pgb	W	Y	F	V	F	W	H	K	NG	ST	–
trHb or 2/2 Hb	Truncated Hbs PF01152	trHb1 (HbN)	F	**Y**	F	**Q**L	**Q**L	F	H	LIV	FV	VI	–
		trHb2 (HbO) type i[5]	F	**Y**	FH	ATS	**Q**	F	H	IV	RA	**W**	–
		trHb2 (HbO) type ii	F	Y*	**Y***	A	L	F	H	I	RA	**W**	–
		trHb3 (HbP)	F	**Y**	F	H	I	F	H	F	F	**W**	–

The table shows conserved side chains in the proximal haem pocket (yellow), distal pocket (blue) and positioned equatorial to the δ methene (white). Where more than one residue is common at a particular position, the most frequently encountered residues are listed.
Abbreviations used: truncated Hb (trHb), non-symbiotic Hb (nsHb), flavohaemoglobin (FHb), unicellular single domain globin (SDgb), globin coupled sensor (GCS), protoglobin (Pgb), modified tyrosyl residue (Y*), position not conserved (n.c.).
[1] Side chains in these positions, where underlined, donate hydrogen bonds to O_2 ligand.
[¶] Hexacoordinate Hbs.
[2] Universally conserved proximal haem ligand.
[3] Side chains in these positions, where underlined, make hydrogen bond interactions with HisF8.
[4] Sensor single-domain globins (SSDgbs) also belong to this phylogenetic group, but as structures are currently available this group is omitted from the table.
[5] The set of class 2 type i trHbs includes all class 3 nsHbs.

by Royer et al. [10,11]).

Each globin polypeptide binds a single molecule of iron-protoporphyrin-IX (haem b; Fig. 2A). The haem molecule is amphipathic—it contains two charged propionate groups that interact with water and/or polar amino acid side chains on the surface of the globin, and the remainder of the haem molecule is largely hydrophobic in nature and binds in the hydrophobic interior of the globin, surrounded by apolar side chains. Each haem has a central iron atom that is coordinated by four equatorial N ligands, one from each of the four pyrrole rings of the porphyrin. Haem is bound to the protein via a coordinate covalent bond from an axial N ligand provided by the imidazole side chain of HisF8 (Fig. 2B, D), together with multiple non-covalent interactions between the porphyrin and globin. Whilst the iron atom of the haem makes a coordinate covalent bond with diatomic gaseous ligands such as O_2, CO, NO, HNO, NO_2^- and H_2S, the globin fold provides the essential environment to achieve reversible and selective ligand binding. The plane of the porphyrin divides the haem pocket into two regions—the Fe-coordinating HisF8 side chain occupies the proximal haem pocket, leaving diatomic ligands bind on the opposite face of the porphyrin, which is the distal haem pocket.

It is worth noting that, besides being the cofactor in Hb, haem has other essential roles in biochemistry. Haem is present in five of the six classes of enzymes recognised by the Enzyme Commission (they are absent only in ligases) [12]. Haem b, as well as other haems, chlorophyll, and vitamin B_{12} (cobalamin) are all synthesised from a common pyrrole precursor. Vitamin B_{12} cofactor is used in radical generation by the class II ribonuceotide reductase (RNR) enzymes, which are essential for all DNA-based life; a similar cofactor may have been used in the prototypical RNR enzyme present in the last universal common ancestor [13], suggesting that tetrapyrrole synthesis is very ancient indeed. Biosynthesis of porphyrin occurs inside the cell where it is to be used (i.e., haem is not transported), via a series of reactions that take place in the cytoplasm and mitochondria [14].

2.2. Distribution and functions of Hbs across three kingdoms of life

Both 3-on-3 Hbs and trHbs (2/2 Hbs) are found in bacteria, archaea and eukaryotes, suggesting that both structural classes were present in the last universal common ancestor. Sequence phylogeny indicates that 3-on-3 Hbs are divided into two families, and five sub-families (Table 1 and Fig. 1) [15,16], which, to some degree, represent functional groupings. Thus, many members of the plant and metazoan Hb sub-family bind O_2 with moderate affinity (O_2 association equilibrium constant, K_{O2} ~1–20 μM^{-1}) and have roles in O_2 storage or transport (Sections 3, 4.2 and 7). The flavohaemoglobin (FHb) and single-domain globin (SDgb) sub-families are found only in bacteria, algae, and fungi and are nitric oxide dioxygenase (NOD) enzymes that protect against nitrosative stress by converting toxic NO to nitrate (reviewed in [17], and see Section 5). These Hbs typically have high O_2 affinity (K_{O2} 10–1000 μM^{-1}). FHbs are chimeric proteins with an N-terminal Hb domain and C-terminal FAD/NAD binding domain with a conserved ferredoxin reductase fold (see Section 5.3). Curiously the whole Mb-like family group is absent in archaea.

The second family of 3-on-3 Hbs, the sensor globins, is absent from

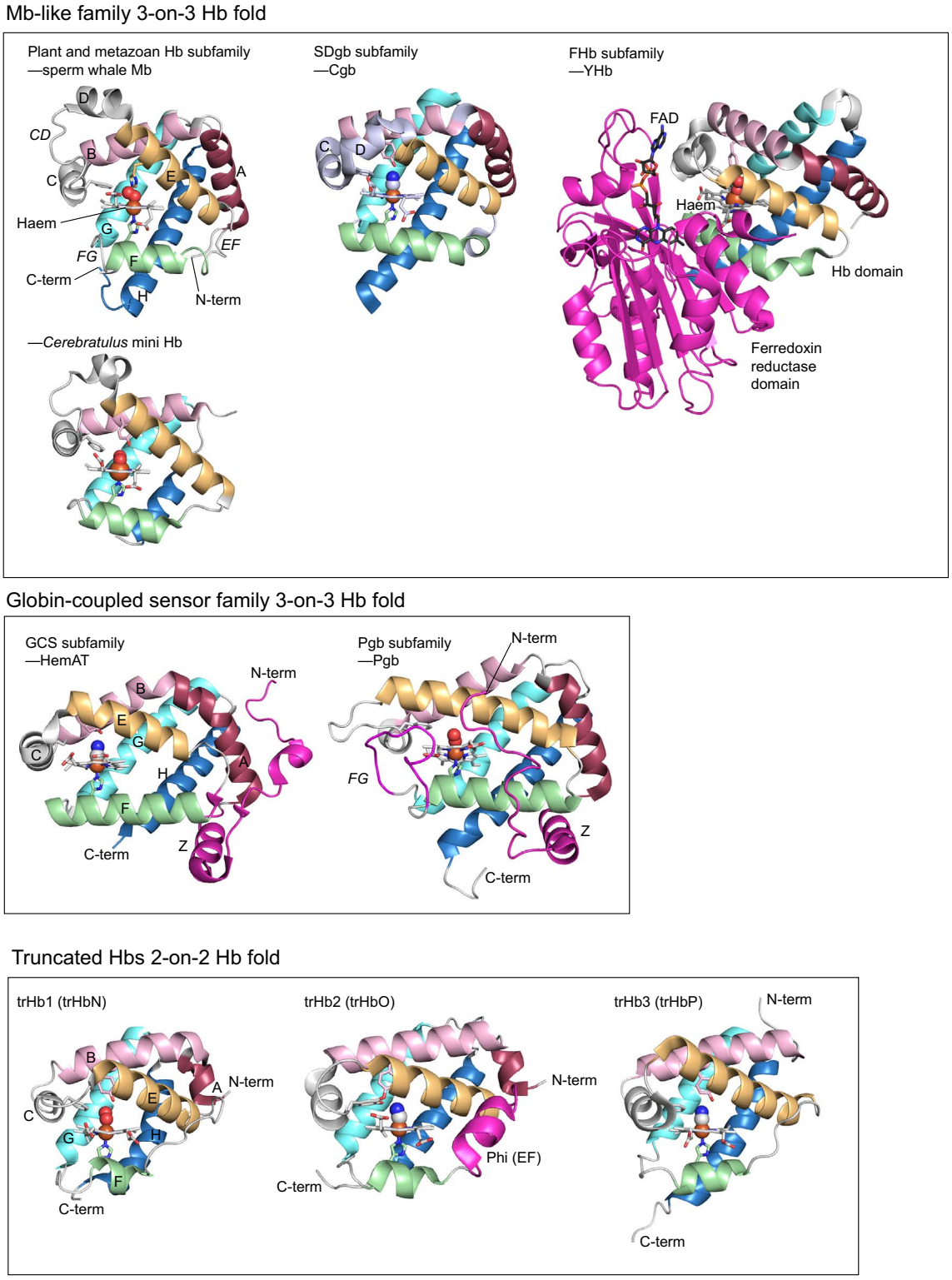

Fig. 1. Conserved and variable features of Hb tertiary structure. The figure shows tertiary structures that are representative of the major Hb families and sub-families (see also Table 1). Most Hbs from the plant and metazoan Hb sub-family are highly similar to sperm whale Mb (pdb 2mgm) [152]; variations include the *Cerebratulus lacteus* mini Hb (1kr7) [161]. Other families/sub-families are represented by Cgb from *Campylobacter jejuni* (2wy4) [107], YHb from *Saccharomyces cerevisae* (4g1v) [105], HemAT from *Bacillus subtilis* (1or4) [397], Pgb from *Methanosarcina acetivorans* (2veb) [63], trHb1 (trHbN) from *Tetrahymena pyriformis* (3aq5) [174], trHb2 (trHbO) from *Mycobacterium tuberculosis* (1ngk) [178], trHb3 (HbP) from *Campylobacter jejuni* (2ig3) [180]. Conserved α-helices that comprise the canonical 3-on-3 tertiary structure are colour-coded as follows: A (red-brown), B (pink), E (yellow/tan), F (green), G (cyan), H (blue). Functionally important loops (CD, EF, FG) are also labelled. Conserved elements of the 2-on-2 Hb fold are coloured as for 3-on-3 Hbs. Additional secondary structure elements present in Mb, but variably present in other Hbs are coloured grey. Additional structural elements that are unique to individual Hb sub-families are coloured magenta. Features of the haem pocket are shown in more detail in Figs. 3 and 4. (For interpretation of the references to colour in this figure legend, the reader is referred to the web version of this article.)

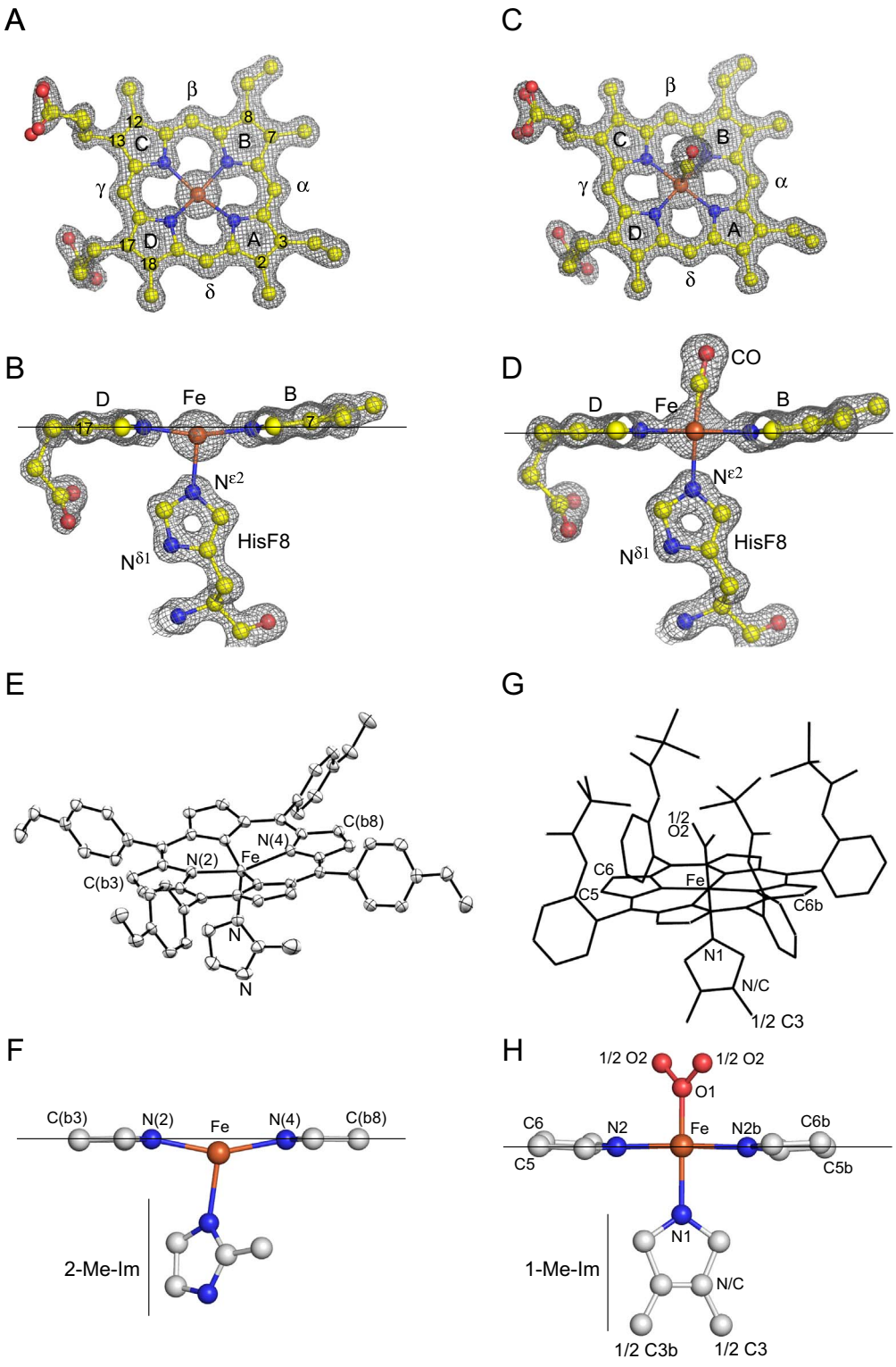

Fig. 2. Haem stereochemistry in Mb and model porphyrins. (A, B) Haem group and proximal HisF8 residue from the crystal structure of unliganded Mb, a high-spin 5-coordinate Fe(II) complex, determined at a resolution of 1.15 Å (pdb 1bzp) [185]. The $2F_O–F_C$ electron density map (mesh) is contoured at 2 σ. The atom colour coding is as follows: iron (orange), oxygen (red), nitrogen (blue), carbon (yellow). Pyrrole rings (Roman letters) and methene bridge positions (Greek letters) are indicated. Substituents at the β-pyrrolic positions (numbered according to the IUPAC convention) are: methyl ($-CH_3$; positions 2, 7, 12, 18), vinyl ($-CH{=}CH_2$; positions 3, 8), and propionate ($-CH_2CH_2COOH$; positions 13, 17). Viewed along the plane of the porphyrin ring (panel B), only the B and D pyrrole rings are shown for clarity. The Fe atom is displaced 0.29 Å out of the plane defined by the four pyrrole N atoms (horizontal line), towards HisF8. (C, D) Haem group and proximal HisF8 residue from Mb (CO), a low-spin 6-coordinate Fe(II) complex, determined at a resolution of 1.15 Å (pbd 1bzr) [185]. The Fe atom is in plane with four pyrrole N atoms (0.015 Å displacement towards CO). Figure panels A–D were prepared from coordinates and structure factors deposited in the Protein Data Bank, using the software, PYMOL. (E, F) Crystal structure of the synthetic porphyrin, Fe(T*p*-OCH_3PP)(2-MeHIm), a high-spin 5-coordinate Fe(II) complex with low O_2 affinity that serves as a synthetic model of unliganded T state Hb [36]. In E, atom positions are shown as thermal vibration ellipsoids (50% probability). (G, H) Crystal structure of Fe(TpivPP)(1-MeIm)(O_2), a synthetic model of Mb(O_2) [41]. The O_2 and 1-methyl imidazole ligand are statistically disordered with 1/2 occupancy at two positions. Panels E–H were prepared from data deposited at the Cambridge Crystallographic Data Centre (CCDC) using the CCDC software program MERCURY (E, G) or PYMOL (F, G). Hydrogen atoms are omitted throughout this figure. (For interpretation of the references to colour in this figure legend, the reader is referred to the web version of this article.)

eukaryotes. Of the sensor globins, the two-domain globin-coupled sensors (GCSs; Section 6) are best understood; these proteins are typically sensors of O_2, NO, or CO that regulates aerotactic responses to these ligands (reviewed [18]). These proteins sometimes show low O_2 affinities ($K_{O2} < 1\ \mu M^{-1}$; [19]). Other subfamilies of the sensor globins are less well characterised. The third major phylogenetic family of Hbs defines a separate structural class, the trHbs. TrHbs comprise at least 3 subfamilies (trHb1/2/3, also called trHbN/O/P, or trHb groups I/II/III) [20,21]. Structure and ligand binding has been characterised for numerous trHbs, but physiological functions have only been tentatively assigned and appear quite diverse. Some trHbs have extremely high O_2 affinity (K_{O2} 5000–22,000 μM^{-1}; e.g. [22]) suggesting that they are likely to have enzymatic functions. TrHbs exist as single-domain proteins, or as chimeras with putative oxidoreductase or signalling domains [23,24]. Of the chimeric Hbs, only the FHbs have been crystallized in their multidomain form.

The implication from phylogenetics is that all Hb families arose in bacteria and, today, about half of bacterial genomes contain Hbs [16].

Consequently, functions of the extant bacterial Hbs reflect possible functions of the ancestral Hb. An ancestral Hb would have operated in a largely anoxic, or local microaerophilic, environment, prior to a significant rise in global O_2 2.4 billion years ago [25]. Thus, enzymatic scavenging of toxic O_2 and NO [26], sulfur metabolism [27], or sensing and signalling in response to O_2, NO, or CO [16], are possible ancestral functions. When compared to bacterial Hbs, vertebrate Hbs (such as RBC Hb and Mb) share highest sequence similarity to SDgb proteins, and it has been suggested that lateral transfer of the SDgb gene(s) to the primitive unicellular eukaryote occurred around the time of the endosymbiotic events that generated mitochondria and plastids [28]. Mb and erythrocyte Hb still retain physiological roles in NO removal (see Section 5.4), in addition to O_2 storage and transport.

3. Structure-function relationships of the haem pocket

3.1. A 5-coordinate haem with an axial imidazole base is essential for O_2 binding

O_2 binding is the hallmark feature of Hbs. Pioneering work using synthetic porphyrins as models of the Hb biosite established two essential conditions for high affinity and reversible O_2 binding. These requirements are: (1) a 5-coordinate haem with an axial base, such as imidazole (Fig. 2A, B) or pyridine, and (2) a mechanism to prevent irreversible haem oxidation. This important work is comprehensively described in a series of excellent reviews [29,30,31]. The following section briefly describes the importance of an axial base, and the non-bonding interactions that protect the haem group from solvent and limit irreversible haem oxidation.

As with other transition metal complexes, haem ligands make co-ordinate, or dative, σ bonds with the metal centre in which both electrons are donated from a lone pair on the ligand (O_2/CO/NO, etc.). Studies of free haems and synthetic porphyrins show that four-co-ordinate metallo-porphyrins have little interest in O_2 binding, whereas 5-coordinate Fe(II) prophyrins with an axial imidazole base bind O_2 with high affinity. This can be rationalised by considering the energy of the d_{z^2} orbital relative to the other four metal d orbitals. By standard convention, only the d_{z^2} orbital is oriented perpendicular to the porphyrin plane and has σ-type geometry that is necessary to participate in σ bonding with an incoming O_2/CO/NO ligand. In 4-coordinate haem, the d_{z^2} orbital has low energy and so is fully occupied with d-shell electrons from Fe(II) and, thus, unable to participate in bonding to O_2. By contrast, in 5-coordinate haem with an axial base, the energy separation between the five metal d orbitals is reduced, allowing the 5 d-shell electrons of Fe(II) to spread out, partially freeing up the d_{z^2} orbital (see [32,33] for illustrated explanations). Magnetic susceptibility measurements, first made by Pauling and Coryell [34,35], established that 5-coordinate deoxy HbFe(II) has 4 unpaired electrons (it is high spin; S = 2), and recent Mössbauer spectroscopy shows that the ground state electronic configuration for 5-coordinate deoxy Mb, deoxy Hb and synthetic high spin Fe(II) porphyrins with an axial imidazole base is $(d_{xz})^2(d_{yz})^1(d_{xy})^1(d_{z^2})^1(d_{x^2}-y^2)^1$ [36,37]. It appears that the partly filled d_{z^2} orbital is a pre-requisite for Fe—O_2 bonding. Interestingly, experiment and density function theory (DFT) suggest that the electronic ground state with an axial imidazole is distinct, even compared to complexes with a similar base such as pyridine [36,37,38], and this might be important for O_2 binding in ways that are not yet fully understood.

3.2. Side chain packing around the haem group prevents irreversible Fe oxidation and haem dissociation

Without the protection afforded by the globin fold, free Fe(II) porphyrins are oxidised in seconds to Fe(III) species, which are unable to bind O_2. In contrast, Fe(II) haemoproteins are stable for days. Broadly two mechanisms are responsible for oxidation of haems. The first is the μ-peroxo mechanism, which is initiated upon reaction of a (porphinato) Fe(II)(O_2) species with a second unligated (porphinato)Fe(II). The result is the generation of μ-oxo dimers with an Fe(III)–O–Fe(III) centre (see [30]). In the presence of water, and at room temperature, the conversion to μ-oxo dimers occurs on a ms time scale. This reaction is essentially blocked in haem proteins by the bulk of the globin protein, which prevents close approach of two haem moieties. In order for synthetic model compounds to reversibly bind O_2, the pathway to μ-oxo dimers must be sterically blocked, as was achieved by James Collman and co workers with the famous picket fence porphyrins, which are still the only synthetic (porphinato)Fe(II)(O_2) complexes for which x-ray crystal structures have been reported (Fig. 2G, H) [39,40,41], although a large number of alternative designs function as O_2 binders [29,30,31].

The second pathway for haem oxidation involves the net transfer of one electron from Fe(II) to O_2, generating Fe(III) haem and superoxide. The reaction is termed autooxidation. The rate of autooxidation shows a biphasic response to O_2 concentration, suggesting that it occurs in haem proteins by different mechanisms in high [O_2] ($P_{O2} > P_{50}$; where P_{50} is O_2 partial pressure (P_{O2}) at which 50% of O_2 binding sites are saturated) or at low [O_2] ($P_{O2} < P_{50}$) [42]. At high [O_2], a process with unimolecular kinetics dominates, which might involve protonation of bound O_2 followed by dissociation of a neutral superoxide radical (HOO·), or reductive displacement of a superoxide anion (O_2^-·) by hydroxyl or other anionic species ([43] and references therein). Recent combined quantum mechanics/molecular mechanics (QM/MM) calculations show that the reductive displacement of O_2^-· is the more energetically favourable process [44]. The reductive displacement overcomes the energetic penalty that would be incurred to separate negatively charged O_2^-· from the $Fe(III)^+$ haem in a purely dissociative mechanism. At low [O_2], a bimolecular reaction takes over, in which an electron is transferred from Fe(II)(H_2O) haem (the water molecule is weakly co-ordinated), to an O_2 molecule that is in the distal haem pocket but not coordinated to Fe(II) (an outer sphere electron transfer), generating superoxide anion (O_2^-·). Consequently, interactions that stabilise bound O_2 (see Section 3.6) or prevent water entry into the haem pocket (below) slow the rate of autooxidation [42,45,46].

Close packing of apolar side chains around the porphyrin, and entrance to the haem pocket, as well as polar interactions with the haem propionates, are important for high affinity haem binding, and preventing ingress of water to the haem pocket. Sequence alignment of Hbs [5], including non-symbiotic plant Hbs [47,48], FHbs and SDgbs [49,50], GCSs and Pgbs [51] and trHbs [8,21,50,52,53], shows that residues in Van der Waals contact with the porphyrin (such as residues at positions CD1, F4, FG5, G5, G8, H15 and H19) have conserved physicochemical properties, with bulky apolar Met, Ile, Leu, Val and Phe side chains being heavily represented in these positions. Aromatic residues, particularly Phe, but also Trp, are common in the haem pocket presumably because π-stacking or edge-to-face (T-stacking) interactions with the porphyrin macrocycle are highly stabilising [54]. For example, PheCD1, which makes π-stacking interactions with pyrrole ring C, is the second-most highly conserved globin residue after HisF8. Only in GCSs is PheCD1 replaced with Leu or Ile [51], and, in trHb2, PheCD1 can be replaced by polar His or Tyr [50], which play a specialised role in electrostatic stabilisation of ligands (Section 3.7). In Mb, the disruption of hydrophobic protein-porphyrin interactions by mutagenesis results in a 10–100-fold increase in the rate of haem loss, due to hydration and scission of the Fe–HisF8 bond [46,55], and this translates directly to a loss of overall protein stability [56]. Polar or basic residues (commonly Lys, Arg, His, Ser) are typically found at one or more of the surface positions F7, FG3, CD3 (or CE3 when the D helix is absent) and E10, where they make stabilising electrostatic interactions with the haem propionates [45,55].

A number of Hbs have additional, unusual, protein-porphyrin contacts. For example, Pgbs and trHb2s (Fig. 1) have loops or additional helical elements that partially bury the propionates [57]. The trHb1s from cyanobacteria *Synechocystis* [58,59,60] and *Synechococcus* [61]

are highly unusual in having a covalent bond between the side chain of HisH16 and the vinyl group of pyrrole ring A [59]. The high-resolution (≤ 1.7 Å) crystal structures of these proteins also show highly ruffled porphyrins [61,62]. A similarly distorted prophyrin occurs in Pgb from *Methanosarcina acetivorans* (1.3-Å resolution) [63]), which lacks covalent attachment of the porphyrin ring. In-plane (compression of the porphyrin core) and out-of-plane (ruffling) distortions, presumably induced by protein-porphyrin contacts, are thought to alter O_2 affinity through changes in porphyrin electronic structure [64–68], and may contribute to the high O_2 affinities of trHb and Pgb proteins. Finally, a small number of globins have been discovered that don't bind haem at all [69,70]. In these proteins, the size of the haem-pocket cavity is dramatically reduced, and, in one case, is occupied by a fatty acid [70].

3.3. Steric interactions between the proximal His and the porphyrin ring lower iron reactivity

Reactivity of haem Fe is predominantly determined by the nature of the axial ligand (see Section 3.1); however, although all Hbs coordinate haem Fe through the same axial imidazole (the side chain of HisF8), the O_2 affinities of Hbs still vary widely—dissociation rate constants span seven orders of magnitude, ranging from 10^{-3} to 10^{4} s^{-1} [71]. Side chains in the proximal haem pocket control reactivity of the iron through two mechanisms: (1) steric interactions that perturb the geometry of the haem–HisF8 interaction (compared to a free haem–imidazole) and (2) changes in the basicity of the HisF8 side chain brought about by electrostatic (hydrogen bonding) interactions (the topic of Section 3.4).

Steric effects can influence Hb affinity because ligand binding *requires* a change in the stereochemistry (or 'shape') of the haem coordination complex (see early reviews by Hoard [72], Perutz [33] and Scheidt [32]). Work in synthetic porphyrins [36,37,73–77] has demonstrated the following general rules (of course, with notable exceptions):

- In general, 5-coordinate porphyrins are high spin (4 or 5 unpaired electrons in the case of Fe(II) or Fe(III), respectively), square pyramidal complexes with the Fe atom displaced 0.39–0.54 Å out of the plane defined by the four pyrrole N atoms, and the porphyrin skeleton domed towards the axial base (Fig. 2E, F)
- On the other hand, 6-coordinate porphyrins are low spin (0 or 1 unpaired electron for Fe(II) or Fe(III), respectively), octahedral coordination complexes in which the porphyrin is flat, and Fe lies in the porphyrin plane (displacement from the pyrrole N plane ≤ 0.11 Å) (Fig. 2G, H)

On this basis, steric interactions that hinder movement of the iron into the porphyrin plane resist the high spin to low spin transition that is required by O_2 binding, and, consequently, reduce O_2 affinity. Such steric effects arise largely from interactions between the porphyrin ring and the proximal imidazole base itself, and the magnitude of the effect depends upon the position and orientation of the imidazole base with respect to the porphyrin, which, in haem proteins, is controlled by the protein structure.

Rotation or tilting of the imidazole with respect to porphyrin draws the Fe–His bond out of a perfectly axial position and increases steric interaction between imidazole and porphyrin. In Hb α chains, a steric clash between the HisF8 imidazole and the porphyrin in 6-coordinate (ligated) structure contributes to ~1000-fold lowering of the O_2 affinity of the T state (see Section 7.7). Smaller effects have been demonstrated in picket fence porphyrins with a sterically hindered proximal base (2-methyl imidazole, shown in Fig. 2E, F, or 1,2-dimethyl imidazole) which show ~100-fold lower affinity for O_2 than do compounds with an unhindered base (1-methyl imidazole, Fig. 2G, H) [78–80].

The azimuthal angle of the HisF8 side chain with respect to the pyrrole nitrogens is another factor that modulates steric interactions (Fig. 3) and therefore has the potential to modulate O_2 affinity. The effect of azimuthal angle has been studied in sperm whale myoglobin (Mb) [81–84], mammalian Hb [85,86] and plant leghaemoglobin (LHb) [84,87], using an innovative approach devised by Doug Barrick. In this approach, HisF8 was mutated to Gly, and an active haem site was reconstituted by the addition of free imidazole base, which naturally occupies the proximal haem pocket and coordinates the Fe(II) haem [81]. A HisF8 → Gly substitution in sperm whale Mb results in ~4-fold increased O_2 and CO binding affinity, largely due to a decreased dissociation rate constant [84]. Crystal structures reveal that the exogenous imidazole adopts an unhindered staggered position [81,83], rather than the hindered eclipsed position seen in the wild-type protein. In Mb, the HisF8 side chain makes a hydrogen bond to the side chain of SerF7, which appears to stabilise the eclipsed position, based on observations that SerF7 → Ala, Val, Leu mutations increase Fe reactivity [88]. Soybean LHb has O_2 affinity that is 20-fold higher than Mb (K_{O2} 23 μM^{-1}) [89,90] and this has been attributed to smaller steric effects in the plant protein. In the crystal structure of unliganded LHb, the proximal HisF8 imidazole shows ~50% occupancy in two staggered positions, separated by ~90°, suggesting that this side chain is more mobile than HisF8 in other globins [91]. In LHb, HisF8 → Gly mutations (with exogenous imidazole added) cause a small *decrease* in ligand affinity [84], consistent with HisF8 already being fully unhindered in the high affinity wild-type protein. The role of the proximal pocket in controlling ligand affinity was confirmed by swapping the F helices of LHb and Mb: a three-fold decrease in O_2/CO affinity occurred for a chimera carrying the Mb F-helix, whereas a five-fold increase in affinity was conferred on a chimera carrying the Lb F-helix [84]. Circumstantial evidence that a staggered imidazole position contributes to affinity comes from structural studies of Hbs with the highest O_2 affinities. For example, Hbs from parasitic *Paramphistomum epiclitum* (K_{O2} 3300 μM^{-1} [92,93]), rice nsHb1 (K_{O2} 1800 μM^{-1} [94]), trHb1 from *Synechocystis* sp. (K_{O2} 17,000 μM^{-1} [95]), trHb2 from *Geobacillus stearothermophilus* (K_{O2} 13,200 μM^{-1} [96]) and trHb2 from *M. tuberculosis* (K_{O2} ≥ 7900 μM^{-1} [97]), all have a staggered proximal imidazole with an azimuthal angle close to the ideal 45°.

3.4. Hydrogen bonding of the proximal histidine modulates Fe reactivity

The second major factor influencing iron reactivity in Hbs is hydrogen bonding between the proximal HisF8 side chain and residues in the proximal pocket (Fig. 4). Whilst HisF8 coordinates haem Fe through a lone pair on the side chain $N^{\varepsilon 2}$ atom, the protonated $N^{\delta 1}$ atom is free to participate in hydrogen bonding to other chemical groups.

Resonance Raman and density functional theory (DFT) calculations show that hydrogen bonding through $N^{\delta 1}$ alters the electronic properties of the proximal imidazole such that it can donate more or less negative charge to the haem Fe, and this modulates the Fe—XO bond strength (where X is C, N, or O) [98–101]. Interestingly, DFT calculations suggest that moderate strength hydrogen bond, e.g., to a carbonyl acceptor group, results in synergic enhancement of π-backbonding from Fe to O_2 and σ-donation from O_2 to Fe, thus stabilising Fe—O_2 [101]. On the other hand, a strong hydrogen bond to His $N^{\delta 1}$ increases the imidazolate character of the His side chain, causing it to donate more negative charge to the haem, and resulting in σ-donor competition with the XO ligand for the Fe d_{z^2} acceptor orbital. This competition weakens the Fe—XO bond. It has been noted that haems with strong electron donating axial ligands, such as imidazolate or thiolate ligands, frequently have similar binding affinities for NO/CO/O_2 ligands, compared to haems with a neutral axial imidazole (see Section 3.6), suggesting that electronic properties of the proximal His have a role in ligand discrimination, in addition to overall affinity and reactivity of the Fe—XO complex [102,103].

In light of the above, it is interesting that hydrogen bonding from a neutral HisF8 imidazole to the carbonyl group of residue F7 is common in O_2 transport Hbs, and that proximal haem pocket interactions are

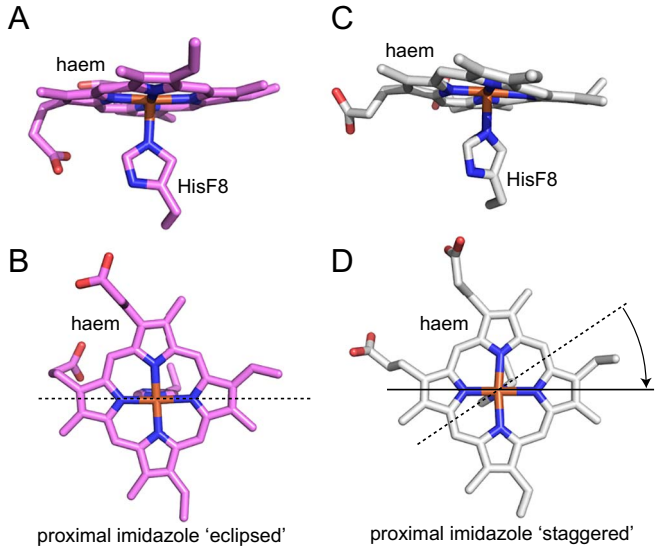

Fig. 3. Steric hindrance between HisF8 and the porphyrin ring. (A, B) In sperm whale Mb, the proximal imidazole base is eclipsed by the closest pyrrole nitrogen atoms—azimuthal angle ~0°. (C, D) In LHb, the azimuthal angle (arrow) is ~30°, close to the maximum staggered position of 45°.

quite different in the bacterial FHbs [104,105] and SDgbs [106,107], which function primarily as NOD enzymes (Fig. 4). In FHbs and SDgbs, a carboxylate (GluH23) and phenol (TyrG5) pair is highly conserved in the proximal haem pocket, and makes strong hydrogen bond interactions that stabilise HisF8 as an imidazolate. σ-Donor competition between O_2 and the axial imidazolate increases negative charge on O_2, which favours NOD enzyme activity [17,105–108]. A similarly positioned carboxylic acid is found in the haem enzymes, horse radish peroxidase (HRP) and cytochrome *c* peroxidase (CcP), and contributes to the mechanism of O—O bond cleavage [109,110].

Measurements of the Fe–His bond stretching frequency (νFe–His) together with potentiometry have confirmed the chemical similarity of haem sites from FHb/SDgb sub-families and peroxidase enzymes. Thus, stretching frequencies for 5-coordinate *Campylobacter jejuni* Cgb (251 cm^{-1}) [106,107], *Vitreoscilla* SDgb (252 cm^{-1}), and *E. coli* Hmp (244 cm^{-1}) [108] are significantly higher than for unliganded Mb (220 cm^{-1}) [111–113] and unliganded Hb (~215 cm^{-1}) [114–117], and similar to values from cytochrome *c* peroxidase (248 cm^{-1}) and HRP (244 cm^{-1}) enzymes [118,119]. The Fe(III)/Fe(II) midpoint potential for Cygb is −134 mV at pH 7 [107], and for *E. coli* Hmp it is −121 mV [120]; both are considerably lower than Mb (+58 mV) or mammalian Hb (+150 mV) [121], and closer to midpoint potentials for HRP (−250 mV) [122] and Cytochrome c peroxidase (−194 mV) [123].

It is worth noting that coordinating haem through lone pairs on S or O atoms (Cys, Met or Tyr side chains) as seen in other non-Hb haem proteins, causes even greater shifts in oxidation potential according to hard-soft acid-base principles [124]. Thus, haem proteins with 5-coordinate Tyr/− (−303 mV) or His/Tyr (−550 mV) arrangements have much lower redox potentials and strongly favour Fe(III) centres [124]. A HisF8 → Tyr mutant of Mb has a midpoint potential ~250 mV lower than the wild type [125]. This has important clinical relevance in the form of the methaemoglobinopathies, wherein mutations of proximal HisF8 or distal HisE7 to Tyr (all these natural Hb variants are referred to as HbMs) cause rapid oxidation to Fe(III) methaemoglobin (metHb), which is unable to transport O_2 (biochemical and clinical correlates of natural Hb variants are reviewed in [126]).

3.5. The Fe—O_2 bond is polar

Whilst the proximal HisF8 plays a dominant role in controlling Fe reactivity, residues in the distal haem pocket are important for controlling affinity and selectivity through more direct interactions with ligands. Because NO, CO and O_2 are similar sized apolar molecules, discrimination between these by Mb and other Hbs must occur at the level of the Fe—XO complexes [127], which have substantially different electronic properties [98,99]. The precise electronic structure of the Fe—O_2 bond has been debated since the 1936 papers on this subject were first published by Pauling and Coryell [29,30,34,35,128–134]. Infrared spectroscopy of the O—O bond clearly supports formal reduction of bound oxygen to superoxide; thus the νO—O frequency in Hb(O_2) (1107 cm^{-1}) [135], Mb(O_2) (1103 cm^{-1}) [136] and synthetic (porphinato)Fe(II)(O_2) complexes (1150 cm^{-1}) [137] are clearly in a range expected for O_2^- (1150–1100 cm^{-1}) [29,137], and not for molecular O_2 (1555 cm^{-1}) or peroxide (O_2^{2-}; 842 cm^{-1}) [29]. This is consistent with the formal superoxo model, Fe(III)$^+$(O_2^-), proposed by H. G. Weiss [128,129]. A bonding model involving σ-donation from an electron pair on O_2^- to Fe(III), with minimal contribution from π-backdonation, is generally accepted [99], although computational studies and Mössbauer spectroscopy indicate the net charge transfer is less that ± 1 e^- [131,138]. Whatever the model, there is consensus that the Fe—O_2 bond is highly polar. In comparison, smaller decreases in νC—O (from 2145 to ~1950 cm^{-1}) and νN—O (from 1877 to ~1600 cm^{-1}) upon haem binding suggest less transfer of electronic charge to these ligands and hence less polar Fe(II)(CO) and Fe(II)(NO) complexes [98]. The mechanisms by which Hbs discriminate between polar and non-polar ligand adducts are discussed next.

3.6. Hydrogen bonding with HisE7 stabilises bound O_2 in Mb and RBC Hb

Selective stabilisation of bound O_2 over CO and NO is physiologically important to prevent poisoning by endogenous CO/NO, which, although present at very low levels, have dramatically stronger binding to Fe(II) haems. The intrinsic high CO affinity of Fe(II) haems is demonstrated by binding experiments in apolar solvents, which show the equilibrium constant for CO binding (K_{CO}) is ~10^4 greater than K_{O2} ([30,31,127] and references therein). Haem proteins with an apolar distal haem pocket have similar preferences for CO over O_2—for these proteins, the ratio K_{NO}:K_{CO}:K_{O2} is typically in the order of ~10^6:~10^3:1 [102]. If this were true of Hb or Mb, then CO produced by normal haem catabolism (porphyrin cleavage at the α methene by haem oxygenase) would result in poisoning. Poisoning does not happen because K_{CO}:K_{O2} is reduced to 25:1 for Mb [139]. The mechanism is an increase in the affinity for O_2, relative to CO, arising from electrostatic interactions between the partial negative charge on bound O_2 and polar side chains in the distal pocket (Fig. 5) [127]. Anticorrelation of νFe—XO and νX—O stretching frequencies has been used extensively to probe the electrostatic potential of the distal haem site in Hbs and other haem proteins, and is reviewed elsewhere [99,140].

Pauling was the first to propose [128] that hydrogen bonding with the distal HisE7 stabilised partial negative charge on O_2 ligand in mammalian RBC Hb and Mb (Fig. 5, top left), and this hydrogen bonding was subsequently confirmed experimentally by Raman [141–143], EPR [144], X-ray crystallography [145,146], neutron diffraction [147] and NMR [148]. The theory that electrostatic interactions selectively enhance O_2 binding has also been borne out by extensive mutagenesis studies in muscle Mb (reviewed by [127,149]) and by computational studies [66,150]. For example, substitution of HisE7 with Val, the side chain of which cannot form hydrogen bonds, causes a > 1000-fold increase in the O_2 dissociation rate constant (k_{O2}), and a 100-fold decrease in the equilibrium association constant, K_{O2} [151].

In their quantitative review of O_2/CO/NO binding, Phillips and Olson [127] show that a polar E7 side chain has two distinct effects on ligand binding kinetics. The first effect is that polar HisE7 causes a small (~10-fold) *decrease* in the binding rate constant for O_2 or CO, compared to model synthetic porphyrins in apolar solvent, or haem pocket mutants with an apolar E7 side chain [139]; the reason is that

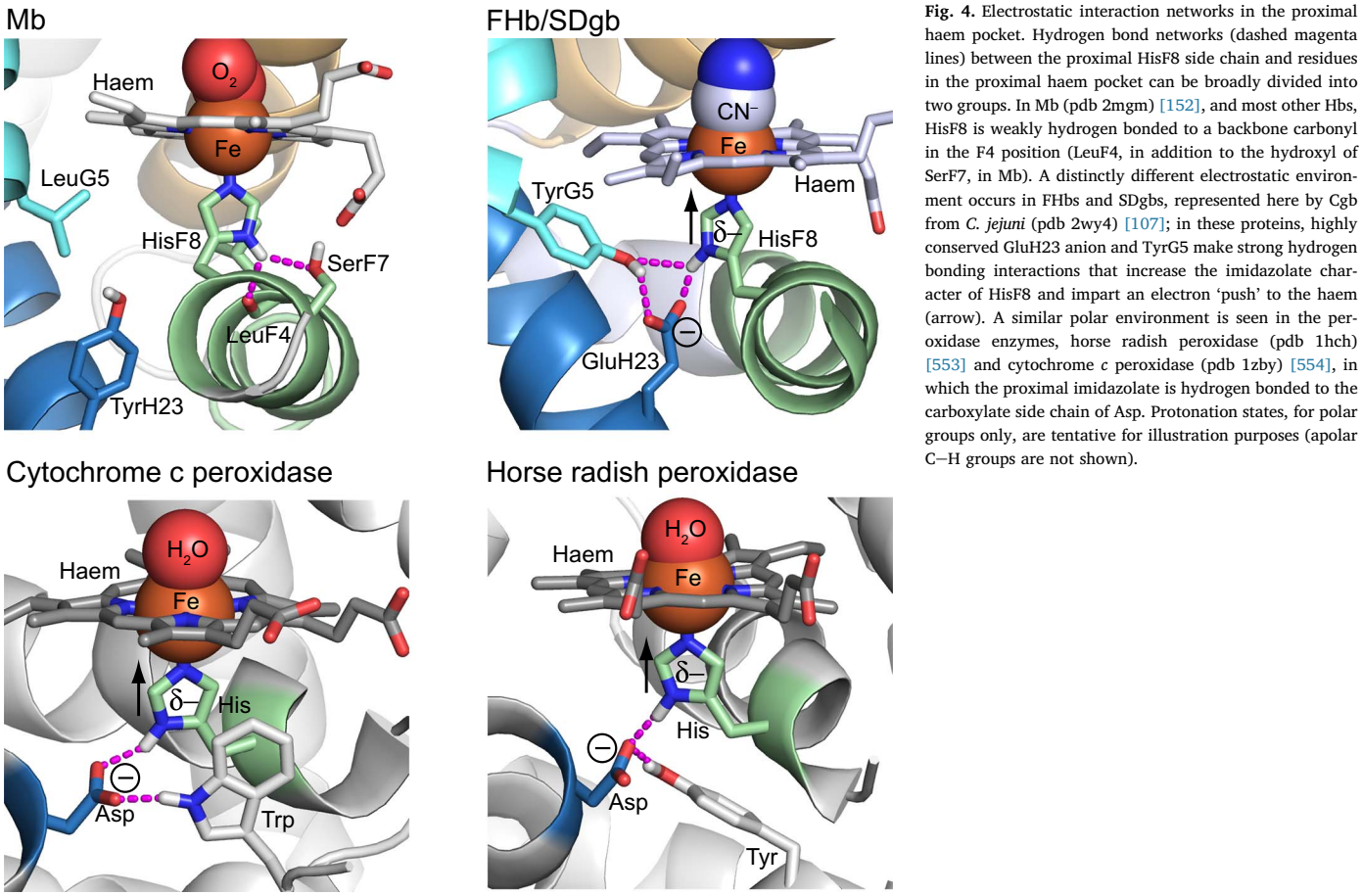

Fig. 4. Electrostatic interaction networks in the proximal haem pocket. Hydrogen bond networks (dashed magenta lines) between the proximal HisF8 side chain and residues in the proximal haem pocket can be broadly divided into two groups. In Mb (pdb 2mgm) [152], and most other Hbs, HisF8 is weakly hydrogen bonded to a backbone carbonyl in the F4 position (LeuF4, in addition to the hydroxyl of SerF7, in Mb). A distinctly different electrostatic environment occurs in FHbs and SDgbs, represented here by Cgb from *C. jejuni* (pdb 2wy4) [107]; in these proteins, highly conserved GluH23 anion and TyrG5 make strong hydrogen bonding interactions that increase the imidazolate character of HisF8 and impart an electron 'push' to the haem (arrow). A similar polar environment is seen in the peroxidase enzymes, horse radish peroxidase (pdb 1hch) [553] and cytochrome *c* peroxidase (pdb 1zby) [554], in which the proximal imidazolate is hydrogen bonded to the carboxylate side chain of Asp. Protonation states, for polar groups only, are tentative for illustration purposes (apolar C–H groups are not shown).

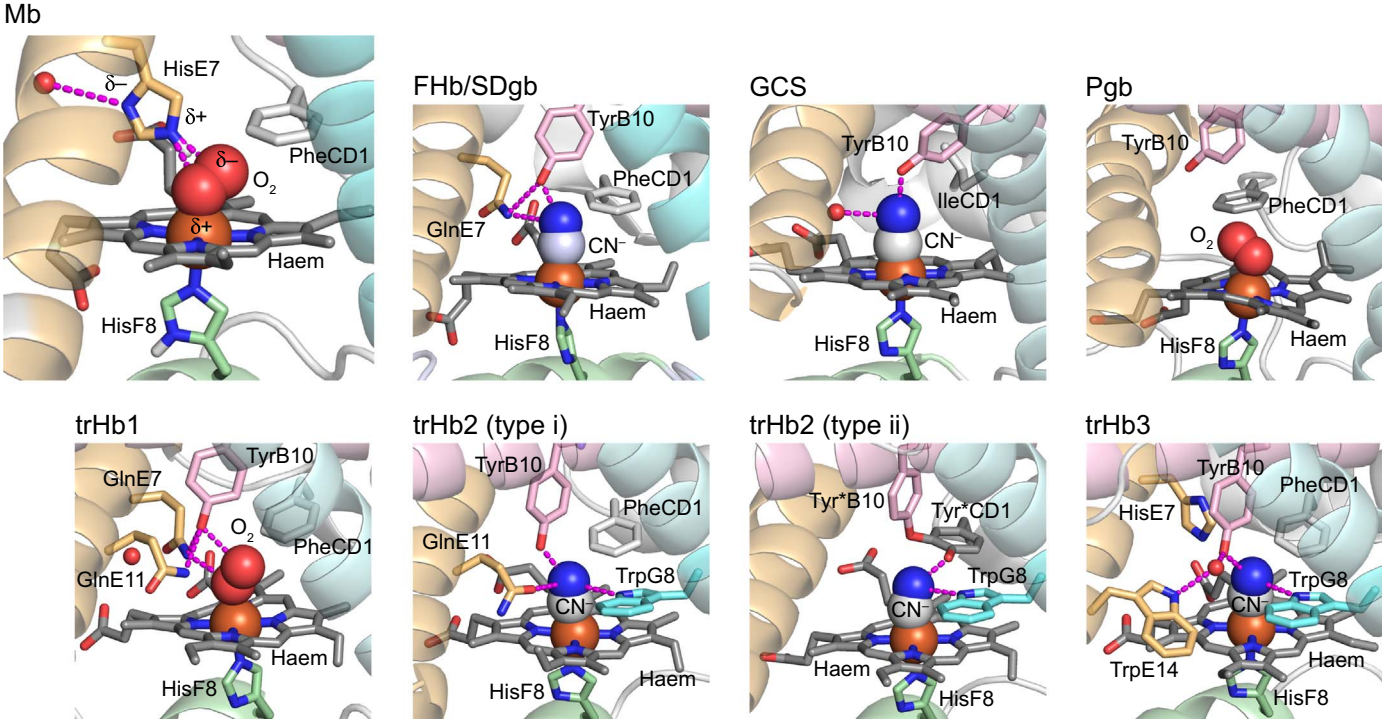

Fig. 5. Electrostatic interactions stabilise ligand in the distal haem pocket. Hydrogen bond networks (dashed magenta lines) between Fe-coordinated ligand (either ferrous ligand, O_2, or ferric ligand, CN^-) and side chains in the distal haem pocket are highly varied. Networks are shown for the following representative x-ray crystal structures: sperm whale Mb (pdb 2mgm) [152], with protonation states of HisE7/F8 $N^{\delta 1}$ and $N^{\epsilon 2}$ atoms shown, based on neutron diffraction [555] (apolar C–H groups are not shown); Cgb from *C. jejuni* (pdb 2wy4) [107]; HemAT from *B. subtilis* (pdb 1or4) [397]; Pgb from *M. acetivorans* (pdb 2veb) [63]; trHb1 from *T. pyriformis* (pdb 3aq5) [174]; trHb2 from *B. subtilis* (pdb 1ux8) [53]; trHb2 from *M. tuberculosis* with covalently linked TyrB10–TyrCD1 (pdb 1ngk) [178]; and trHb3 from *C. jejuni* (pdb 2ig3) [180].

electrostatic interactions with HisE7 stabilise a non-coordinated water molecule in the haem pocket of unliganded Mb that must dissociate to allow room for diatomic ligands to enter the haem pocket [152,153]. More recently the reverse exchange of CO for water has been measured [153] and the role of non-coordinated water molecules in controlling ligand binding rates has been shown in other Hbs [154]. Together, these results show that the hydrogen bonding potential of residues in the distal pocket contributes significantly to the overall kinetic barrier for O_2 binding.

The second effect of the polar E7 side chain, as suggested by Pauling, is to stabilise polar Fe–ligand complexes. In the case of O_2 binding to Mb, the small negative effect of HisE7 on the ligand *association* is offset by a ~1000-fold decrease in the *dissociation* rate constant of the polar $Fe(III)^+(O_2^-)$ complex. The net result is ~100-fold increase in O_2 affinity of Mb with HisE7 compared to Mb mutants with apolar side chains at the E7 position [127]. Mutant studies suggest that hydrogen bonding with HisE7 contributes around -3.5 kcal mol^{-1} to O_2 binding affinity in Mb, and around -2 kcal mol^{-1} in the Hb α and Hb β chains [155]. These values are similar to those obtained from QM computational approaches, which are in the range -3.7 to -6.8 kcal mol^{-1} for Mb [66,150,156]. For apolar Fe(II)(CO) complexes, the positive contribution from weak hydrogen bonding to HisE7 is smaller than the negative contribution from steric interference by water in the distal pocket, leading to an overall ~5-fold drop in K_{CO} for Mb compared to apolar haem pocket mutants of Mb [127]. For NO, it appears that a ~10-fold stabilisation of NO by hydrogen bonding is almost exactly offset by the 10-fold reduction in K_{NO} due to water in the haem pocket. In summary, hydrogen bonding interactions in the distal pocket increase Hb affinity and selectivity for O_2 ligand by lowering the $Hb(O_2)$ dissociation rate.

3.7. Hydrogen bonding networks in the distal pocket are highly varied

Taking a broad view of Hb structure, it is striking that the plant and metazoan Hb sub-family is the only group in which distal HisE7 is conserved and acts as the sole hydrogen bond donor to bound ligand (Table 1). In other families, a more extended hydrogen bond network involving two or more polar side chains is typical (Fig. 5). One of these polar residues is almost always TyrB10, which replaces Phe, Ile or Leu at the corresponding position in Mb. The FHbs and SDgbs share highly conserved TyrB10 and GlnE7 residues in the distal pocket, which hydrogen bond with bound ligand [105,157,158]. An extended polar network in the distal pocket is typically associated with higher O_2 binding affinities and is also a feature in the haem enzymes HRP and CcP [102]. Some typical and atypical features of the hydrogen bond network in each of the three Hb families (Table 1) are briefly discussed next.

Even within the restricted group of plant and metazoan Hbs, O_2 affinities vary over at least 3 orders of magnitude (e.g., see [92]). Mb-like Hbs from parasitic nematodes such as *Paramphistomum epiclitum* (TyrB10/TyrE7; K_{O2} 3300 μM^{-1}) [92,93] and *Ascaris suum* (TyrB10/GlnE7; K_{O2} 425 μM^{-1}) [159,160] bind O_2 with much higher affinity than Mb (K_{O2} 1.1 μM^{-1}) [139], and stabilise O_2 through hydrogen bonding to TyrB10, as seen for the non-plant and metazoan Hbs. However, the identity of side chains in the B10/E7 positions clearly does not tell the whole story, as demonstrated by studies of Hb from nerve tissue of the nemertean worm *Cerebratulus lacteus*. Although clearly clustering with the metazoan Hbs, *C. lacteus* Hb has an unusual truncated structure, missing helix A and most of H [161], and, although it has a TyrB10/GlnE7 sequence in the distal pocket, it exhibits only moderate O_2 affinity (K_{O2} 1.3 μM^{-1}) that is very similar to that of Mb. Crystal structures indicate an extended hydrogen bond network in the distal pocket involving TyrB10, GlnE7, and ThrE11, of which TyrB10 makes the most significant interactions directly with the bound O_2 or CO [161,162]. The lower-than-expected O_2 affinity is attributed to equilibrium between different hydrogen bonding patterns [163,164]: a high affinity state in which the phenol of TyrB10 hydrogen bonds to the O_2 or CO ligand, and a lower affinity in which TyrB10 phenol is hydrogen bonded to the side chain of ThrE11 and a lone pair on phenolic O of TyrB10 is directed towards the ligand with consequent electrostatic repulsion of the ligand [163,164]. Evidence for this explanation comes from molecular dynamics (MD) and QM/MM calculations [163,165], and by the fact that mutation of ThrE11 → Val causes a 1000-fold reduction in the O_2 dissociation rate constant and a 130-fold decrease in K_{O2} [164]. A much smaller 7-fold decrease in CO dissociation rate constant for the E11Thr → Val mutant is also consistent with the proposed model as Fe(II)(CO) is expected to be less sensitive to electrostatic effects. A similar equilibrium may explain moderate affinity (K_{O2} 1.2 μM^{-1}; [166]) in trHb1 from *Paramecium caudatum* [167].

Unlike the case of Mb (Section 3.6), mutation of distal HisE7 → Val (or Ala or Leu) in soybean LHb causes little change in O_2 affinity [87,90], suggesting little electrostatic stabilisation of ligands by HisE7 in LHb. The reason appears to be that interactions between HisE7 and TyrB10 constrain the imidazole side chain in a position that reduces hydrogen bonding to O_2. For Mb(CO), and a number of other Hbs, multiple νC—O stretching frequencies, measured by infra-red spectroscopy (IR), indicate the presence of multiple conformational states of HisE7 [168], some of which correspond to conformers with hydrogen bond interactions between protonated $N^{\varepsilon 2}$ of HisE7 and the CO ligand [66]. In the case of LHb, the presence of a single major νC—O peak led Kundu et al. to suggest that HisE7 is restrained by a hydrogen bond from TyrB10 to $N^{\delta 1}$ of the imidazole [169]. Mutation of TyrB10 freed HisE7 to adopt other conformations (as evidenced by multiplicity of νC—O) and increased O_2 affinity, suggesting that electrostatic interactions between HisE7 and ligand were enhanced [87,167,169]. Although a hydrogen bond from TyrB10 to HisE7 is not seen in the crystal structure [90], computational studies indicate that TyrB10-interacting and non-interacting conformers of HisE7 are populated in solution, and that the HisE7 rotamer with a hydrogen bond to TyrB10 makes weaker electrostatic interactions with O_2 [167].

Structural plasticity appears to be common in the distal pocket of proteins in the sensor Hb family, suggesting this might be linked to signal transduction mechanisms. The distal haem pocket in several bacterial globin-coupled sensors (GCS) undergoes conformational change such that TyrB10 can coordinate bound ligand or swing away to generate a low affinity state [19] [170]. This group of Hbs is notable for low conservation of PheCD1 (can be Phe, Ile or Leu) and there is considerable variation at E7 and E11 that is not seen in other Hb groups. In one GCS from *Geobacter sulfurreducens*, HisE11 and HisF8 form hexacoordinate haem [171] (Section 4). In Pgb from *Methanosarcina acetivorans*, TyrB10 is conserved but the distance from the haem site means this side chain only makes a small contribution to ligand affinity [63,172]. *M. acetivorans* is an obligate anaerobe that lives in marine sediments where it is thought to metabolise CO, hence CO binding ineractions with Pgb have been of interest. Complex CO binding kinetics [172] and structural plasticity in the distal haem pocket [173] suggest an equilibrium between a high affinity liganded state with hydrogen bonding from TrpB9 to CO, and a lower affinity state in which this interaction is absent. These varied properties demonstrate that there is still much to discover about the structural basis for ligand affinity in this group.

Finally, members of the bacterial trHb family typically have high ligand affinities and display a number of distinctive distal pocket features. Hydrogen bond networks in the distal pocket of these proteins frequently involve multiple polar side chains that interact with each other, as well as with bound haem ligands (Fig. 5, bottom row). Crystallographic studies have identified distal pocket hydrogen bond networks comprising side chains of TyrB10, GlnE7 and GlnE11 in trHb1 proteins, and mutations at any of these positions increase O_2 dissociation and autooxidation rates [8,174–176]. A hydrogen bonding to ligand through the indole N of TrpG8 is a distinctive feature of trHb2 [53,96,177–179] and trHb3 proteins [180–182]; in each case, the

indole ring of TrpG8 lies parallel to the porphyrin ring and makes additional π-stacking interactions with the porphyrin macrocycle. Some trHb2s (type ii in Table 1) have a distal pocket with an unusual post-translational modification, whereby a pair of tyrosine side chains are linked via a covalent bond between the O^{η} atom of TyrB10 and the $C^{\varepsilon 2}$ atom of TyrCD1 [178]; the remaining hydroxyl of TyrCD1 donates a hydrogen bond to the O_2 ligand. These π-stacking interactions and covalent modifications are expected to stabilise electrostatic interactions with haem ligands.

The trHb3 group is notable as the only group outside the plant and vertebrate Hbs in which HisE7 is conserved. In the crystal structure of trHb3 from *C. jejuni*, HisE7 does not make a hydrogen bond with the bound CN^- ligand [180]; however, RR, mutagenesis and MD simulations indicate that TyrB10, TrpG8 and His E7 all contribute to the hydrogen bond network [181,182]. Mutation of TyrB10 and HisE7 to apolar residues *increases* the O_2 affinity dramatically, from $K_{O2} = 222\ \mu M^{-1}$ in the wild-type protein, to $K_{O2} = 15{,}000\ \mu M^{-1}$ [181], suggesting that TrpG8 on its own makes a highly stabilising interaction that is moderated by the extended hydrogen bond network. MD simulations suggest that multiple hydrogen bond networks may coexist in *C. jejuni* trHb3 to lower O_2 affinity, as also proposed for *Cerebratulus lacteus* miniHb, LHb, and *P. caudatum* trHb1 (see above), suggesting this might be a common mechanism to regulate ligand affinity [182].

3.8. Steric hindrance as a mechanism for discriminating haem ligands

The different geometry of linear Fe—C—O (~180°) versus bent Fe—O—O (~120°) and moderately bent Fe—N—O (~140°) provide for potential steric selection of ligand binding, as proposed by Collman [137]. Initial reports of a bent Fe—C—O conformation in MbCO structures were found to be artifacts of isotropic refinement of anisotropic crystals, due to limited resolution in the original x-ray diffraction studies [183]. Model porphyrins [31] and crystal structures of Mb determined with atomic (1 Å) resolution [184,185], as well as numerous other protein structures, show that CO invariably binds with a linear geometry. Although steric hindrance is not required for a quantitative explanation of CO/O_2 selectivity [127], Collman points out [31] that a linear Fe—C—O unit does not discount a role for sterics CO/O_2 discrimination as a mechanism in other Hbs. The rationale is that steric hindrance does alter relative stabilities 1000-fold in synthetic porphyrin models *without* substantial Fe—C—O distortion; instead distortions in the porphyrin core [36,37,77], that may be too small to be detected in the majority of protein crystals, are implicated.

3.9. The distal haem pocket captures diatomic ligands prior to Fe–ligand bond formation

Whilst ligand dissociation rate constants are predominantly controlled by iron reactivity (proximal haem pocket effects) and electrostatic stabilisation of Fe—XO, rate constants for ligand binding are controlled by accessibility of the iron and capture of ligand into the distal haem pocket. The effect of polar residues and water in the distal pocket on ligand association rate has already been mentioned (Section 3.6). Hydrophobic residues in the distal haem pocket have a strong influence on ligand association rates by providing a hydrophobic pocket into which O_2/CO/NO can bind prior to reaction with the haem Fe. Residues LeuB10, PheCD1, ValE11, IleG8 determine the size of the distal haem pocket and have effects on O_2 binding rates [186–188]. A smaller volume increases the number of collisions of O_2 with the Fe centre—as illustrated by LeuB10 → Phe mutants of Mb [189,190] and Hb [191], which increase the affinity and the rate of geminate CO rebinding following photolysis, whereas mutation to Ala has the opposite effect. ValE11 is highly conserved in O_2 transport Hbs and has a subtle steric interaction that is destabilising to the distal pocket water molecule in unliganded Mb, but not substantial enough to significantly hinder haem ligands [187,188]. In the β subunit of RBC Hb, ValE11 hinders ligand binding in the T, but not R, quaternary state (see Section 7.7). In addition to forming the ligand binding/rebinding cavity, hydrophobic residues in the distal pocket have important effects on haem binding, lowering autooxidation rates, and making steric interactions to position polar side chains. For example, PheCD4 helps to position HisE7 for hydrogen bonding in Mb [192].

3.10. Diatomic ligands enter the distal haem pocket by defined pathways

The driving 'force' that concentrates ligands to the haem pocket is the hydrophobic effect that causes hydrophobic O_2/CO/NO to partition from the solvent water to the apolar cavities in the distal haem pocket [153,193]; the pathway of ligand diffusion from the exterior of protein to the distal haem site dictates the kinetics. Perutz proposed entry of O_2 to the haem pocket of Mb and Hb via a solvent channel created by an outward rotation of the HisE7 side chain [194,195]. The E7 gating mechanism is supported by the everted position of the HisE7 side chain in crystal structures of Mb carrying bulky ligands [196–198], and also in crystals of MbCO at pH 4 [199], where it was supposed that the low pH increases the cationic state of HisE7, thus increasing its solvent exposure. Even at pH 7.0, atomic-resolution structures of Mb reveal ~20% occupancy of the everted HisE7 side chain conformation [184]. In solution, the multiplicity of the νCO stretching frequencies can be explained using MD [200] and QM/MM [66] as arising from a mix of hydrogen bonded and everted, or open, states of HisE7.

An alternative route for ligand migration is diffusion via a longer pathway of atom-sized hydrophobic cavities in the protein. Xe is a relatively large and inert atom that binds with low affinity purely through Van der Waals interactions and has been used extensively as a probe for internal cavities. Crystal structures of Mb under pressurised Xe atmosphere show Xe molecules bound in a number of cavities within the protein matrix [201,202]. When the Fe–ligand bond is broken, naturally by thermal energy or induced by photolysis, the ligand molecule is positioned close to the haem-Fe from which it can rebind (geminate rebinding with ps–ns time constants), or diffuse to the bulk solvent and be replaced by ligand diffusing in from the solvent (bimolecular rebinding). The Xe-binding sites in Mb have been proposed as transient sites for O_2/CO/NO ligands migrating to the haem pocket [203]; however, filling cavities with Xe under pressure had no effect on geminate or bimolecular CO binding for Hb [191] and only small effects on the slow (μs) phase of geminate rebinding in Mb (reflecting a small fraction of geminate rebinding from internal Xe sites) [71,204,205]. The results described above suggest that Xe-binding cavities in Hb and Mb are not major routes of ligand migration.

Mutational, crystallographic and kinetic studies of laser flash photolysis of Hb(CO) and stopped-flow spectrophotometry by Olson, Gibson and colleagues suggest that the E7 gate is the predominant pathway for ligand entry in Mb [71,204] and Hb α and β chains [155,191,206]. Royer and colleagues [207,208], using similar methods, identified the E7 gate as the major route of ligand entry and exit in HbI from the clam *Sapharca inaequivalvis*, which is representative of a group of dimeric metazoan Hbs that have a dimer interface formed by the E and F helices. Interestingly, the MD results of Boechi et al. [193] suggest that HisE7 does not provide a physical barrier to O_2 diffusion in the closed state, but rather, in the open state, creates a hydrophobic site, corresponding to a shallow free energy well (-2 kcal mol^{-1} compared to O_2 in solvent), above the edge of the porphyrin ring and ~5 Å from the iron into which ligand would be captured if traversing the E7 channel. Depth of energy well was directly related to the bimolecular rate constant for entry into the haem pocket in Mb mutants. MD simulations of RBC Hb reveal a similar E7-linked hydrophobic cavity and suggest that opening of the E7 gate regulates ligand association rate in the β chain [209]. Together these results suggest HisE7 as a common gas migration pathway in plant and metazoan 'HisE7' Hbs; it is clear, however, that other ligand migration pathways operate in different

groups of Hbs.

In particular hydrophobic tunnels have emerged as major routes of ligand diffusion in the trHb1 and trHb2 families and some other Hbs. Channels or tunnels are formed by contiguous or nearly contiguous series of cavities leading from the exterior of the protein to the haem pocket in the trHb1 proteins from *Paramecium caudatum* [8,210], *Chlamydomonas eugametos* [8,210] and *Mycobacterium tuberculosis* [210–212], and in trHb2 from *Mycobacterium tuberculosis* [178,213,214] the thermophilic *actinobacterium*, *Thermobifida fusca* [215,216], Pgb from *Methanosarcina acetivorans* [63] and the metazoan *C. lacteus* Hb [161,165,217,218]. Compared to the cavities in Mb (13–45 $Å^3$), the tunnel cavities are much larger (180–400 $Å^3$), are lined with hydrophobic residues forming a barrier to water, and can accommodate multiple Xe atoms consistent with diffusion pathways for apolar ligands [210]. The locations of cavities are conserved between members of the trHb1 family, but distinct from those in Pgb and *C. lacteus* Hb, suggesting separate evolutionary origins. MD simulations have demonstrated that ligand migration through these systems of cavities can account for the observed kinetics of ligand binding [154,210,214,219]. MD studies also show that non-coordinated waters, stabilised by the polar residues in the distal pocket of trHbs, create a barrier to the final step of ligand migration and have a strong effect on the overall ligand binding kinetics [154,220,221]. Bustamante et al. suggest that, although ligand migration occurs through the apolar tunnels, water in the distal pocket may still exchange with the bulk solvent through an E7-like gate [154]. Finally, trHb3 proteins lack conserved hydrophobic tunnels seen in trHb1 and trHb2; trHb3 is the only group outside the plant and metazoan Hb group to conserve HisE7; the distal HisE7 side chain adopts a partially outward facing conformation in one molecule of the asymmetric unit in crystals of trHb3 from *Campylobacter jejuni* [180], all suggesting that an E7 gate mechanism may be at play.

4. Hexacoordinate Hbs (HxHbs)

4.1. HxHbs as physiological and pathophysiological states

In free haem, the binding of one axial imidazole generates much higher affinity for binding a second base in the remaining sixth metal coordination site, leading to rapid formation of a bis-imidazole complex. Bis-imidazole coordination dramatically reduces affinity for diatomic ligands, through a competition effect, unless interaction with the second imidazole can be selectively hindered [222]. In Mb, erythrocyte Hb, and many other Hbs, the distal HisE7 can potentially coordinate the haem, but is restrained from doing so by the protein matrix; under mild denaturing/non-physiological conditions, however, formation of a reversible 6-coordinate bis-histidyl complex can occur in Mb and Hb [223,224]. Bis-histidyl coordination favours Fe(III) over Fe(II) oxidation state and so can be coupled with Fe oxidation. Under pathophysiological conditions, 6-coordinate Fe(III) haems, termed hemichromes, can potentially involve protein groups other than HisE7 as Fe ligands, and are formed as part of an irreversible process of Hb oxidation and denaturation [225]. It is now known that bis-histidyl haem coordination also has an important physiological role in RBC Hb production (Section 4.3). What is more, there are a large number of Hbs that constitutively employ reversible haem coordination by a side chain in the distal haem pocket as part of normal physiological function, and these are referred to as hexacoordinate Hbs (HxHbs).

The largest group of HxHbs are the non-symbiotic Hbs (nsHbs) from plants [226,227]. Plant nsHbs form three phylogenetic groups: class 1 and class 2 nsHbs have a 3-on-3 Hb structure, a third class of plant nsHbs has a 2-on-2 trHb fold. All class 1 and 2 nsHbs, for which coordination state has been reported, have hexacoordinate haems [226]. In mammals, a neural-specific Hb, neuroglobin (Ngb) [228–231], and ubiquitously expressed cytoglobin (Cygb) [232,233] are HxHbs. A third vertebrate HxHb, globin X, has been found in fish and amphibians [234,235]. *Drosophila melanogaster* Hb [236] and a neural Hb from bivalve mollusc, *Spisula solidissima* [237], are other examples of HxHbs from the metazoan subfamily. In all these cases the distal HisE7 serves as the sixth metal ligand.

Outside the plant and metazoan Hbs, HisE7 is generally not conserved and only a handful of bacterial Hbs are known to be HxHbs. Cases that have been established by crystallography include group I trHbs from cyanobacteria *Synechocystis* sp. and *Synechococcus* sp., which have HisF8/HisE10 coordination [58,60,61,62,238]; a highly unusual HisF8/LysE10 coordination in trHb1 from the alga *Chlamydomonas reinhardtii* [239]; and, a single GCS, from *Geobacter sulfurreducens* with HisF8/HisE11 [171]. The class 3 plant nsHbs have a trHb fold, and can form pentacoordinate or hexacoordinate structures. The mechanisms that regulate haem coordination are unclear but, in *A. thaliana* trHb, a role for an N-terminal extension to the conserved Hb domain is implicated [47,240]. Multiple hexacoordinate states involving TyrCD1 or TyrB10 in trHb2 from cold-adapted *Pseudoalteromonas haloplanktis* have been suggested [241]. A survey of all these proteins suggests that hexacoordination does not segregate with a particular biological function and several functions, similar to 5-coordinate Hbs, seem likely as described below.

4.2. Some HxHbs may function as O_2 transporters

A physiological role in O_2 transport or storage typically requires O_2 binding with P_{50} in order of 1 Torr. Because HisE7 competes with O_2 for Fe binding in HxHbs, the intrinsic O_2 affinity of the 5-coordinate species must typically be > 10-fold greater than in Mb to achieve a similar overall K_{O2}. Consequently, O_2 dissociation rates may then be too slow to facilitate O_2 diffusion (k_{O2} in order of $1\,s^{-1}$ is required) [226,227,242]. The plant class 2 nsHbs have binding parameters consistent with O_2 transport function—K_{O2} $2.9 \pm 3.5\,\mu M^{-1}$ (P_{50} ~0.2 Torr) and k_{O2} $1.1 \pm 1.2\,s^{-1}$, and may help to maintain cellular metabolism under conditions of hypoxia, although this is just one theory (reviewed by [227]). *Drosophila melanogaster* HxHb binds O_2 with a P_{50} of 0.12 Torr [243] and knock out studies support a role in O_2 transport or signalling [244]. Neural specific HxHb from the bivalve mollusc (*Spisula solidissima*) binds O2 with a P_{50} of 0.3–0.6 Torr, in a similar range to 5-coordinate neural globins from the annelid (*Aphrodite aculeate*; P_{50} 1.1 Torr) and nemertean worm (*Cerebratulus lacteus*; P_{50} 0.6 Torr), and a role for these proteins in O_2 delivery to nerve cells is well established [245]. All these proteins are expressed at high concentration (1–3 mM) as required to facilitate O_2 diffusion. On the other hand, vertebrate Ngb is expressed at μM concentration in most neural tissues arguing against a transport function, except in retinal rod cells, where Ngb concentrations of 0.1–0.2 mM may facilitate O_2 supply to mitochondria during visual activity [246]. Cygb, Ngb and globinX also display high rates of autooxidation that make a role in O_2 transport unlikely [226,246]. Cygb has been shown to regulate NO signalling in the vascular system [247] and is efficiently reduced by the cytochrome b_5/cytochrome b_5 reductase system [248], satisfying multiple criteria as a bona fide NOD enzyme. Cygb is ubiquitously expressed and so might have a general role in protecting electron transport proteins from NO toxicity [17]. Knocking down Ngb expression increases hypoxic neuronal injury in vitro and ischemic cerebral injury in vivo, suggesting roles in scavenging reactive O_2 or NO species, or in signal transduction (reviewed by [249]). Globin X is distantly related to Ngb, but is non-neuronal [235] and has recently been shown to have a nitrite reductase activity in fish RBCs [234].

For class 1 nsHbs, O_2 transport function is unlikely as the average K_{O2} is $410\,\mu M^{-1}$ (P_{50} 0.002 Torr) due to very high intrinsic reactivity of the 5-coordinate haem, coupled with weak hexacoordination and strong electrostatic stabilisation of bound O_2 by distal HisE7 [227]. An alternative possibility is that class 1 nsHbs detoxify NO (see Section 5). The reaction with NO involves oxidation of the haem Fe, and so an efficient reduction mechanism is needed for catalytic turnover.

Interestingly, HxHbs have more rapid reduction kinetics than 5-coordinate Hbs in vitro [250], although a cognate reductase for nsHbs in vivo has yet to be identified and is an important criterion for assigning a biological NOD function [251].

4.3. Hexacoordination linked to protein conformational change

A number of cases show that conversion between 5-coordinate and hexacoordinate haem can be linked to a 'signalling' function, such as protein-protein interaction or redox regulation, through a coupled conformational change in the globin protein. An example is the interaction between α-Hb stabilising protein (AHSP) and α subunit of RBC Hb (hereafter referred to as simply 'α' for simplicity). AHSP performs a chaperone function by stabilising nascent free α until the Hb β subunit (hereafter referred to as simply as β) becomes available to form a functional tetramer. In this way, AHSP protects developing erythroid cells from harmful effects that otherwise arise from α redox activity, haem loss and precipitation [252–254]. AHSP binds to α that has an oxidised Fe(III) haem ~100-fold more tightly (K_D 0.17 nM) than it binds to α with a functional Fe(II) haem centre (K_D 17 nM) [255–257], largely due to 100-fold lower dissociation rate constant of the AHSP·αFe(III) complex [257]. Greater stability of the AHSP·αFe(III) complex arises because, upon AHSP binding, αFe(III) undergoes a conformational change coupled to conversion of the 5-coordinate haem to a HisF8/HisE7 hexacoordinate haem [256,258–260]. In contrast, conversion of AHSP·αFe(II) to the hexacoordinate complex is thermodynamically unfavourable [260].

AHSP also binds to α(O_2), and the AHSP·α(O_2) complex converts to a HisF8/HisE7 hexacoordinate complex with a half-life of 14–23 min (pH 7, 37 °C) by an autooxidation mechanism [261,262]. A steric interaction between a cis-prolyl residue of AHSP and the G helix of α promotes autooxidation and α conformational change [256,258,263–265]. The physiological importance is to convert all free forms of α that are not paired with β to a redox-inert state with low cytotoxicity.

AHSP binds more tightly to α with an Fe(III) centre, compared to α with an Fe(II) centre, and, hence, stabilises the Fe(III) oxidation state over Fe(II). The degree of stabilisation has been measured as a large drop in the redox midpoint potential of α from + 40 mV to − 78 mV (in 1 M glycine, pH 6.0, 8 °C) [266]. The lower redox potential and the hexacoordinate structure physically blocks ligand access and inhibits reactions with H_2O_2 and other species that would otherwise generate harmful radicals through redox cycling [258–260,266]. It is well established that bis-imidazole coordination favours Fe(III) over Fe(II) in model haem systems, and the lower redox potentials for 6-coordinate Hbs compared to 5-coordinate Hbs confirms this pattern in haemoproteins [230,267,268]. This is also clearly demonstrated by Hb mutations that switch the native 5-coordinate or 6-coordinate structure. For example, a double HisE7 → Val, ValE11 → His mutation in Mb generates a hexacoordinate haem and shifts the redox midpoint potential from + 76 mV [269] to − 128 mV [270]. In another study mutations that converted HxHbs to pentacoordinate structures, increased the redox midpoint by + 112 mV or + 146 mV in two instances [268]. The interesting thing about the AHSP·α complex is that the presence of Fe(III) or Fe(II) haem is sufficient to tip the balance between two different protein conformations—Fe(III) haem selects hexacoordination coupled with conformational switch to the high-affinity AHSP·α complex, whereas, Fe(II) haem selects pentacoordination and retains the native-like conformation. The overall effect is to trap oxidised (non functional) α, whilst allowing reduced (functional) α to more rapidly dissociate and rebind β.

To perform its chaperone function, AHSP binds to α with a high on rate (k_{on} ~10^7 M^{-1} s^{-1}) [257], which is 20-fold greater than the rate constant for α binding to β. At the same time, the greater stability of the α·β dimer ensures a net transfer of α from AHSP·α to α·β; the transfer is 100-fold faster for 5-coordinate AHSP·αFe(II) compared to 6-coordinate AHSP·αFe(III). Once formed, bis-histidyl α can be reduced by metHb reductase whilst in complex with AHSP, or after transfer to β, to generate functional Hb [262]. There is evidence that Hb chains are initially synthesised with Fe(III) haems, in which case AHSP·α complexes may be the major pathway for incorporation of native Fe(II) α chains into mature Hb (see [271] and references therein). In this scenario the bis-histidyl intermediate might actually facilitate haem reduction, as faster reduction kinetics for 6-coordinate haem, compared to 5-coordinate haem has been shown in other systems [250]. Finally AHSP can also bind and stabilise α apoprotein in a partially folded state, suggesting it might facilitate haem insertion into nascent α chains [254,255,272].

A second example of structural change linked to hexacoordination involves allosteric regulation of vertebrate Ngb and Cygb. Ngb and Cygb are allosterically regulated by intermolecular disulfide bond formation, suggesting they may respond to cellular redox stress [273–276]. In Ngb, reduction of the CysCD7–CysD5 disulfide bond lowers O_2 affinity from a P_{50} of 0.67–1 Torr in the oxidised state [230,274,277] to 7.5–10 Torr in the reduced state (and a similar drop in O_2 affinity is seen for Ngb with Cys residues mutated to Gly or Ser) [274,277]. Ngb undergoes considerable conformational change upon ligand binding, including conversion from a 6-coordinate unliganded to liganded state, a 'sliding' of the haem group, and movement of the F, CD, EF, FG regions [278,279]. High hydrostatic pressure has been used to shift the equilibrium between the 5-coordinate and 6-coordinate unliganded states, suggesting that the conformation or flexibility of the CD region is an important determinant of 6-coordination in the unliganded state [280,281], although the role of the disulfide was not addressed directly in these studies. A strand-to-helix transition in the CD loop upon disulfide formation has been proposed as the mechanism of redox control [282] and gains some support from the only crystal structure of wild-type human Ngb in the oxidised state [283] compared with that of a triple-Cys mutant which cannot form a disulfide bond [284]. Ngb is also allosterically regulated by H^+ [277] and by phosphorylation [285]. The nature of disulfide bonding in Cygb is more uncertain due to the formation of both intra- and inter-molecular disulfide linked species in vitro. One study by Lechauve et al. found that reduction of an intramolecular CysB2–CysE9 disulfide bond increases P_{50} from 0.2 to 2 Torr, similar to the effect seen in Ngb [276], although others have found the change in affinity to be < 2-fold [274]. There is evidence that Fe coordination in Cygb is also regulated by lipid binding [286].

Finally, HxHb from *Synechocystis* undergoes a large conformational change on binding to the ferric ligands, CN^- and N_3^- [62], which involves a hinging motion of the E helix, rearrangement of hydrogen bonding around the pyrrole D propionate, and the formation of an extra turn in the F helix. Large conformational changes in response to ligand binding are unusual for Hbs and it is attractive to speculate that they represent novel signalling mechanisms.

5. Hbs and protection from nitrosative stress

5.1. NO production and nitrosative stress

NO is produced in living systems by two general mechanisms: (a) by the nitric oxide synthase (NOS) class of haem-containing enzymes using the amino acid L-arginine as substrate [287], or (b) by the process of nitrate reduction in bacteria [288,289], fungi [290] and plants [291] to liberate energy for metabolism under conditions of low [O_2]. Bacteria and fungi employ a denitrification reaction, which uses nitrate (NO_3^-), instead of O_2, as the terminal electron acceptor to liberate energy under hypoxic conditions. In the process, nitrate is reduced in subsequent steps to nitrite (NO_2^-), NO, N_2O and finally N_2, from which N can be assimilated by nitrogen fixation. A competing process, respiratory ammonification, can convert nitrite directly to ammonia without production of NO [292]. An alternative nitrate reduction pathway, that also generates NO, operates under hypoxic conditions in plants [291]. As a

signalling molecule, NO has numerous roles in eukaryotes and prokaryotes including regulation of smooth muscle by binding to the haem-enzyme guanylate cyclase (generating the second messenger, cyclic-GMP), targeted killing of pathogens by macrophages and other cells in the immune system [293], transcriptional regulation of bacterial virulence [294], and, induction of ethylene production in plants [295]. NO acts on its signalling targets at nM concentration, but is also toxic through inhibiting many other haem- or iron-containing enzymes at similar concentrations, as well as generating non-specific damage through radical chemistry, all of which contribute to nitrosative stress (reviewed in [17]). In particular, NOD activity is likely to be important in many cell types to prevent potent (nM) inhibition of cytochrome *c* oxidase, the terminal oxidase of respiration [17,296].

5.2. Reactions of Hb with NO and other bioactive gases in the haem pocket

It has been known since 1865, when it was shown by Hermann (see [297]), that NO has extremely high affinity for Hb. Under physiological conditions the major Hb/Mb species in mammals are deoxy Hb/MbFe(II) and Hb/Mb(O_2), both of which undergo extremely rapid reaction with NO. Under anaerobic conditions, HbFe(II) and MbFe(II) bind NO reversibly, but with extremely high affinity ($K_{NO} \sim 2 \times 10^{11}\ M^{-1}$) and the bimolecular association rate is close to diffusion controlled ($\sim 10^8\ M^{-1}\ s^{-1}$) [155,187,297,298]. Upon exposure to O_2, the ferrous nitrosyl HbFe(II)(NO) species converts to metHb and nitrate (NO_3^-) [299] at a rate governed by the slow dissociation of NO from Fe(II) haems (k_{NO} is 10^{-4} to $10^{-5}\ s^{-1}$) [300,301]. On the other hand, the reaction of NO with Mb(O_2) or Hb(O_2) to form metHb and nitrate is extremely fast (bimolecular rate constant $\sim 1 \times 10^8\ M^{-1}\ s^{-1}$) [302] and similar in speed to bimolecular reaction of NO to unliganded Hb; in both cases the rate-limiting step is capture of NO into the distal haem pocket [187,189]. Reaction products of Mb(O_2) or Hb(O_2) in excess NO are exclusively metHb and nitrate [303]. Additional reaction products, such as S-nitrosated Hb (see Section 5.4) and nitrite (NO_2^-) have been reported at low (physiological) [NO]:[Hb] mixing ratios [304]; however these products may arise from artificially high local [NO] as a mixing artefact of bolus NO addition, as, when NO donors are used, nitrosation products and NO_2^- account for < 1% of the NO consumed [305,306].

The NO induced oxidation of Hb(O_2) proceeds by an NO dioxygenation (NOD) mechanism [307]. The NOD reaction involves capture of NO in the distal pocket of HbO_2, where it reacts with bound O_2 to form an Fe(III) *cis*-peroxynitrite transition state, $Fe(III)^+(OONO^-)$, that immediately isomerises to an $Fe(III)^+(NO_3^-)$ complex [308–310]. Both O atoms of the bound O_2 are incorporated into the NO_3^-, as determined by ^{18}O labelling, confirming the NOD mechanism [311]. The transient $Fe(III)^+(NO_3^-)$ intermediate dissociates in < 1 ms at neutral pH, but can be observed spectrophotometrically at high pH [308]. An alternative pathway proceeding by reaction of non-coordinated O_2 in the distal pocket of HbFe(II)(NO), termed O_2 nitrosylation, has been proposed [312], but problems with this mechanism have been raised by Gardner [17]. The NOD mechanism is consistent with kinetics of NO reactions with vertebrate Hb/Mb and bacterial FHbs, and is likely to be a general mechanism for NO reaction with Hb over a wide range of O_2 concentrations in vivo.

In an authoritative review of the NOD mechanism, Gardiner [17] identifies several key features of Hbs that promote NOD activity as follows. (1) High O_2 affinity promotes the NOD reaction, which proceeds through the O_2 ligated haem, and mutations that reduce O_2 affinity increase NO-inhibition of the NOD reaction. Hbs for which the physiological importance of NOD enzyme activity has been demonstrated, have O_2 binding affinity orders of magnitude higher than Hbs that function in O_2 transport. (2) Sufficient space is required in the distal haem pocket to capture both O_2 and NO ligands efficiently and allow formation of the Fe(III) *cis*-peroxynitrite transition state, and these structural features have been conserved in evolution of FHbs and vertebrate Hbs. (3) The radical nature of the $Fe(III)^+(O_2^-)$ centre (Section 3.5) may promote rapid reaction with NO through radical pairing. (4) A mechanism for univalent reduction of the ferric Hb back to the starting ferrous form is needed for catalytic turnover. Identifying an effective reduction pathway in vivo is essential before assigning a NOD function to any particular Hb because virtually all Hbs can demonstrate NOD activity in vitro under suitable assay conditions [251].

In bacterial FHbs, Fe(II) haem is regenerated by the C-terminal oxidoreductase domain in order to maintain NOD enzyme turnover, providing incontrovertible evidence for an enzymatic function in these proteins. In mammalian Hb, NOD activity (together with autooxidation) generates Fe(III) metHb, and this is reduced back to functional Fe(II) Hb by cytochrome b_5, which, in turn, receives electrons from cytochrome b_5 reductase (also called metHb reductase). Both FHb and cytochrome b_5 reductase are flavin-containing enzymes that receive reducing equivalents from NADPH. Thus the overall NOD reaction is

$$2NO + 2O_2 + NAD(P)H \rightarrow 2NO_3^- + NAD(P)^+ + H^+ \quad (1)$$

The flavin adenine dinucleotide has an important feature, in that it can exist in an oxidised (FAD), one-electron reduced (semiquinone; ·FADH) or fully reduced ($FADH_2$) state, and can therefore act as mediator between single-electron reduction of Fe(III) haem and the two-electron oxidation/reduction of NADPH/$NADP^+$ [313]; two Fe(III) Hb reduction cycles must occur for every NADPH turned over.

The above paragraphs details reactions of ferrous Hb species with NO. An interesting feature of NO is that, unlike CO and O_2, NO can also bind to Fe(III) haems, albeit with much lower affinity (k_{on} $1.5 \times 10^5\ M^{-1}\ s^{-1}$; K_D 7×10^{-5} M for Mb) [314]. The ferric nitrosyl Fe(III)(NO) complex has some Fe(II)(NO^+) character (see [315]). Here, NO^+ is isoelectronic with CO and the Fe—N—O unit adopts a linear structure, like Fe—C—O (and unlike the bent ferrous Fe(II)(NO·) complex). The Fe(II)(NO^+) character also confers reactivity towards nucleophiles. An example is the reductive nitrosylation of metMb (or metHb) by excess NO inder anaerobic conditions to form nitrite:

$$[Fe(III)(NO) \leftrightarrow Fe(II)(NO^+)] + OH^- + NO \rightarrow HbFe(II)(NO) + NO_2^- + H^+ \quad (2)$$

In this reaction, the nucleophilic OH^- reacts with Fe(II)(NO^+) to form an Fe(II)(ONOH) intermediate with a bimolecular rate constant of $\sim 3 \times 10^2\ M^{-1}\ s^{-1}$ for Mb and $\sim 3 \times 10^3\ M^{-1}\ s^{-1}$ for Hb [316]. Chemical and biochemical features of reductive nitrosylation are reviwed by Ford [315]. A ferric nitrosyl haem is also an intermediate in the nitrite reductase reaction that converts NO_2^- to NO in bacterial denitrification (essentially the reverse of reductive nitrosylation) [317]. It has long been known that deoxygenated HbFe(II) can react with nitrite under anaerobic conditions to form Hb(II)NO and met(III)Hb by the following linked reactions [318].

$$HbFe(II) + NO_2^- + H^+ \rightarrow HbFe(III) + NO + OH^- \quad (3)$$

$$HbFe(II) + NO \rightarrow HbFe(II)(NO) \quad (4)$$

The reason for highlighting these reactions is that they may be important for the biological function of some Hbs, such as in metabolism of nitrogen oxides under anoxic conditions by the nitrate reductase reaction [319], and they are also implicated in serveral putative mechanisms of NO signalling by mammalian Hb and Mb, as described in Section 5.4.

Several other oxides of nitrogen are of pharmacological interest; one of these is nitroxyl (HNO, also called azanone). Whether HNO is produced endogenously in mammals is controversial, but conversion of exogenously supplied HNO to NO is chemically plausible and may account for some of its biological effects. Nevertheless HNO has distinct pharmacology suggesting some unique biological chemistry [320]. Like NO, HNO is reactive to both Fe(II) and Fe(III) haems, and promotes similarly fast oxidation of Mb(O_2) to metMb [321]. One potentially important difference is that, unlike NO, HNO reacts directly and rapidly

with thiols (10^6 to 10^7 M^{-1} s^{-1}) [321].

Finally, hydrogen sulfide (H_2S) reacts with Hb(O_2) and ferryl HbFe (IV)(O) species to generate sulfhaems, which have a sulfur atom incorporated into the haem pyrrole B leading to defective O_2 binding and clinical cyanosis [322]. Nevertheless some organisms living in sulfur rich environments, such as hydrothermal vents and mangrove swamps, form symbiotic relationships with sulfide-oxidising γ-proteobacteria and produce globins that transport H_2S. The clam, *Lucina pectinata*, has three Hbs, two that transport O_2, and a third, HbI, which binds H_2S with high affinity and releases it by slow dissociation from the Fe(III) haem or by haem reduction [323].

5.3. Bacterial and yeast FHbs, and uni-cellular single-domain globins (SDgbs)

FHbs were the first bacterial Hbs to be described [324,325]. They contain three domains—an N-terminal globin domain, a central FAD-binding domain and a C-terminal NADP-binding domain; the FAD and NAD binding domains combine to form a conserved ferredoxin reductase fold [104]. Residues of the haem pocket implicated in NOD activity are highly conserved across FHbs, as are residues surrounding the flavin cofactor that play roles in electron transfer from NADP [326]. FHbs from *E. coli* [251,327], *Salmonella enterica* [328], *Salmonella typhimurium* [329], *Ralstonia entropha* [330], *Staphylococcus aureus* [331], *Bacillus subtilis* [332], and *Saccharomyces cerevisiae* (yeast) FHb [333,334] have been shown to protect their host organisms from nitrosative stress in gene knockout studies, considered the gold standard for assigning biological function [16]. In *E. coli*, expression of HMP is regulated by the transcription factor FNR (fumarate and nitrate reduction) [335], which is a master regulator controlling response to anoxia and oxidative and nitrosative stress [307]. In a number of cases, resistance to nitrosative stress conferred by FHb contributes to pathogen virulence [329,331,336].

An unusual feature of some FHbs is the ability to accommodate the aliphatic chain of a fatty acid into the haem pocket. The FHb from *Ralstonia eutropha* (formerly *Alcaligenes eutrophus*; a soil and water bacterium of interest in bioremediation due to its ability to decompose chlorinated aromatics) was isolated with a molecule of phosphatidylethanolamine or phosphatidylglycerol in the haem pocket [337]. Instability of *R. eutropha* FHb in the absence of lipid suggests a constitutive complex [158]. HMP from *E. coli* has only been crystallized in the absence of lipid [157], but, nevertheless, binds to unsaturated or cyclopropanated fatty acids in solution with nanomolar affinity [338]. Resonance Raman and x-ray absorption fine structure (EXAFS) suggest lipid-bound HMP has a 6-coordinate high-spin iron centre, which the authors attribute to an unusual coordinate bond donated by π electrons from an unsaturated moiety of the lipid [339]. The lipid alters kinetics of CO/O_2 binding, although the significance of this is not clear [326]. It has been suggested that the lipid interaction serves to colocalise FHb with the respiratory chain complexes in the membrane [326]. Reduction of membrane lipid hydroperoxides has been demonstrated for HMP [340], suggesting a role in reversing oxidative membrane damage. In contrast, FHb from the yeast, *Saccharomyces cerevisiae*, appears not to bind any lipid [105]. Taken together, the data suggest diversification of function among FHbs from different groups of organisms. FHbs from *S. cerevisiae* [105] and *R. eutropha* FHb [158] have been crystallized with a variety of bulky azole ligands (potent FHb inhibitors [341]) in the haem pocket, and comparisons of these structures with apo and lipid-bound structures has led to the hypothesis that the NAD, FAD, and Hb domains undergo relative motions during the catalytic cycle, perhaps to regulate electron transfer between the NAD and FAD cofactors [158].

Turning to the single domain Hbs, a NOD function for SDgb from *Campylobacter jejuni* (Cgb) has been demonstrated by gene deletion [342], biochemistry [107,181] and expression analyses [342,343]. The physiological role of SDgb from *Vitreoscilla stercoraria* (VHb) has not yet been conclusively demonstrated (the organism is not amenable to genetic modification), but VHb fused with a FHb reductase domain has been extensively used in biotechnology applications to protect against nitrosative stress [344,345]. Although evidence that SDgs function generally as NOD enzymes is emerging, an important piece of the puzzle—identifying the reductase for SDgb proteins in vivo—remains to be solved. Many bacterial trHbs are also likely to be NOD enzymes [346]. A role in nitrosative stress response has been demonstrated genetically for trHbs from *Synechococcus* [347], *Chlamydomonas reinhardtii* [348,349], *Mycobacterium* species [350,351] and the antarctic marine bacterium *Pseudoalteromonas haloplanktis* [352].

5.4. Reactions of mammalian Mb and Hb with NO

The finding that Hb(O_2) is a potent inhibitor of venous and arterial relaxant responses provided key evidence in the original discovery that NO is the endothelium-derived relaxing factor [353]. It is now accepted that NO is a central regulator of blood flow, and that Hb inside RBCs plays a central role in destroying NO through the NOD reaction, thereby providing a sink for NO that is produced by endothelial NO synthase (eNOS) and preventing NO reaching toxic levels [354]. Whilst the lifetime of NO inside the RBC is < 1 μs, physical barriers to NO diffusion such as the RBC membrane and the unstirred layer proximal to the membrane, as well as flow effects that draw RBCs away from the endothelium towards the centre of the vessel lumen, all combine to increase the lifetime of NO to the ms timescale in the lumen wall, and allow NO to accumulate to physiologically active concentrations (see [305,355] and references therein). The importance of this compartmentalisation is dramatically demonstrated by the rapid increase in blood pressure that occurs, due to consumption of NO in the endothelium, when Hb is released into plasma under pathological conditions [356]. Several experiments have demonstrated that NOD is the primary mechanism of NO removal in vivo. First, human subjects breathing NO experienced a rise in metHb and nitrate levels in stoichiometric amounts, as expected for NOD reaction, with minimal levels of alternative reaction products [357]. Second, transfusion of recombinant Hb mutants into rabbits reveals a linear relationship between NOD activity, determined spectrophotometrically in vitro, and the rise in arterial blood pressure in vivo [309].

In addition to the established paracrine function of NO discussed above, evidence is emerging for endocrine signalling by nitrogen oxides in a number of physiological systems, including the cardiovascular system. Due to the short half-life of NO, endocrine signalling would require conversion of NO to another chemical form and back to NO at the target tissue; two 'transportable' nitrogen oxides that have received considerable attention from the field are nitrite (NO_2^-) and S-nitrosothiols (R–SNO), as outlined briefly in the following paragraphs.

In humans, nitrite comes from diet, from reduction of nitrate by microorganisms (e.g., crypts of tongue) or from spontaneous oxidation of NO, which is generated by endogenous NOS enzymes [358]. Endogenous production accounts for the major fraction of circulating nitrite under normal circumstances. Nitrite has vasodilatory activity, and a mechanism has been proposed whereby nitrite is converted to NO by nitrite reductase reaction with deoxyHb [359,360]. Enhancement of the reaction under reduced oxygen saturation and acid conditions suggested this could operate under allosteric control [360–362]. A major challenge to the nitrate reductase concept is that any NO produced would immediately be consumed by the NOD reaction or remain tightly bound to HbFe(II), and would not escape the RBC. An alternative suggestion is that nitrite and NO react in some combination with metHb to generate N_2O_3, which can diffuse out of the RBC and decompose to liberate NO in the vessel wall. The ferric nitrosyl species might form first and react with the nucleophilic NO_2^- [315,363–365].

$$[\mathrm{Fe(III)(NO)} \leftrightarrow \mathrm{Fe(II)(NO^+)}] + \mathrm{NO_2^-} \rightarrow \mathrm{HbFe(II)} + \mathrm{N_2O_3} \quad (5)$$

Or, alternatively an [Fe(III)(NO_2^-) ↔ Fe(II)–NO_2·] species forms first and reacts with ·NO in a radical-radical type interaction

[363,366]. In any case, metHb is a minor (≤ 1%) fraction of total Hb and any reactions involving NO have to compete with the diffusion rate limited reaction with HbFe(II)(O_2) or HbFe(II); thus, the bioactive role of nitrite in regulating blood flow is still not understood [367].

S-nitrosothiol is a second form of transportable 'NO' that has generated a large amount of interest. S-nitrosation is a modification of thiol (R–SH) groups in proteins (cysteine residues), and low molecular weight components (notably glutathione) to form S-nitrosothiol groups (R–SNO; more accurately represented as a combination of three resonance structures see [368]). A model proposed by the Stamler group is that NO binds initially to HbFe(II) and is subsequently transferred to βCys(93)F9 upon oxygenation of tetramers in the lungs; then, as Hb converts to the T state at lower O_2 tension in the microvasculature, the quaternary change in Hb exposes βCys(93)F9 to solvent favouring transfer of the nitroso group to the thiol of another protein or small molecule that can then move out of the RBC, so avoiding the problem of NO inactivation by the NOD reaction [369–374]. This mechanism, however, is controversial on a number of counts. First, other workers found no evidence for a direct transfer of NO from haem to βCys(93)F9 upon oxygenation [365,375,376]. One of the thorny issues is that ≤ 0.1% of Hb βCys(93)F9 sites are nitrosated leading to difficulty in accurately measuring changes in this micropopulation [377]. Second, an allosteric mechanism for regulating the migration of NO from the nitrosyl haem to βCys(93)F9 has not been established.

Nevertheless, S-nitrosation is emerging as a general mechanism of redox based signalling [378] and the biochemistry of S-nitrosation has been extensively studied [321,379]. Early work showed that S-nitrosation of cysteine and glutathione by solutions of NO required the presence of O_2 [380–382], suggesting that oxidation of NO or the thiol group is necessary. In aerobic solution, NO is oxidised to N_2O_3 which has NO^+-like activity and reacts readily with thiol, which is a strong nucleophile.

$$N_2O_3 + RSH \rightarrow RSNO + NO_2^- + H^+ \quad (6)$$

The alternative is one-electron oxidation of the thiol to a thiyl radical, which can pair with the ·NO radical

$$RSH \rightarrow RS\bullet + e^- + H^+ \quad (7)$$

$$RS\bullet + \bullet NO \rightarrow RSNO \quad (8)$$

A third reaction—direct reaction of ·NO with thiol, followed by oxidation of the RSHNO· intermediate—has been proposed [304], but has been considered by others as less likely under physiological conditions [321,379]. Some groups have postulated that intramolecular S-nitrosation in Hb involves coupled oxidation/reduction of the thiol/Fe(II)(NO^+) haem [364,383,384]. Others favour nitrosation of βCys(93)F9 via reaction with N_2O_3 generated via Reaction 5 [315,364,365].

Whatever the mechanism, genetic evidence supports a physiogical role for βCys(93)F9, which is notable as one of only three residues conserved across all mammalian and bird Hbs (the others being HisE7 and PheCD1), in cardiovascular function. Experiments on mice with RBCs expressing human Hb showed that a βCys(93)F9 → Ala mutation caused no gross changes in systemic and pulmonary arteriole blood pressure [385], but did show defects in peripheral blood flow under normoxic and hypoxic condutions [386] and increased the severity of ischemic injury and mortality in models of myocardial infarction [387] consistent with a role in NO signalling.

In summary, whilst there is evidence that nitrite and S-nitrosation products have biological activity, the physiology of NO and Hb is dominated by the diffusion rate-limited NOD reaction of NO with Hb (O_2) and autooxidation of HbFe(II)(NO) species, as described in the opening paragraphs of Section 5.2. To conclude this section, it has recently been discovered that Hb and Mb are expressed at low levels in a variety of tissues outside RBCs and muscle, where they may have roles in NO signalling (see [17,246]). Examples include erythrocyte Hb chains expressed in neurons and endothelial cells of blood vessels [388–393]. As one example, Hb α subunit is expressed in arteriole endothelial cells, where it regulates NO signalling to smooth muscle in redox sensitive manner consistent with a NOD activity [389].

6. Hbs in O_2 sensing

The two-domain globin GCSs, sensor single-domain globins (SSDgbs), and more distantly related Pgbs, form a family of sensor Hbs present in ~30% of globin-containing bacterial and archaeal genomes [51,394]. Of these, the GCSs have been the most widely studied. GCSs comprise an N-terminal Hb domain and a variable C-terminal signalling domain [395,396].

The structures of the Hb domains from several GCSs have been determined, together with ligand binding and enzymatic activities (reviewed by [18]), yet the precise roles of SDGs in vivo are still poorly understood due to a lack of genetic and physiological studies [16]. Homology of the C-terminal GCS domain to proteins of known function is currently the best guide to likely physiological roles of GCSs. Thus, HemAT from the archaeon *Halobacterium salinarum* and HemAT from the Gram-positive bacterium *Bacillus subtilis* carry a C-terminal methyl accepting chemotaxis protein (MCP) domain, suggesting they sense O_2 in order to trigger an aerotactic response [397,398]; a model for O_2 signal transduction has been proposed for these proteins [397]. A globin coupled histidine kinase from *Anaeromyxobacter* sp. shows histidine kinase activity in response to O_2 or CO binding [399]. A number of GCSs have a C-terminal diguanylate cyclase domain and produce the bacterial second messenger, bis-(3′-5′)-cyclic diguanosine monophosphate (*c*-di-GMP), to regulate biofilm formation, in response to O_2 binding [400,401]. Histidine kinase and *c*-di-GMP represent two major second-messenger signalling pathways in bacteria. Interestingly a new class of Hb coupled to adenylate cyclase has recently been discovered in the eukaryotic parasite *Leishmania* [402] and Gram-negative bacterium *Vibrio brasiliensis* [403]; these proteins function in oxidative stress responses and appear to be structurally related to a non-haem globin involved in stress signalling in Gram-positive *B. subtilis* [69].

7. The role of human RBC Hb in O_2 transport

7.1. Natural genetic variants of RBC Hb

Since Linus Pauling and colleagues [404] described the basis of sickle cell anaemia as a specific chemical defect in Hb caused by a change in a single allele—the first 'molecular disease'—insight into almost every feature of Hb molecular function has come from study of natural Hb variants and their associated clinical consequences (reviewed [126]). There are over 1000 mutations in Hb genes that have been described [405], largely giving rise to single amino acid changes, most of which are catalogued on the Globin Gene Server (http://globin.cse.psu.edu) [406]. Although the clinical correlates of natural Hb sequence variation are beyond the scope of this review, a brief mention is made of HbS (βGlu(6)A3 → Val; the sickle cell mutation of Pauling) because it is the most common and medically important Hb variant. The frequency of the β^S allele is attributed to positive genetic selection because it confers survival advantages against malaria [407]. The βGlu(6)A3 → Val substitution switches a negatively charged side chain for a hydrophobic one, which permits deoxygenated Hb in the T quaternary structure to form polymers that disrupt the architecture and flexibility of the RBC, causing multitude of biochemical and physical changes, including the eponymous sickle cell shape. The process of polymerisation and cell deformation is complex; Frank Ferrone has made the major contribution to understanding the physical mechanisms (see for example, [408]). The pathological outcomes of Hb polymerisation are: (1) deformed cells block vessels in the microcirculation causeing ischemia and re-perfusion injuries, and (2) RBCs undergo lysis, resulting in haemolytic anaemia. The pathological, clinical and epidemiological factors have recently been succinctly summarised by Gladwin and

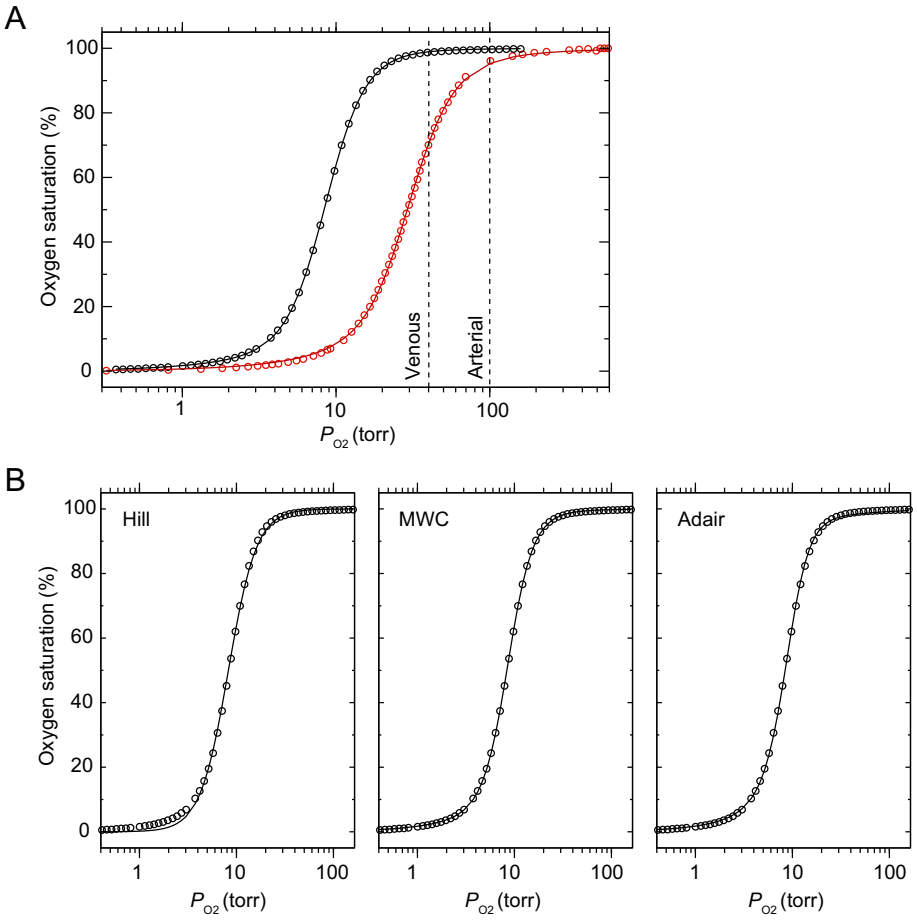

Fig. 6. O_2 saturation curves of RBC Hb. (A) Curves are shown for purified haemoglobin (black circle) in the absence of organic phosphates (1.2 mM Hb, 0.1 M potassium phosphate, pH 7.4, 25 °C), data taken from Imai [420], and for whole fresh blood (red circles) that contained physiological levels of 2,3-DPG (0.89 μmol 2,3-DPG per μmole Hb tetramer) and CO_2 (P_{CO2} = 40 Torr; pH 7.4, 37 °C), data taken from Winslow et al. [556]. The saturation function of the Monod, Wyman, Changeux (MWC) model (Eq. (2) from [415]) was fit to the data using a standard unweighted Levenberg-Marquardt procedure (solid lines). The Hill equation (main text) was also fit to the data (not shown). The derived MWC and Hill parameters for purified Hb in the absence of allosteric effectors were: $L = 7.66 \times 10^6$; $c = 2.578 \times 10^{-3}$; $1/K_T = 58.5$ Torr; $P_{50} = 8.26$ Torr; Hill coefficient (n) = 3. The derived parameters for whole blood in the presence of allosteric effectors were: $L = 1.558 \times 10^4$; $c = 1.66 \times 10^{-2}$; $1/K_T = 150.6$ Torr; $P_{50} = 28.8$ Torr; $n = 2.52$. Typical arterial and venous P_{O2} is 100 and 40 Torr, respectively. (B) A comparison of fitting the equations of Hill (two parameters), MWC (three parameters), and Adair (four parameters) to saturation data for purified Hb as shown in A. Note that the Hill equation deviates considerably from the data, particularly at low P_{O2}. (For interpretation of the references to colour in this figure legend, the reader is referred to the web version of this article.)

colleagues [407].

7.2. Cooperative binding of O_2 to Hb

The solubility of O_2 in water (~0.3 mM at 20 °C and 1 atm pressure) is insufficient to achieve full tissue oxygenation in most animals. Consequently, vertebrates have evolved mechanisms to store (Mb) and transport (Hb) O_2. The concentration of Hb tetramers in RBCs is typically ~5.2 mM (equivalent to ~21 mM haem) and RBCs typically account for 45% of blood volume, giving a theoretical O_2 concentration of ~9 mM. The level of O_2 in air is 21% by volume, which corresponds to ~8.75 mM at 1 atm pressure and 20 °C (one mole of gas under these conditions occupies 24.0 l by the ideal gas law). Thus, Hb raises the O_2 concentration in blood to the same level as in air. A plot of O_2 saturation against the partial pressure of O_2 (P_{O2}) has the characteristic sigmoidal shape (Fig. 6) that was first described by Christian Bohr in 1903 [409] and follows a simple empirical relationship, described by A. V. Hill in 1910 [410]

$$Y = \frac{P_{O2}{}^n}{(P_{50}{}^n + P_{O2}{}^n)}$$

In this equation, Y is the fraction O_2 saturation, and P_{50} is the value of P_{O2} at which 50% of the O_2-binding sites are occupied. The factor, *n*, called the Hill coefficient, measures cooperativity—the tendency for binding (or dissociation) at one site to promote binding (or dissociation) at all other sites. Positive cooperativity ($n > 1$) ensures a large release of O_2 over the relatively small change in P_{O2} between the lungs (P_{O2} ~100 Torr) and the venous blood (PO_2 ~40 Torr), as shown by dashed lines in Fig. 6A. Although the Hill equation gives no insight into *how* cooperatively is achieved, it is still widely used as a convenient description of O_2 affinity and cooperativity for different Hbs. However, as shown in Fig. 6B, the Hill equation, with only 2 fitted parameters, fails to accurately capture the O_2 saturation profile, particularly at low P_{O2}.

Quantitative models that describe cooperative O_2 binding and give insight into the molecular mechanisms started with G. S. Adair, who, in 1925, showed that Hb contained four binding sites for O_2 [411]. The binding model of Adair, with four binding constants, accurately captures the complete O_2 saturation curve (Fig. 6B). The development and rigorous testing of models, including the sequential binding models of Adair [412] and, later, Koshland, Némethy and Filmer (the KNF model) [413], has been the subject of excellent reviews [414–417]. In particular, the Monod, Wyman and Changeux (MWC) 'two-state concerted' model [418], based on the concept of allostery proposed by Monod and Jacob in 1961 [419], has endured as a theoretical basis for understanding cooperative O_2 binding. Key features of the MWC model, drawn on in later sections are:

- Hb adopts *two* alternative and distinct quaternary structures, termed the tense (T) and relaxed (R) states that are in equilibrium. In the absence of O_2, the T quaternary conformation is much more stable than R ($[T_o] / [R_o] \gg 1$, where $[T_o]$ and $[R_o]$ are the molar concentrations of the unliganded T and R states)
- Quaternary and tertiary conformations are strictly coupled. In the T state, *all four* subunits have a tertiary (*t*) conformation with low O_2 affinity (association equilibrium constant K_T), whereas in the R state, *all four* subunits have a tertiary conformation (*r*) with high O_2 affinity (K_R)

Because O_2 has higher affinity for empty sites in the R quaternary state, the T ↔ R equilibrium must shift towards R with the addition of O_2, according to Le Châtelier's principle. The basis for cooperativity is

that the T ↔ R quaternary switch requires a *concerted* switch of *all* subunits to low or high affinity. In the MWC model, it is important to note that O_2 binding to an individual site does *not* increase the O_2 binding affinity of other sites within that tetramer, other than to increase the probability of a switch to the R quaternary structure; in other words, there is no cooperativity *within* the T or R quaternary states. The MWC model gives quantitative fit to the O_2 saturation curve generated under a given set of solution conditions, using just three independent parameters L, K_T and K_R. Fitted values for the MWC parameters can be interpreted as follows, with reference to typical data obtained for highly purified Hb (Fig. 6A, black data points and fitted curve; data from [420]). The value L is the equilibrium constant between the R and T quaternary states with zero O_2 molecules bound ($L = [T_o] / [R_o]$). In the current example, $[T_o] / [R_o] = 7.66 \times 10^6$, showing that $[R_o]$ is negligible. The values for K_T and K_R are typically presented as $c = K_T / K_R$ and $1 / K_T$. In the current example, $c = 2.6 \times 10^{-3}$, showing that affinity of T is $\sim 10^3$-fold lower than the affinity of R. Also, for every n O_2 bound (for $0 \le n \le 4$ sites) the quaternary equilibrium constant increases by a factor c^n; thus, with all four O_2 sites occupied the value of $[T_4] / [R_4] = L{\cdot}c^n = 3.4 \times 10^{-4}$, in other words $[R_o]$ is now negligible. These parameters are significantly modulated by pH, salt, organic phosphate concentration and temperature [421–423], as demonstrated by displacement of the red and black curves in Fig. 6, and discussed in following sections. The parameter values presented in this paragraph are for illustrative purposes, and the reader is encouraged to consult the orginal works (e.g., references above) where more sophisticated fitting, such as weighting based on experimental errors will be employed.

An extension of the MWC model, proposed by Eaton, Henry and coworkers and called the tertiary two-state (TTS) model, successfully predicts kinetics, as well as thermodynamics, of O_2 binding (Section 7.9) and also accurately models O_2 binding globally across different conditions of pH, temperature and allosteric effectors [415,416,424,425]. The distinguishing feature of the TTS model is that the two tertiary subunit conformations, *t* and *r*, exist in equilibrium within *both* T *and* R quaternary states. In other words, tertiary and quaternary structural changes are not strictly coupled as they are in the original MWC model. Instead, T quaternary and *t* tertiary structures are mutually stabilising, as are the R and *r* structures, thus cooperativity still arises from a shift from T to R in the presence of O_2, according to Le Châtelier.

7.3. Hb is allosterically regulated by H^+, CO_2 and 2,3-diphosphoglycerate

In addition to positive allosteric action of O_2, other physiologically important allosteric effectors lower O_2 affinity. In his 1904 study, Bohr found that CO_2 lowered O_2 binding affinity [409]; this response, which is due to decreasing pH, is called the Bohr effect. CO_2 arising from respiration is converted to carbonic acid ($CO_2 + H_2O \leftrightarrow H_2CO_3$) inside erythrocytes by carbonic anhydrase. Carbonic acid dissociates to bicarbonate (HCO_3^-) and H^+. Bicarbonate is released back into the plasma in exchange for Cl^-, whereas H^+ accumulates inside erythrocytes. This is the primary mechanism for CO_2 transport—bicarbonate in the serum accounts for 70–80% of CO_2 transport, with another 15–20% of CO_2 being carried as carbamino Hb (by reaction of CO_2 with the terminal amine groups of α and β chains)[426–428], and the remaining ~7% CO_2 is transported by dissolution. In the lungs, the above reactions are reversed. Details of the physiological interplay between O_2 and CO_2 transport have been reviewed recently [429]; for the purpose of the present review, however, we are interested in how H^+ (and also Cl^-) act as allosteric inhibitors of Hb through the Bohr effect.

The alkaline Bohr effect describes the decrease in O_2 affinity with a decrease in pH in the range pH 7.9–6.3 and is defined as $\partial \log(P_{50})/\partial pH$. Under physiological conditions (0.1 M Cl^-, pH 7.4) the magnitude of the Bohr effect is − 0.5 [430], which also corresponds to ~0.5H^+ released per O_2 bound [431]. The Bohr protons come from ionisable groups in Hb, for which the affinity for H^+ is greater in the unligated state compared to the O_2 ligated state; in other words, the pK of the ionisable group is significantly increased in the unligated state of Hb. On chemical grounds, His side chains or the terminal amino groups are the most likely sources of the Bohr protons. Ho, Lukin, and colleagues measured H^+ dissociation by NMR to determine the pK of all 26 surface His side chains in T and R. They found that the pK of βHis(146)HC3 increases from 6.4 in the ligated R state to 7.9 in the unliganded T state, and accounts for 60% of the Bohr effect [432] consistent with predictions of Perutz [433] and Kilmartin and Wootton [434]. The alkaline Bohr effect is reduced by approximately 50% in the absence of Cl^-, and virtually all of the chloride-independent contribution of the Bohr effect occurs through βHis(146)HC3 [432]. The chloride-dependent Bohr effect is still not completely understood; there is no consensus about the binding sites for Cl^- and the effect is more likely to arise from a network of electrostatic interactions involving a large number of residues, which together stabilise additional H^+ binding in the T state [431]. A more extreme version of the Bohr effect, called the Root effect [435] is of physiological importance in many species of bony fish, but is still poorly understood at the structural level (for example, see [436]).

In addition to CO_2 and H^+, organic phosphates also regulate (lower) the affinity of vertebrate Hb. In some species, such as human and horse, 2,3-diphosphoglycerate (2,3-DPG), is an allosteric inhibitor [437,438]; in the absence of 2,3-DPG Hb affinity remains too high to effectively release O_2 in the tissues (Fig. 6A, compare black and red traces). 2,3-DPG is produced in mammalian RBC as a secondary metabolite of glycolysis and in human RBCs is ~5 mM (approximately equimolar with Hb tetramers). Other mammalian species, such as cattle and sheep, have naturally 'low affinity' Hbs with low sensitivity to 2,3-DPG. Typically, Hbs with high intrinsic oxygen affinity have P_{50} values in the range 4–6 Torr, whereas low affinity Hbs have P_{50} values in the range 10–20 Torr, as measured in conditions of 0.05 M Bis-Tris, 0.1 M NaCl, pH 6.5–7.5, at 20–25 °C [439]. Inositol pentaphosphate (IPP) is the corresponding allosteric regulator of Hb in birds, and ATP or GTP performs this function in reptiles and fish. In humans, 2,3-DPG concentration increases in response to prolonged hypoxia over hours or days during acclimatisation to altitude, or anaemia, in order to increase O_2 delivery [429]. In pregnancy 2,3-DPG can increase up to 30%, which, coupled with a relative insensitivity of foetal Hb ($\alpha_2\gamma_2$) to 2,3-DPG [440], facilitates O_2 transport to the foetus.

7.4. Quaternary interactions mediate cooperative O_2 binding

The first structures of Hb, solved by Max Perutz and colleagues at 5.5 Å, showed that Hb is a dimer-of-dimers, with two equivalent α·β dimers arranged with a two-fold rotational symmetry [3,441] (cover, this issue). The dimer-of-dimers is realised in solution as the equilibrium αβ + αβ ↔ (αβ)·(αβ). Within the (αβ)·(αβ) tetramer, α makes two different contact interfaces with β, one within the permanent αβ dimer, designated the $\alpha_1\beta_1$ interface, and a second across the dimer-of-dimers (allosteric) interface, designated $\alpha_1\beta_2$ (there are, of course, symmetry related $\alpha_2\beta_2$ and $\alpha_2\beta_1$ interfaces). The 5.5-Å resolution data obtained by Perutz showed that the two permanent αβ dimers rotate by 15° with respect to one-another in the liganded [3] compared to unliganded [441] tetramer, and, in doing so, narrow the separation between the β subunits in liganded Hb. In this quaternary transition, Perutz saw a connection with the thermodynamic R (high affinity) and T (low affinity) states from MWC model.

At this point it is important to note that proteins are flexible entities and that a crystal structure can only represent a subset of the conformational ensembles present in solution. Although the majority of Hb structures determined by crystallography are highly similar to the original 'T' or 'R' structures, a number of liganded structures with different rotations of the αβ dimers have been crystallized [442,443]. A liganded 'R2' structure with αβ dimer rotation of ~23° relative to the T structure [442] is represented by at least 14 structures in the Protein Data Bank [444]. It was proposed that the R2 structure represented the true end

point for the quaternary transition in solution [445], but it was shown later that R and R2 have the same high O_2 affinity [446]. Using other structural methods, namely NMR [447–453] and wide-angle X-ray scattering (WAXS) [454], studies by Chein Ho and others indicate that the time-averaged solution structure of liganded Hb is unlikely to be identical to crystallized structures (reviewed in [431]). Most recently, the Cryo-EM structure of Hb(CO) has been determined at a resolution of 2.3 Å, and this is highly similar to the R2 crystal structure [455]. The unifying view is that the thermodynamic R state corresponds to an ensemble of structures in a relatively flat energy landscape, rather than a single unique structure [431,456,457]. Unlike dimer rotation angles, specific side chain contacts at the $\alpha_1\beta_2$ interface (described in [458,459]) are largely conserved in liganded Hbs crystallized in different R-like states (R, RR etc.) implying that these $\alpha_1\beta_2$ intermolecular contacts have greater relevance to the thermodynamic R state than dimer rotation angles [457,460].

Early studies showed that quaternary interactions across the $\alpha_1\beta_2$ interface lower the intrinsic O_2 affinity of haems in the T state. This is clearly demonstrated by the fact that isolated Hb α and β monomers [461] and permanent αβ dimers [462] bind O_2 non-cooperatively and with high affinity similar to that of R state tetramers. In fact, as first noted by Wyman [463] and extensively explored by Ackers and co-workers (reviewed [464–467]), the αβ + αβ ↔ (αβ)·(αβ) binding equilibrium is thermodynamically linked to O_2 saturation. Thus, the dimer-tetramer affinity is much higher for deoxy Hb ($K_A \sim 4 \times 10^{10}\ M^{-1}$) than for fully ligated Hb(O_2) ($K_A \sim 9 \times 10^{5}\ M^{-1}$) [466,468–470] ($K_A$ values given for the condition 0.1 m Tris.HCl, 0.1 M NaCl, 1 mM EDTA, pH 7.4, 21.5 °C). In contrast, the association constant for α·β heterodimerisation ($K_A \sim 5 \times 10^{11}\ M^{-1}$) is independent of O_2 ligation state [471], indicating the absence of allosteric transitions across this interface. The free energy change for binding $4O_2$ to two αβ dimers is -33.2 kcal mol^{-1}; for binding $4O_2$ to an (αβ)·(αβ) tetramer it is -26.9 kcal mol^{-1}; the difference is 6.3 ± 0.2 kcal mol^{-1} [465,466], which is the (unfavourable) free energy that must be supplied from O_2 binding in order to switch from T to R conformation and is also called the cooperative free energy of binding. It is worth noting an alternative definition of cooperative free energy, also frequently used, as the difference in free energy between binding of the first and fourth O_2 molecule; this can be obtained directly from a transformation of the Hill plot (given knowledge of the intrinsic binding affinities of α and β subunits) [472] and has a value of 3.7 kcal mol^{-1} measured under the same conditions as above.

7.5. Structural features that distinguish high affinity R from low affinity T

Based on his structures of liganded [473,474] and unliganded horse Hb [475] at 2.8 Å-resolution, together with knowledge of synthetic porphyrins from the work of L. J. Hoard [72–75], Perutz proposed his stereochemical mechanism for cooperative effects in Hb. In the stereochemical mechanism, interaction between the haems (cooperativity) results from a switch between two (coupled tertiary and quaternary) structures, where one structure (tertiary *t* in T) resists the stereochemical changes required (see Section 3.3) by O_2 binding (therefore has low affinity), and one structure (tertiary *r* in R) does not (therefore is high affinity) [430,458]. The structural features that characterize the unliganded T [457,475,476] and liganded R states [457,473,474,477] have been reviewed (for example, see [430]) and some key points are outlined in the following paragraph.

First, structural changes are restricted to the 'allosteric core', which includes the haem and contiguous structural elements, including HisF8, the F helix and the FG corner (the FG corner sits at the allosteric $\alpha_1\beta_2$ interface) [458,459,478–481]. Second, the T and R quaternary structures are characterised by different sets of side chain interactions at the allosteric $\alpha_1\beta_2$ interface (as introduced in the previous section). The FG corners from Hb α and β subunits both contribute to the allosteric interface but behave quite differently. The interfacial contacts made by αFG corners change very little during the quaternary transition, and hence these are termed 'hinge' contacts; whereas, βFG makes different set of side chain contacts in T and R, and so these are termed 'switch' contacts [430]. There are no structural differences at the $\alpha_1\beta_1$ interface detectible from x-ray diffraction studies, suggesting each αβ dimer behaves as a single unit during the allosteric transition. Third, ~0.4 Å movement of the Fe atom into the plane of the porphyrin ring, which occurs upon ligand binding, is amplified through a pivoting movement of helix F to a much larger displacement of the FG corners. Although the $\alpha_1\beta_1$ interface does not undergo structural changes, the permanent αβ dimer does change *shape* as the αFG and βFG corners within the same αβ dimer move ~2.5 Å closer together in R compared to T [459,479]; this movement presumably forces dimer rotation and requires one of the FG corners (βFG) to switch partners.

7.6. The unliganded T and liganded R structures are unstrained

With all the structural data available, can we understand the structural basis for O_2 affinity in RBC Hb? Perutz proposed that affinity is lowered in quaternary T because the T structure resists stereochemical changes at the haem required by O_2 ligation [458,482]. To look for evidence of strain in the haem, imposed by the protein, the haem centre of Hb has been compared with model haems (Fig. 2). The findings are (1) that model 5-coordinate high spin Fe(II) porphyrins [36,37,77,78,483,484] have similar stereochemistry to the haems of unliganded T [457,476], and (2) synthetic 6-coordinate, low spin, O_2-ligated porphyrins [39,41] have the same stereochemistry as liganded R state Hb [457,477]. Other sensitive spectroscopic tests have been applied which conclude that the above porphyrin species are excellent models for deoxy Hb and Hb(O_2) [484–486]. As well as establishing that Fe moves ~0.4 Å into the porphyrin plane in the T ↔ R transition, the above studies show that strain in both unliganded T and liganded R must be low. A similar conclusion is reached based on energy minimisation of Hb haems [478]. The essential point is that substantial strain is only expected when there is a miss-match between the haem stereochemistry and the tertiary or quaternary state, for example, *liganded* tertiary *t* in quaternary T [478]. Unliganded Hb has been crystallized in the T state from solutions containing PEG, and subsequently liganded to obtain structures of ligated *t* in T which do show some porphyrin ring distortions and lengthening of the Fe–N^{ε}, particularly at the α haems, indicative of a strained conformation (reviewed in [430]).

7.7. Strain in the liganded T state: structural basis for the low affinity of T

As concluded at the end of the preceeding section, ligation of tertiary *t* within quaternary T introduces strain into the structure—-meaning that the energies of certain bonding or non-bonding interactions within the Hb tetramer are raised (e.g., bonds are stretched), and this partially offsets a favourable energy change from Fe—O_2 bond formation, and so lowers O_2 affinity overall. For ligation of tertiary *r* in quaternary R the restraining interactions—equivalent to the cooperative free energy—have been removed. It is interesting to consider two aspects of the strain mechanism. Firstly, there are interactions at the haem that directly alter O_2 affinity (reviewed in general terms in Section 3). Based on differences between the liganded and unliganded Hb structures available in 1970, Perutz identified strain in the Fe–His bond, resisting in-plane movement of the Fe atom, as a key factor [458]. At the same time, Perutz also identified steric interference between ValE11 and O_2 in the distal pocket of the β chains in T state Hb. These mechanisms (discussed in the next paragraphs) are now understood quite well. A second aspect of the strain mechanism—identifying the full network of molecular interactions that quantitatively account for the cooperative free energy—has been harder to answer. Perutz' original concept was that eight salt bridges present in T, but not R, stabilised the T structure, and that the cooperative free energy was required for breaking these bonds [458]. However, considerable evidence

now indicates that quaternary salt bridges do not make a large contribution to the low affinity of T (see discussions in [430,478,487,488]). Structure-based computational approaches suggest that cooperative free energy comes from multiple steric interactions, mostly within the allosteric core, including steric interactions with the haem and at the $\alpha_1\beta_2$ interface, as well as the C-terminal regions that form T-specific salt bridges, rather than being located in a small number of discrete bonding interactions [209,489–493].

Returning to proximal and distal interactions at haem. Resonance Raman spectroscopy (RR) provides a wealth of information about haem structure, but the stretching frequency of the Fe–His bond (νFe-His) [112,494] is one of the only parameters showing a simple correlation with O_2 binding affinity [495,496] and so has been extensively used to track allosteric changes in Hb. Although there is no evidence for large strains in crystal structures of unliganded T state Hb, RR is sensitive to much smaller changes bond parameters. A lower νFe–His frequency in T state deoxy Hb (215–216 cm^{-1}) [114–116] compared to Mb (220 cm^{-1}) [111–113] or the isolated Hb α (223 cm^{-1}) or β (224 cm^{-1}) chains [494] reflects increased Fe–His tension in the deoxy T state. Similar decreases of 10–16 cm^{-1} in νFe–His are seen in hindered versus unhindered model porphyrins [497] [498]. These differences correspond to strain energies of < 0.3 kcal mol^{-1} [478,499] (less than a tenth of the cooperative free energy), consistent with the conclusions above that strain on the haem in unliganded T state is small. However, the correlation of νFe–His in the unliganded state with O_2 affinity suggests that small strains in the unliganded molecule are converted to proportionally larger strains in the ligated tertiary *t* state. Unfortunately, νFe–His is not resonance-enhanced in the 6-coordinate liganded complexes so strains in ligated complexes cannot be measured directly in the same way.

Multiple lines of evidence indicate that Fe–His strain is greater in α chains than in β. Early evidence came from studies of NO adducts. NO exerts a strong trans effect on Fe(II) that weakens the proximal Fe–His bond. In the background of strong stabilisation of the T state using the allosteric effector, inositol hexaphosphate (IHP), NO binding ruptures the Fe–His bond in the α chains in solution [500–502] and also in a crystal structure of T state Hb(NO) [503]. Rupture of the α Fe–His has also been seen in a crystal of T state Hb(CN) [504]. As α Fe–His remains intact in R state Hb(NO) and Hb(CN), the above data indicate that increased strain in liganded T, compared to liganded R, is sufficient to rupture the Fe–His bond.

Using their approach described in Section 3.3, Barrick and colleagues specifically ablated the Fe–His bond in α or β, or in both chains [85,86]. They showed that Hb retaining only α Fe–His had similar CO affinity to intact Hb, retained substantial cooperativity, and retained signatures of the quaternary transition in ^{1}H NMR spectra. On the other hand, tetramers retaining only β Fe–His had > 10-fold increase in CO affinity, essentially lost cooperativity and showed diminished markers of quaternary transition. These data demonstrate that strain transmitted specifically through α Fe–His substantially lowers O_2 affinity and is a major determinant of quaternary switching. QM/MM implementation of an in silico version of the Barrick experiment also show that reduced O_2 affinity in α is almost entirely due to proximal effects (strain in the Fe–His bond), whereas proximal effects account for very little of the reduced affinity of β [209]. Recently νFe–His has been measured separately for α and β chains within quaternary T by using mixed protohaem/mesohaem hybrid tetramers, showing νFe–His is lower in α chains (207 cm^{-1}) than in β chains (218 cm^{-1}) [116]. Subsequently, Bringas et al. have used computational methods to produce geometry optimised structures of *liganded* T and find that the Fe–His is dramatically strained in Hb α (Fe–N^{ε} bond length of 2.20 Å) compared to isolated haem (Fe–N^{ε} bond length 2.12 Å), and this difference disappeared in the optimised R quaternary structure [209]. In the same structures, β Fe–His was less perturbed, and, in fact, slightly compressed (2.08 Å in T versus 2.09 Å in R).

Increased Fe–His strain in α is attributed to greater off-axis rotation of HisF8 imidazole in Hb α [480]. The smaller strains in β Fe–His arise from force on the porphyrin from side chains surrounding HisF8, in particular from PheG5 [480,493,505]. Affinity in β chains is lowered predominantly, not by Fe–His strain, but by a more distributed set of steric effects surrounding the haem [209,480,493], including interference between O_2 ligand and ValE11 in the distal haem pocket [458,506–508]. A new finding from recent QM/MM work is that a shift in HisE7 gate equilibrium towards the open state occurs for β, but not α, upon T → R transition leading to an increased ligand binding rate [209]. The net result, as consistently shown by experiment [155,509,510,511] and computation [209,493], is that α and β chains have similar O_2 affinity in T, probably within a factor of two, and similar increase in affinity upon T → R transition, consistent with the proposal that functional equivalence is important in maintaining high cooperativity [510]. Nevertheless, despite progress over ~60 years of research since the first pioneering work of Perutz, it seems the structural basis for cooperative free energy is still not completely understood [488].

7.8. Allosteric effectors act by shifting the tertiary *t* ↔ *r* equilibrium

Early pioneering work described in Section 7.4 provides strong evidence that *quaternary* interactions underpin cooperative O_2 binding (so-called homotypic allosteric interaction). The discovery of allosteric mechanisms that operate at the *tertiary* structural level has emerged from efforts to understand how heterotypic allosteric effectors (inhibitors) change O_2 affinity. Co-crystal structures with human T Hb show one binding site for the allosteric inhibitor, 2,3-DPG, between the two β chains at the entrance to the central Hb cavity, with negative charges on the 2,3-DPG interacting with multiple positively charged groups on Hb [512,513]. This site was predicted by Perutz [433], who suggested that closer positioning of the β chains in the R state would block 2,3-DPG binding to R, and that the action of 2,3-DPG could be explained by preferential binding to, and stabilisation of, the T state, equivalent to a 15–30-fold increase in the MWC parameter, L (L = $[T_0]$ / $[R_0]$). However, precise measures of ligand equilibria and kinetics over a wide range of conditions show that up to 50% of the decrease in P_{50} induced by 2,3-DPG arises from a change in the intrinsic O_2 affinities of the T and R states, K_T and K_R [421,422,514,515]. This proposal breaks one of the central postulates of the MWC model—that there is no allostery *within* T or R quaternary states. And, lowering of K_T and K_R is even more dramatic with potent synthetic allosteric effectors such as IHP, Bezafibrate (BzF) and L35 [421,514,516]. These effectors have multiple binding sites, in the Hb central cavity and on the surface of Hb, and bind to both T and R quaternary structures [481,517–519]. Furthermore, IHP and L35 also lower the O_2 affinity of semihaemoglobins, which are dimeric forms containing a haem group in only one α or β chain, emphasising a mechanism that is independent of quaternary structure [520].

A series of elegant experiments, using Hb in crystals or in gels, have shown that allosteric effectors act by shifting the tertiary *t* ↔ *r* equilibrium. The first set of experiments was stimulated by the discovery that T state deoxy Hb can be crystallized from solutions containing PEG and subsequently liganded without the crystals being destroyed [521,522]. Using this method, Eaton, Henry and co-workers showed that T state Hb crystals bound O_2 non-cooperatively and with low affinity (P_{50} = 148 Torr at pH 7.2, 15 °C) and with no Bohr effect [511,523]. The O_2 affinity in the crystals was equal to the low extreme of affinity in solution, which can only be attained by adding strong allosteric inhibitors IHP and BzF together (these bind to separate sites to have combined effect) [421,422]. The same allosteric inhibitors had no effect on the extreme low affinity of the crystals [524]. An explanation, put forward by Rivetti et al. [523], is that the T state Hb in solution contains both high affinity *r* and low affinity *t tertiary* structures in equilibrium, and allosteric inhibitors shift the tertiary equilibrium in the *r* → *t* direction, thus lowering O_2 affinity without a change in

quaternary state. Crystallization freezes out the equilibrium in favour of the lower energy *t* tertiary structure in quaternary T, and crystal forces resist changes in tertiary or quaternary structure rendering the crystals insensitive to allosteric effectors.

The second set of important experiments was inspired by the discovery that embedding Hb in silica gel dramatically slows quaternary switching, from a timescale of μs in solution to days in the gel state [525]. Deoxy T state Hb embedded in silica gel has a P_{50} of ~12 Torr at pH 7.0, 15 °C in the absence of allosteric effectors, and a P_{50} of ~139 Torr in the presence of IHP (2 mM) and BzF (2 mM), matching the values obtained under similar conditions in solution [526,527]. Furthermore, the Bohr effect is of similar magnitude in silica gels and in solution, indicating that increased H^+ binding lowers O_2 affinity independent of quaternary changes [526,527]. It can also be shown that Hb crystallized in the R state [446], or embedded in silica gels [525], can be deoxygenated and rebinds O_2 with high affinity (P_{50} 0.1–0.3 Torr) [446], similar to the 4th oxygen binding to R in solution.

Results in Hb crystals and Hb in silica gels demonstrate that cooperative O_2 binding requires quaternary structural changes. In addition, silica gels permit tertiary structural changes whilst restraining quaternary changes, and, in doing so, demonstrate that tertiary level changes account for most of the effect of IHP/Bzf, and most of the chloride dependent and independent Bohr effect.

7.9. The kinetic pathway from haem-ligand interactions to quaternary changes

The final sections of this review consider the time scales of structural changes involved in ligand binding to Mb and to Hb, and the causative sequence of events that underlies tertiary and quaternary transitions in Hb. The kinetics of ligand binding in Mb was revealed in flash photolysis experiments pioneered by Quentin H. Gibson and others. Flash photolysis of Hb(CO) generates unliganded Hb in the R state, that subsequently relaxes back towards the equilibrium unliganded T state on a μs–ms time scale; bimolecular rebinding of CO occurs with a fast and a slow rate, corresponding to binding to the R and T deoxy states [528–531]. Monitoring the fraction of CO rebinding to R and T enabled Sawicki and Gibson to measure the R → T quaternary transition to occur with a time constant of ~20 μs [532]. By measuring on even shorter time scales, Eaton, Henry and colleagues found that a fraction of sites switch to lower affinity tertiary states with a time constant < 1 μs, and proposed that a *r* → *t* tertiary structural change *precedes* quaternary structural changes [533]. This conclusion is consistent with later computational kinetic models developed by Martin Karplus and coworkers [414,491,492,534]. Silica gels came to the fore again due to their capacity to dramatically slow tertiary, and essentially freeze quaternary, structural changes. After laser photolysis of Hb(CO) in silica gels, two bimolecular CO rebinding rates can be separated, with time constants of ~25 ms (slow) and ~1 ms (fast) at 20 °C [488], corresponding to binding to *t* (low affinity) and *r* (high affinity) subunits. The same fast and slow CO rebinding rates can be detected in both R and T quaternary state, implying that *t* (or *r*) is functionally identical in T and R [425,488,535], an idea that underpins the TTS model of allostery [415,416,424,425].

One of the current frontiers in understanding Hb function is to trace the kinetic pathway of the tertiary and quaternary transition over the period of fs–ms as it occurs in solution. For the much simpler Mb system, a full 3D picture of structural changes down to the ps time domain has been obtained by time-resolved x-ray diffraction methods and spectroscopy. Following the synchronised severing of the Fe—CO bond in Mb(CO) with a laser light pulse, stereochemical changes including doming of the porphyrin and movement of Fe ~0.3 Å out of the porphyrin plane occur with biphasic kinetics with a fast 50–70 fs phase and slower ~0.4 ps phase [111,536–540]. The sudden change in haem geometry compresses the Fe–His bond, which can be detected within 1 ps by time-resolved RR as the appearance of a νFe–His signal at 222 cm^{-1}—the increased value of νFe–His, compared to the 220 cm^{-1} value measured for unliganded Hb at equilibrium, indicates bond shortening [111]. The change in haem geometry introduces strain into the protein, which relaxes with stretched exponential kinetics [541] and a time constant of ~100 ps [111]. Time-resolved Laue crystallography has revealed a series of Mb x-ray structures at ~1.8 Å resolution, with the first data set obtained within 100 ps after photolysis, and a number of subsequent structures obtained out to the μs time point [542,543]. The data shows correlated motions of helix C, F, H away from the haem, and movement of helix A, E towards the haem within 100 ps of Fe—CO photolysis, suggesting an 'upward' force on haem and a 'downward' force on proximal His is generated in the initial photoproduct [542,543]. Tilting motions of the haem and conformational changes in distal haem pocket residues, including HisE7, are larger than differences between the static HbCO and Hb structures [542,543]. The invention of the x-ray free electron laser has allowed x-ray diffraction [544] and x-ray scattering [545] analysis to be extended down to the ps time domain. The experiment has shown that a global expansion of Mb occurs within 1 ps of Fe—CO photolysis, after which the protein undergoes oscillatory motions with a ~4 ps period that decay away to equilibrium; the effect has been dubbed a 'protein quake' [544,545]. Future development of these techniques may see the first complete, atomic level, deterministic model for any protein.

Turning back to the structural transitions of the more complex Hb molecule. Although the T and R endpoints are related through simple rotation of αβ dimers (together with a small ~1 Å translation movement), the process of the T ↔ R transition involves two separate and sequential rotations involving different sub domains of Hb, rather than a single rotation [534]. Evidence supporting a two-step transition comes from several experimental studies. First, time-resolved magnetic CD [546] and RR [547] show that the βTrp(37)C3–αAsp(94)G1 hydrogen bond in the hinge region rearranges with a time constant of ~2 μs following photolysis of HbCO; whereas, the αTyr(42)C7–βAsp(99)G1 hydrogen bond in the switch region rearranges with a time constant of 21 μs [547]. Time resolved WAXS, which is a sensitive to global protein shape, indicates that the major quaternary reorganisation in the R → T directions takes place in the 2 μs phase [548]. This could correspond to the major quaternary transition in the minimum energy pathway calculations of Fischer and Karplus (who model the reverse, T → R transition) [534]. According to Spiro, the major R → T rotation proceeds reorganisation of side chains in the switch region into their T-specific contacts, including the formation of the αTyr(42)C7–βAsp(99)G1 hydrogen bond, but these switch region contacts are still needed to attain the high-affinity *t* tertiary structure [549]; however, some uncertainty remains in correlating reorganisation of the switch contacts in the Karplus model with markers of the T-state specific contacts as reported by RR [534].

A further series of experiments by Spiro and co-workers was designed to resolve events in the Hb α and β subunits, and to correlate changes at the haem sites with reorganisation of the hinge and switch regions, as reported by changes in the RR marker bands [116,505,550]. As with Mb, compression of the Fe–His bond occurs in < 1 ps following photolysis of HbCO—indicated by appearance of νFe–His at 230 cm^{-1} [115,117,550]—and is followed by relaxation of the protein in a series of steps over a μs time scale, compared to sub-ns relaxation in Mb [551,552]. RR measurements obtained from protohaem/mesohaem hybrid Hbs [116,505] show that νFe–His in β evolves earlier than in α, with an initial reduction in β νFe–His at ~3 μs coinciding with the proposed rotation of the αβ dimers to establish the quaternary T hinge contacts. The α chain evolution occurs later, and with a more dramatic reduction in νFe–His at 20 μs [116], coinciding with the proposed rotation of the α subunits to establish the T switch contacts [116,505].

8. Concluding remarks

Work on Mb and RBC Hb has ushered in many of the great

breakthroughs in molecular biology (to use the term in its original and widest sense), including such conceptual leaps as the theory of allostery, as well as driving the development of methods that have revolutionised biology, like protein crystallography. Now exciting new prospects lie on the horizon, made possible by the application of powerful new time-resolved spectroscopic methods, the growing capability of computational chemistry to tackle macromolecular systems and metal centres, and the x-ray free electron laser, to name a few. With these tools it is hoped that the first complete deterministic description of protein function might be achieved for Mb or other robust single subunit Hbs. Beyond this, and despite the remarkable progress of ~60 years, a complete structural explanation for oxygen affinity in RBC Hb remains an unsolved problem. Another promising space for future research comes from the avalanche of genomic data, particularly from bacterial species, which is revealing the true extent of Hb diversity. This vast sequence space is sure to throw up new Hb functions and mechanisms through biochemical and biophysical studies. At the same time, the biological functions of many Hbs remain elusive despite extensive knowledge of their structure and chemistry; thus genetic studies in the host organsisms are crucial to soundly attribute function. The unexpected diversity of Hbs in vertebrates is another new and open field. Until recently Mb and RBC Hb were the only known vertebrate Hbs; now Cygb, Ngb, globin E, globin Y, globin X and androglobin have been discovered, and the tissue distribution of even Mb and Hb α/β subunits is much wider than originally understood. The role of these proteins in vertebrate physiology is grist to the mill. There is plenty to occupy the new wave of Hb researchers.

References

[1] J.C. Kendrew, G. Bodo, H.M. Dintzis, R.G. Parrish, H. Wyckoff, D.C. Phillips, A three-dimensional model of the myoglobin molecule obtained by x-ray analysis, Nature 181 (1958) 662–666.

[2] J.C. Kendrew, R.E. Dickerson, B.E. Strandberg, R.G. Hart, D.R. Davies, D.C. Phillips, V.C. Shore, Structure of myoglobin: a three-dimensional Fourier synthesis at 2 A. resolution, Nature 185 (1960) 422–427.

[3] M.F. Perutz, M.G. Rossmann, A.F. Cullis, H. Muirhead, G. Will, A.C. North, Structure of haemoglobin: a three-dimensional Fourier synthesis at 5.5-A. resolution, obtained by X-ray analysis, Nature 185 (1960) 416–422.

[4] A.M. Lesk, C. Chothia, How different amino acid sequences determine similar protein structures: the structure and evolutionary dynamics of the globins, J. Mol. Biol. 136 (1980) 225–270.

[5] O.H. Kapp, L. Moens, J. Vanfleteren, C.N. Trotman, T. Suzuki, S.N. Vinogradov, Alignment of 700 globin sequences: extent of amino acid substitution and its correlation with variation in volume, Protein Sci. 4 (1995) 2179–2190.

[6] T.A. Freitas, S. Hou, E.M. Dioum, J.A. Saito, J. Newhouse, G. Gonzalez, M.A. Gilles-Gonzalez, M. Alam, Ancestral hemoglobins in archaea, Proc. Natl. Acad. Sci. U. S. A. 101 (2004) 6675–6680.

[7] L. Holm, C. Sander, Structural alignment of globins, phycocyanins and colicin A, FEBS Lett. 315 (1993) 301–306.

[8] A. Pesce, M. Couture, S. Dewilde, M. Guertin, K. Yamauchi, P. Ascenzi, L. Moens, M. Bolognesi, A novel two-over-two α-helical sandwich fold is characteristic of the truncated hemoglobin family, EMBO J. 19 (2000) 2424–2434.

[9] W.E. Royer Jr., H. Sharma, K. Strand, J.E. Knapp, B. Bhyravbhatla, Lumbricus erythrocruorin at 3.5 A resolution: architecture of a megadalton respiratory complex, Structure 14 (2006) 1167–1177.

[10] W.E. Royer Jr., J.E. Knapp, K. Strand, H.A. Heaslet, Cooperative hemoglobins: conserved fold, diverse quaternary assemblies and allosteric mechanisms, Trends Biochem. Sci. 26 (2001) 297–304.

[11] W.E. Royer Jr., H. Zhu, T.A. Gorr, J.F. Flores, J.E. Knapp, Allosteric hemoglobin assembly: diversity and similarity, J. Biol. Chem. 280 (2005) 27477–27480.

[12] L.J. Smith, A. Kahraman, J.M. Thornton, Heme proteins–diversity in structural characteristics, function, and folding, Proteins 78 (2010) 2349–2368.

[13] D. Lundin, G. Berggren, D.T. Logan, B.M. Sjoberg, The origin and evolution of ribonucleotide reduction, Life (Basel) 5 (2015) 604–636.

[14] P. Ponka, Cell biology of heme, Am J Med Sci 318 (1999) 241–256.

[15] S.N. Vinogradov, D. Hoogewijs, X. Bailly, R. Arredondo-Peter, M. Guertin, J. Gough, S. Dewilde, L. Moens, J.R. Vanfleteren, Three globin lineages belonging to two structural classes in genomes from the three kingdoms of life, Proc. Natl. Acad. Sci. U. S. A. 102 (2005) 11385–11389.

[16] S.N. Vinogradov, M. Tinajero-Trejo, R.K. Poole, D. Hoogewijs, Bacterial and archaeal globins - a revised perspective, Biochim. Biophys. Acta 1834 (2013) 1789–1800.

[17] P.R. Gardner, Hemoglobin: a nitric-oxide dioxygenase, Scientifica (Cairo) 2012 (2012) 683729.

[18] M. Martinkova, K. Kitanishi, T. Shimizu, Heme-based globin-coupled oxygen sensors: linking oxygen binding to functional regulation of diguanylate cyclase, histidine kinase, and methyl-accepting chemotaxis, J. Biol. Chem. 288 (2013) 27702–27711.

[19] W. Zhang, J.S. Olson, G.N. Phillips Jr., Biophysical and kinetic characterization of HemAT, an aerotaxis receptor from *Bacillus subtilis*, Biophys. J. 88 (2005) 2801–2814.

[20] M. Nardini, A. Pesce, M. Milani, M. Bolognesi, Protein fold and structure in the truncated (2/2) globin family, Gene 398 (2007) 2–11.

[21] J.P. Bustamante, L. Radusky, L. Boechi, D.A. Estrin, A. Ten Have, M.A. Marti, Evolutionary and functional relationships in the truncated hemoglobin family, PLoS Comput. Biol. 12 (2016) e1004701.

[22] M. Couture, T.K. Das, P.Y. Savard, Y. Ouellet, J.B. Wittenberg, B.A. Wittenberg, D.L. Rousseau, M. Guertin, Structural investigations of the hemoglobin of the cyanobacterium *Synechocystis* PCC6803 reveal a unique distal heme pocket, Eur. J. Biochem. 267 (2000) 4770–4780.

[23] M.D. Hade, J. Kaur, P.K. Chakraborti, K.L. Dikshit, Multidomain truncated hemoglobins: new members of the globin family exhibiting tandem repeats of globin units and domain fusion, IUBMB Life 2017 (2017).

[24] A. Bonamore, A. Attili, F. Arenghi, B. Catacchio, E. Chiancone, V. Morea, A. Boffi, A novel chimera: the "truncated hemoglobin-antibiotic monooxygenase" from *Streptomyces avermitilis*, Gene 398 (2007) 52–61.

[25] A.H. Knoll, M.A. Nowak, The timetable of evolution, Sci. Adv. 3 (2017) e1603076.

[26] M.T. Forrester, M.W. Foster, Protection from nitrosative stress: a central role for microbial flavohemoglobin, Free Radic. Biol. Med. 52 (2012) 1620–1633.

[27] X. Bailly, S. Vinogradov, The sulfide binding function of annelid hemoglobins: relic of an old biosystem? J. Inorg. Biochem. 99 (2005) 142–150.

[28] S.N. Vinogradov, D. Hoogewijs, X. Bailly, K. Mizuguchi, S. Dewilde, L. Moens, J.R. Vanfleteren, A model of globin evolution, Gene 398 (2007) 132–142.

[29] R.D. Jones, D.A. Summerville, F. Basolo, Synthetic oxygen carriers related to biological systems, Chem. Rev. 79 (1979) (189-179).

[30] M. Momenteau, C.A. Reed, Synthetic heme dioxygen complexes, Chem. Rev. 94 (1994) 659–698.

[31] J.P. Collman, R. Boulatov, C.J. Sunderland, L. Fu, Functional analogues of cytochrome c oxidase, myoglobin, and hemoglobin, Chem. Rev. 104 (2004) 561–588.

[32] W.R. Scheidt, C.A. Reed, Spin-state/stereochemical relationships in iron porphyrins: implications for the hemoproteins, Chem. Rev. 81 (1981) 543–555.

[33] M.F. Perutz, Regulation of oxygen affinity of hemoglobin: influence of structure of the globin on the heme iron, Annu. Rev. Biochem. 48 (1979) 327–386.

[34] L. Pauling, C.D. Coryell, The magnetic properties and structure of the hemochromogens and related substances, Proc. Natl. Acad. Sci. U. S. A. 22 (1936) 159–163.

[35] L. Pauling, C.D. Coryell, The magnetic properties and structure of hemoglobin, oxyhemoglobin and carbonmonoxyhemoglobin, Proc. Natl. Acad. Sci. U. S. A. 22 (1936) 210–216.

[36] C. Hu, A. Roth, M.K. Ellison, J. An, C.M. Ellis, C.E. Schulz, W.R. Scheidt, Electronic configuration assignment and the importance of low-lying excited states in high-spin imidazole-ligated iron(II) porphyrinates, J. Am. Chem. Soc. 127 (2005) 5675–5688.

[37] C. Hu, J. An, B.C. Noll, C.E. Schulz, W.R. Scheidt, Electronic configuration of high-spin imidazole-ligated iron(II) octaethylporphyrinates, Inorg. Chem. 45 (2006) 4177–4185.

[38] M.-S. Liao, S. Scheiner, Electronic structure and bonding in unligated and ligated FeII porphyrins, J. Chem. Phys. 116 (2002) 3635–3645.

[39] J.P. Collman, R.R. Gagne, C.A. Reed, W.T. Robinson, G.A. Rodley, Structure of an iron(II) dioxygen complex; a model for oxygen carrying hemeproteins, Proc. Natl. Acad. Sci. U. S. A. 71 (1974) 1326–1329.

[40] G.B. Jameson, F.S. Molinaro, J.A. Ibers, J.P. Collman, J.I. Brauman, E. Rose, K.S. Suslick, Structural changes upon oxygenation of an iron(II)(porphyrinato)(imidazole) complex, J. Am. Chem. Soc. 100 (1978) 6769–6770.

[41] G.B. Jameson, G.A. Rodley, W.T. Robinson, R.R. Gagne, C. Reed, J.P. Collman, Structure of a dioxygen adduct of (1-methylimidazole)-meso-tetrakis (α,α,α,α-o-pivalamidophenyl) porphinatoiron (II). An iron dioxygen model for the heme component of oxymyoglobin, Inorg. Chem. 17 (1978) 850–857.

[42] R.E. Brantley Jr., S.J. Smerdon, A.J. Wilkinson, E.W. Singleton, J.S. Olson, The mechanism of autooxidation of myoglobin, J. Biol. Chem. 268 (1993) 6995–7010.

[43] K. Shikama, A controversy on the mechanism of autoxidation of oxymyoglobin and oxyhaemoglobin: oxidation, dissociation, or displacement? Biochem. J. 223 (1984) 279–280.

[44] J.P. Arcon, P. Rosi, A.A. Petruk, M.A. Marti, D.A. Estrin, Molecular mechanism of myoglobin autoxidation: insights from computer simulations, J. Phys. Chem. B 119 (2015) 1802–1813.

[45] R.T. Aranda, H. Cai, C.E. Worley, E.J. Levin, R. Li, J.S. Olson, G.N. Phillips Jr., M.P. Richards, Structural analysis of fish versus mammalian hemoglobins: effect of the heme pocket environment on autooxidation and hemin loss, Proteins 75 (2009) 217–230.

[46] E.C. Liong, Y. Dou, E.E. Scott, J.S. Olson, G.N. Phillips Jr., Waterproofing the heme pocket. Role of proximal amino acid side chains in preventing hemin loss from myoglobin, J. Biol. Chem. 276 (2001) 9093–9100.

[47] N. Mukhi, S. Dhindwal, S. Uppal, A. Kapoor, R. Arya, P. Kumar, J. Kaur, S. Kundu, Structural and functional significance of the N- and C-terminal appendages in *Arabidopsis* truncated hemoglobin, Biochemistry 55 (2016) 1724–1740.

[48] X. Bai, J. Long, X. He, J. Yan, X. Chen, Y. Tan, K. Li, L. Chen, H. Xu, Overexpression of spinach non-symbiotic hemoglobin in *Arabidopsis* resulted in decreased NO content and lowered nitrate and other abiotic stresses tolerance, Sci Rep 6 (2016) 26400.

[49] A.D. Frey, P.T. Kallio, Bacterial hemoglobins and flavohemoglobins: versatile

proteins and their impact on microbiology and biotechnology, FEMS Microbiol. Rev. 27 (2003) 525–545.
[50] J.B. Wittenberg, M. Bolognesi, B.A. Wittenberg, M. Guertin, Truncated hemoglobins: a new family of hemoglobins widely distributed in bacteria, unicellular eukaryotes, and plants, J. Biol. Chem. 277 (2002) 871–874.
[51] T.A. Freitas, J.A. Saito, S. Hou, M. Alam, Globin-coupled sensors, protoglobins, and the last universal common ancestor, J. Inorg. Biochem. 99 (2005) 23–33.
[52] E. Dumont, S. Jokipii-Lukkari, V. Parkash, J. Vuosku, R. Sundstrom, Y. Nymalm, S. Sutela, K. Taskinen, P.T. Kallio, T.A. Salminen, H. Haggman, Evolution, three-dimensional model and localization of truncated hemoglobin PttTrHb of hybrid aspen, PLoS One 9 (2014) e88573.
[53] L. Giangiacomo, A. Ilari, A. Boffi, V. Morea, E. Chiancone, The truncated oxygen-avid hemoglobin from *Bacillus subtilis*: X-ray structure and ligand binding properties, J. Biol. Chem. 280 (2005) 9192–9202.
[54] A.B. Cowley, M.L. Kennedy, S. Silchenko, G.S. Lukat-Rodgers, K.R. Rodgers, D.R. Benson, Insight into heme protein redox potential control and functional aspects of six-coordinate ligand-sensing heme proteins from studies of synthetic heme peptides, Inorg. Chem. 45 (2006) 9985–10001.
[55] M.S. Hargrove, A.J. Wilkinson, J.S. Olson, Structural factors governing hemin dissociation from metmyoglobin, Biochemistry 35 (1996) 11300–11309.
[56] M.S. Hargrove, J.S. Olson, The stability of holomyoglobin is determined by heme affinity, Biochemistry 35 (1996) 11310–11318.
[57] A. Pesce, M. Bolognesi, M. Nardini, Protoglobin: structure and ligand-binding properties, Adv. Microb. Physiol. 63 (2013) 79–96.
[58] J.A. Hoy, S. Kundu, J.T. Trent 3rd, S. Ramaswamy, M.S. Hargrove, The crystal structure of *Synechocystis* hemoglobin with a covalent heme linkage, J. Biol. Chem. 279 (2004) 16535–16542.
[59] J.A. Hoy, B.J. Smagghe, P. Halder, M.S. Hargrove, Covalent heme attachment in *Synechocystis* hemoglobin is required to prevent ferrous heme dissociation, Protein Sci. 16 (2007) 250–260.
[60] B.C. Vu, A.D. Jones, J.T. Lecomte, Novel histidine-heme covalent linkage in a hemoglobin, J. Am. Chem. Soc. 124 (2002) 8544–8545.
[61] B.B. Wenke, J.T. Lecomte, A. Heroux, J.L. Schlessman, The 2/2 hemoglobin from the cyanobacterium *Synechococcus* sp. PCC 7002 with covalently attached heme: comparison of X-ray and NMR structures, Proteins 82 (2014) 528–534.
[62] J.T. Trent III, S. Kundu, J.A. Hoy, M.S. Hargrove, Crystallographic analysis of *Synechocystis* cyanoglobin reveals the structural changes accompanying ligand binding in a hexacoordinate hemoglobin, J. Mol. Biol. 341 (2004) 1097–1108.
[63] M. Nardini, A. Pesce, L. Thijs, J.A. Saito, S. Dewilde, M. Alam, P. Ascenzi, M. Coletta, C. Ciaccio, L. Moens, M. Bolognesi, Archaeal protoglobin structure indicates new ligand diffusion paths and modulation of haem-reactivity, EMBO Rep. 9 (2008) 157–163.
[64] Y. Jin, M. Nagai, Y. Nagai, S. Nagatomo, T. Kitagawa, Heme structures of five variants of hemoglobin M probed by resonance Raman spectroscopy, Biochemistry 43 (2004) 8517–8527.
[65] C. Kiefl, N. Sreerama, R. Haddad, L. Sun, W. Jentzen, Y. Lu, Y. Qiu, J.A. Shelnutt, R.W. Woody, Heme distortions in sperm-whale carbonmonoxy myoglobin: correlations between rotational strengths and heme distortions in MD-generated structures, J. Am. Chem. Soc. 124 (2002) 3385–3394.
[66] C. Rovira, B. Schulze, M. Eichinger, J.D. Evanseck, M. Parrinello, Influence of the heme pocket conformation on the structure and vibrations of the Fe—CO bond in myoglobin: a QM/MM density functional study, Biophys. J. 81 (2001) 435–445.
[67] S. Van Doorslaer, L. Tilleman, B. Verrept, F. Desmet, S. Maurelli, F. Trandafir, L. Moens, S. Dewilde, Marked difference in the electronic structure of cyanide-ligated ferric protoglobins and myoglobin due to heme ruffling, Inorg. Chem. 51 (2012) 8834–8841.
[68] D.E. Bikiel, F. Forti, L. Boechi, M. Nardini, F.J. Luque, M.A. Marti, D.A. Estrin, Role of heme distortion on oxygen affinity in heme proteins: the protoglobin case, J. Phys. Chem. B 114 (2010) 8536–8543.
[69] J.W. Murray, O. Delumeau, R.J. Lewis, Structure of a nonheme globin in environmental stress signaling, Proc. Natl. Acad. Sci. U. S. A. 102 (2005) 17320–17325.
[70] G.R. Stranzl, E. Santelli, L.A. Bankston, C. La Clair, A. Bobkov, R. Schwarzenbacher, A. Godzik, M. Perego, M. Grynberg, R.C. Liddington, Structural insights into inhibition of *Bacillus anthracis* sporulation by a novel class of non-heme globin sensor domains, J. Biol. Chem. 286 (2011) 8448–8458.
[71] E.E. Scott, Q.H. Gibson, J.S. Olson, Mapping the pathways for O_2 entry into and exit from myoglobin, J. Biol. Chem. 276 (2001) 5177–5188.
[72] J.L. Hoard, Stereochemistry of hemes and other metalloporphyrins, Science 174 (1971) 1295–1302.
[73] R. Countryman, D.M. Collins, J.L. Hoard, Stereochemistry of the low-spin iron porphyrin, bis(imidazole)-α,β,γ,δ-tetraphenylporphinatoiron(III) chloride, J. Am. Chem. Soc. 91 (1969) 5166–5167.
[74] J.L. Hoard, G.H. Cohen, M.D. Glick, Stereochemistry of coordination group in an iron(III) derivative of tetraphenylporphine, J. Am. Chem. Soc. 89 (1967) 1992–1996.
[75] J.L. Hoard, M.J. Hamor, T.A. Hamor, W.S. Caughey, Crystal structure and molecular sterochemistry of methoxyiron(III) mesoporphyrin-9 dimethyl ester, J. Am. Chem. Soc. 87 (1965) 2312–2319.
[76] J.L. Hoard, W.R. Scheidt, Stereochemical trigger for initiating cooperative interaction of the subunits during the oxygenation of cobaltohemoglobin, Proc. Natl. Acad. Sci. U. S. A. 70 (1973) 3919–3922.
[77] M.K. Ellison, C.E. Schulz, W.R. Scheidt, Structure of the deoxymyoglobin model [Fe(TPP)(2-MeHIm)] reveals unusual porphyrin core distortions, Inorg. Chem. 41 (2002) 2173–2181.
[78] G.B. Jameson, F.S. Molinaro, J.A. Ibers, J.P. Collman, J.I. Brauman, E. Rose, K.S. Suslick, Models for the active site of oxygen-binding hemoproteins. Dioxygen binding properties and the structures of (2-methylimidazole)-meso-tetra(α,α,α,α-o-pivalamidophenyl)porphyrinatoiron(II)-ethanol and its dioxygen adduct, J. Am. Chem. Soc. 102 (1980) 3224–3237.
[79] J.P. Collman, J.I. Brauman, K.M. Doxsee, T.R. Halbert, K.S. Suslick, Model compounds for the T state of hemoglobin, Proc. Natl. Acad. Sci. U. S. A. 75 (1978) 564–568.
[80] D.K. White, J.B. Cannon, T.G. Traylor, A kinetic model for R-and T-state hemoglobin. Flash photolysis of heme-imidazole-carbon monoxide mixtures, J. Am. Chem. Soc. 101 (1979) 2443–2454.
[81] D. Barrick, Replacement of the proximal ligand of sperm whale myoglobin with free imidazole in the mutant His-93 → Gly, Biochemistry 33 (1994) 6546–6554.
[82] D. Barrick, Trans-substitution of the proximal hydrogen bond in myoglobin: II. Energetics, functional consequences, and implications for hemoglobin allostery, Proteins 39 (2000) 291–308.
[83] D. Barrick, F.W. Dahlquist, Trans-substitution of the proximal hydrogen bond in myoglobin: I. Structural consequences of hydrogen bond deletion, Proteins 39 (2000) 278–290.
[84] S. Kundu, B. Snyder, K. Das, P. Chowdhury, J. Park, J.W. Petrich, M.S. Hargrove, The leghemoglobin proximal heme pocket directs oxygen dissociation and stabilizes bound heme, Proteins 46 (2002) 268–277.
[85] D. Barrick, N.T. Ho, V. Simplaceanu, F.W. Dahlquist, C. Ho, A test of the role of the proximal histidines in the Perutz model for cooperativity in haemoglobin, Nat. Struct. Biol. 4 (1997) 78–83.
[86] D. Barrick, N.T. Ho, V. Simplaceanu, C. Ho, Distal ligand reactivity and quaternary structure studies of proximally detached hemoglobins, Biochemistry 40 (2001) 3780–3795.
[87] S. Kundu, M.S. Hargrove, Distal heme pocket regulation of ligand binding and stability in soybean leghemoglobin, Proteins 50 (2003) 239–248.
[88] S.J. Smerdon, S. Krzywda, A.J. Wilkinson, R.E. Brantley Jr., T.E. Carver, M.S. Hargrove, J.S. Olson, Serine92 (F7) contributes to the control of heme reactivity and stability in myoglobin, Biochemistry 32 (1993) 5132–5138.
[89] Q.H. Gibson, J.B. Wittenberg, B.A. Wittenberg, D. Bogusz, C.A. Appleby, The kinetics of ligand binding to plant hemoglobins. Structural implications, J. Biol. Chem. 264 (1989) 100–107.
[90] M.S. Hargrove, J.K. Barry, E.A. Brucker, M.B. Berry, G.N. Phillips Jr., J.S. Olson, R. Arredondo-Peter, J.M. Dean, R.V. Klucas, G. Sarath, Characterization of recombinant soybean leghemoglobin a and apolar distal histidine mutants, J. Mol. Biol. 266 (1997) 1032–1042.
[91] E.H. Harutyunyan, T.N. Safonova, I.P. Kuranova, A.N. Popov, A.V. Teplyakov, G.V. Obmolova, A.A. Rusakov, B.K. Vainshtein, G.G. Dodson, J.C. Wilson, et al., The structure of deoxy- and oxy-leghaemoglobin from lupin, J. Mol. Biol. 251 (1995) 104–115.
[92] A. Pesce, S. Dewilde, L. Kiger, M. Milani, P. Ascenzi, M.C. Marden, M.L. Van Hauwaert, J. Vanfleteren, L. Moens, M. Bolognesi, Very high resolution structure of a trematode hemoglobin displaying a TyrB10-TyrE7 heme distal residue pair and high oxygen affinity, J. Mol. Biol. 309 (2001) 1153–1164.
[93] L. Kiger, A.K. Rashid, N. Griffon, M. Haque, L. Moens, Q.H. Gibson, C. Poyart, M.C. Marden, Trematode hemoglobins show exceptionally high oxygen affinity, Biophys. J. 75 (1998) 990–998.
[94] M.D. Goodman, M.S. Hargrove, Quaternary structure of rice nonsymbiotic hemoglobin, J. Biol. Chem. 276 (2001) 6834–6839.
[95] A.N. Hvitved, J.T. Trent III, S.A. Premer, M.S. Hargrove, Ligand binding and hexacoordination in *Synechocystis* hemoglobin, J. Biol. Chem. 276 (2001) 34714–34721.
[96] A. Ilari, P. Kjelgaard, C. von Wachenfeldt, B. Catacchio, E. Chiancone, A. Boffi, Crystal structure and ligand binding properties of the truncated hemoglobin from *Geobacillus stearothermophilus*, Arch. Biochem. Biophys. 457 (2007) 85–94.
[97] H. Ouellet, L. Juszczak, D. Dantsker, U. Samuni, Y.H. Ouellet, P.Y. Savard, J.B. Wittenberg, B.A. Wittenberg, J.M. Friedman, M. Guertin, Reactions of *Mycobacterium tuberculosis* truncated hemoglobin O with ligands reveal a novel ligand-inclusive hydrogen bond network, Biochemistry 42 (2003) 5764–5774.
[98] T.G. Spiro, M.Z. Zgierski, P.M. Kozlowski, Stereoelectronic factors in CO, NO and O_2 binding to heme from vibrational spectroscopy and DFT analysis, Coord. Chem. Rev. 219 (2001) 923–936.
[99] T.G. Spiro, A.V. Soldatova, G. Balakrishnan, CO, NO and O_2 as vibrational probes of heme protein interactions, Coord. Chem. Rev. 257 (2013) 511–527.
[100] M.A. Marti, D.A. Scherlis, F.A. Doctorovich, P. Ordejon, D.A. Estrin, Modulation of the NO trans effect in heme proteins: implications for the activation of soluble guanylate cyclase, J. Biol. Inorg. Chem. 8 (2003) 595–600.
[101] L. Capece, M.A. Marti, A. Crespo, F. Doctorovich, D.A. Estrin, Heme protein oxygen affinity regulation exerted by proximal effects, J. Am. Chem. Soc. 128 (2006) 12455–12461.
[102] A.L. Tsai, V. Berka, E. Martin, J.S. Olson, A "sliding scale rule" for selectivity among NO, CO, and O(2) by heme protein sensors, Biochemistry 51 (2012) 172–186.
[103] E.J. Murphy, A. Marechal, A.W. Segal, P.R. Rich, CO binding and ligand discrimination in human myeloperoxidase, Biochemistry 49 (2010) 2150–2158.
[104] U. Ermler, R.A. Siddiqui, R. Cramm, B. Friedrich, Crystal structure of the flavohemoglobin from *Alcaligenes eutrophus* at 1.75 A resolution, EMBO J. 14 (1995) 6067–6077.
[105] E. El Hammi, E. Warkentin, U. Demmer, N.M. Marzouki, U. Ermler, L. Baciou, Active site analysis of yeast flavohemoglobin based on its structure with a small ligand or econazole, FEBS J. 279 (2012) 4565–4575.
[106] C. Lu, M. Mukai, Y. Lin, G. Wu, R.K. Poole, S.R. Yeh, Structural and functional properties of a single domain hemoglobin from the food-borne pathogen

Campylobactor jejuni, J. Biol. Chem. 282 (2007) 25917–25928.
[107] M. Shepherd, V. Barynin, C. Lu, P.V. Bernhardt, G. Wu, S.R. Yeh, T. Egawa, S.E. Sedelnikova, D.W. Rice, J.L. Wilson, R.K. Poole, The single-domain globin from the pathogenic bacterium *Campylobacter jejuni*: novel D-helix conformation, proximal hydrogen bonding that influences ligand binding, and peroxidase-like redox properties, J. Biol. Chem. 285 (2010) 12747–12754.
[108] M. Mukai, C.E. Mills, R.K. Poole, S.R. Yeh, Flavohemoglobin, a globin with a peroxidase-like catalytic site, J. Biol. Chem. 276 (2001) 7272–7277.
[109] T.L. Poulos, The role of the proximal ligand in heme enzymes, JBIC, J. Biol. Inorg. Chem. 1 (1996) 356–359.
[110] J.H. Dawson, Probing structure-function relations in heme-containing oxygenases and peroxidases, Science 240 (1988) 433–439.
[111] Y. Mizutani, T. Kitagawa, Ultrafast structural relaxation of myoglobin following photodissociation of carbon monoxide probed by time-resolved resonance Raman spectroscopy, J. Phys. Chem. B 105 (2001) 10992–10999.
[112] J. Kincaid, P. Stein, T.G. Spiro, Absence of heme-localized strain in T state hemoglobin: insensitivity of heme-imidazole resonance Raman frequencies to quaternary structure, Proc. Natl. Acad. Sci. U. S. A. 76 (1979) 549–552.
[113] O. Bangcharoenpaurpong, K.T. Schomacker, P.M. Champion, Resonance Raman investigation of myoglobin and hemoglobin, J. Am. Chem. Soc. 106 (1984) 5688–5698.
[114] M.R. Ondrias, D.L. Rousseau, J.A. Shelnutt, S.R. Simon, Quaternary-transformation-induced changes at the heme in deoxyhemoglobins, Biochemistry 21 (1982) 3428–3437.
[115] J.M. Friedman, T.W. Scott, R.A. Stepnoski, M. Ikeda-Saito, T. Yonetani, The iron-proximal histidine linkage and protein control of oxygen binding in hemoglobin. A transient Raman study, J. Biol. Chem. 258 (1983) 10564–10572.
[116] G. Balakrishnan, M. Ibrahim, P.J. Mak, J. Hata, J.R. Kincaid, T.G. Spiro, Linking conformation change to hemoglobin activation via chain-selective time-resolved resonance Raman spectroscopy of protoheme/mesoheme hybrids, J. Biol. Inorg. Chem. 14 (2009) 741–750.
[117] Y. Mizutani, M. Nagai, Ultrafast protein dynamics of hemoglobin as studied by picosecond time-resolved resonance Raman spectroscopy, Chem. Phys. 396 (2012) 45–52.
[118] G. Smulevich, R. Evangelista-Kirkup, A. English, T.G. Spiro, Raman and infrared spectra of cytochrome c peroxidase-carbon monoxide adducts in alternative conformational states, Biochemistry 25 (1986) 4426–4430.
[119] J. Teraoka, T. Kitagawa, Structural implication of the heme-linked ionization of horseradish peroxidase probed by the Fe-histidine stretching Raman line, J. Biol. Chem. 256 (1981) 3969–3977.
[120] C.E. Cooper, N. Ioannidis, R. D'Mello, R.K. Poole, Haem, flavin and oxygen interactions in Hmp, a flavohaemoglobin from *Escherichia coli*, Biochem. Soc. Trans. 22 (1994) 709–713.
[121] E. Antonini, J. Wyman, M. Brunori, J.F. Taylor, A. Rossi-Fanelli, A. Caputo, Studies on the oxidation-reduction potentials of heme proteins. I. Human hemoglobin, J. Biol. Chem. 239 (1964) 907–912.
[122] H. Yamada, R. Makino, I. Yamazaki, Effects of 2,4-substituents of deuteropheme upon redox potentials of horseradish peroxidases, Arch. Biochem. Biophys. 169 (1975) 344–353.
[123] C.W. Conroy, P. Tyma, P.H. Daum, J.E. Erman, Oxidation-reduction potential measurements of cytochrome c peroxidase and pH dependent spectral transitions in the ferrous enzyme, Biochim. Biophys. Acta 537 (1978) 62–69.
[124] C.J. Reedy, M.M. Elvekrog, B.R. Gibney, Development of a heme protein structure-electrochemical function database, Nucleic Acids Res. 36 (2008) D307–13.
[125] D.P. Hildebrand, D.L. Burk, R. Maurus, J.C. Ferrer, G.D. Brayer, A.G. Mauk, The proximal ligand variant His93Tyr of horse heart myoglobin, Biochemistry 34 (1995) 1997–2005.
[126] C.S. Thom, C.F. Dickson, D.A. Gell, M.J. Weiss, Hemoglobin variants: biochemical properties and clinical correlates, Cold Spring Harb. Perspect. Med. 3 (2013) a011858.
[127] J.S. Olson, G.N. Phillips Jr., Myoglobin discriminates between O_2, NO and CO by electrostatic interactions with the bound ligand, J. Biol. Inorg. Chem. 2 (1997) 544–552.
[128] L. Pauling, J.J. Weiss, Nature of the iron-oxygen bond in oxyhaemoglobin, Nature 203 (1964) 182–183.
[129] J.J. Weiss, Nature of the iron-oxygen bond in oxyhaemoglobin, Nature 202 (1964) 83–84.
[130] J.B. Wittenberg, B.A. Wittenberg, J. Peisach, W.E. Blumberg, On the state of the iron and the nature of the ligand in oxyhemoglobin, Proc. Natl. Acad. Sci. U. S. A. 67 (1970) 1846–1853.
[131] H. Chen, M. Ikeda-Saito, S. Shaik, Nature of the Fe—O_2 bonding in oxy-myoglobin: effect of the protein, J. Am. Chem. Soc. 130 (2008) 14778–14790.
[132] K.L. Bren, R. Eisenberg, H.B. Gray, Discovery of the magnetic behavior of hemoglobin: a beginning of bioinorganic chemistry, Proc. Natl. Acad. Sci. U. S. A. 112 (2015) 13123–13127.
[133] S.A. Wilson, E. Green, Mathews II, M. Benfatto, K.O. Hodgson, B. Hedman, R. Sarangi, X-ray absorption spectroscopic investigation of the electronic structure differences in solution and crystalline oxyhemoglobin, Proc. Natl. Acad. Sci. U. S. A. 110 (2013) 16333–16338.
[134] S.A. Wilson, T. Kroll, R.A. Decreau, R.K. Hocking, M. Lundberg, B. Hedman, K.O. Hodgson, E.I. Solomon, Iron L-edge X-ray absorption spectroscopy of oxy-picket fence porphyrin: experimental insight into Fe—O_2 bonding, J. Am. Chem. Soc. 135 (2013) 1124–1136.
[135] C.H. Barlow, J.C. Maxwell, W.J. Wallace, W.S. Caughey, Elucidation of the mode of binding of oxygen to iron in oxyhemoglobin by infrared spectroscopy, Biochem. Biophys. Res. Commun. 55 (1973) 91–96.
[136] J.C. Maxwell, J.A. Volpe, C.H. Barlow, W.S. Caughey, Infrared evidence for the mode of binding of oxygen to iron of myoglobin from heart muscle, Biochem. Biophys. Res. Commun. 58 (1974) 166–171.
[137] J.P. Collman, J.I. Brauman, T.R. Halbert, K.S. Suslick, Nature of O_2 and CO binding to metalloporphyrins and heme proteins, Proc. Natl. Acad. Sci. U. S. A. 73 (1976) 3333–3337.
[138] K.P. Jensen, U. Ryde, How O_2 binds to heme: reasons for rapid binding and spin inversion, J. Biol. Chem. 279 (2004) 14561–14569.
[139] R.J. Rohlfs, A.J. Mathews, T.E. Carver, J.S. Olson, B.A. Springer, K.D. Egeberg, S.G. Sligar, The effects of amino acid substitution at position E7 (residue 64) on the kinetics of ligand binding to sperm whale myoglobin, J. Biol. Chem. 265 (1990) 3168–3176.
[140] T.G. Spiro, I.H. Wasbotten, CO as a vibrational probe of heme protein active sites, J. Inorg. Biochem. 99 (2005) 34–44.
[141] T. Kitagawa, M.R. Ondrias, D.L. Rousseau, M. Ikeda-Saito, T. Yonetani, Evidence for hydrogen bonding of bound dioxygen to the distal histidine of oxycobalt myoglobin and haemoglobin, Nature 298 (1982) 869–871.
[142] D. Morikis, P.M. Champion, B.A. Springer, S.G. Sligar, Resonance raman investigations of site-directed mutants of myoglobin: effects of distal histidine replacement, Biochemistry 28 (1989) 4791–4800.
[143] M. Unno, J.F. Christiansen, J.S. Olson, J.T. Sage, P.M. Champion, Evidence for hydrogen bonding effects in the iron ligand vibrations of carbonmonoxy myoglobin, J. Am. Chem. Soc. 120 (1998) 2670–2671.
[144] T. Yonetani, H. Yamamoto, T. Iizuka, Studies on cobalt myoglobins and hemoglobins. 3. Electron paramagnetic resonance studies of reversible oxygenation of cobalt myoglobins and hemoglobins, J. Biol. Chem. 249 (1974) 2168–2174.
[145] S.E. Phillips, Structure and refinement of oxymyoglobin at 1.6 A resolution, J. Mol. Biol. 142 (1980) 531–554.
[146] B. Shaanan, The iron-oxygen bond in human oxyhaemoglobin, Nature 296 (1982) 683–684.
[147] S.E. Phillips, B.P. Schoenborn, Neutron diffraction reveals oxygen-histidine hydrogen bond in oxymyoglobin, Nature 292 (1981) 81–82.
[148] J.A. Lukin, V. Simplaceanu, M. Zou, N.T. Ho, C. Ho, NMR reveals hydrogen bonds between oxygen and distal histidines in oxyhemoglobin, Proc. Natl. Acad. Sci. U. S. A. 97 (2000) 10354–10358.
[149] J.S. Olson, G.N. Phillips Jr., Kinetic pathways and barriers for ligand binding to myoglobin, J. Biol. Chem. 271 (1996) 17593–17596.
[150] D.A. Scherlis, D.A. Estrin, Hydrogen bonding and O_2 affinity of hemoglobins, J. Am. Chem. Soc. 123 (2001) 8436–8437.
[151] B.A. Springer, K.D. Egeberg, S.G. Sligar, R.J. Rohlfs, A.J. Mathews, J.S. Olson, Discrimination between oxygen and carbon monoxide and inhibition of autooxidation by myoglobin. Site-directed mutagenesis of the distal histidine, J. Biol. Chem. 264 (1989) 3057–3060.
[152] M.L. Quillin, R.M. Arduini, J.S. Olson, G.N. Phillips Jr., High-resolution crystal structures of distal histidine mutants of sperm whale myoglobin, J. Mol. Biol. 234 (1993) 140–155.
[153] R.A. Goldbeck, S. Bhaskaran, C. Ortega, J.L. Mendoza, J.S. Olson, J. Soman, D.S. Kliger, R.M. Esquerra, Water and ligand entry in myoglobin: assessing the speed and extent of heme pocket hydration after CO photodissociation, Proc. Natl. Acad. Sci. U. S. A. 103 (2006) 1254–1259.
[154] J.P. Bustamante, S. Abbruzzetti, A. Marcelli, D. Gauto, L. Boechi, A. Bonamore, A. Boffi, S. Bruno, A. Feis, P. Foggi, D.A. Estrin, C. Viappiani, Ligand uptake modulation by internal water molecules and hydrophobic cavities in hemoglobins, J. Phys. Chem. B 118 (2014) 1234–1245.
[155] I. Birukou, R.L. Schweers, J.S. Olson, Distal histidine stabilizes bound O_2 and acts as a gate for ligand entry in both subunits of adult human hemoglobin, J. Biol. Chem. 285 (2010) 8840–8854.
[156] I. Degtyarenko, R.M. Nieminen, C. Rovira, Structure and dynamics of dioxygen bound to cobalt and iron heme, Biophys. J. 91 (2006) 2024–2034.
[157] A. Ilari, A. Bonamore, A. Farina, K.A. Johnson, A. Boffi, The X-ray structure of ferric *Escherichia coli* flavohemoglobin reveals an unexpected geometry of the distal heme pocket, J. Biol. Chem. 277 (2002) 23725–23732.
[158] E. El Hammi, E. Warkentin, U. Demmer, F. Limam, N.M. Marzouki, U. Ermler, L. Baciou, Structure of *Ralstonia eutropha* flavohemoglobin in complex with three antibiotic azole compounds, Biochemistry 50 (2011) 1255–1264.
[159] J. Yang, A.P. Kloek, D.E. Goldberg, F.S. Mathews, The structure of *Ascaris* hemoglobin domain I at 2.2 A resolution: molecular features of oxygen avidity, Proc. Natl. Acad. Sci. U. S. A. 92 (1995) 4224–4228.
[160] Q.H. Gibson, R. Regan, J.S. Olson, T.E. Carver, B. Dixon, B. Pohajdak, P.K. Sharma, S.N. Vinogradov, Kinetics of ligand binding to *Pseudoterranova decipiens* and *Ascaris suum* hemoglobins and to Leu-29 → Tyr sperm whale myoglobin mutant, J. Biol. Chem. 268 (1993) 16993–16998.
[161] A. Pesce, M. Nardini, S. Dewilde, E. Geuens, K. Yamauchi, P. Ascenzi, A.F. Riggs, L. Moens, M. Bolognesi, The 109 residue nerve tissue minihemoglobin from *Cerebratulus lacteus* highlights striking structural plasticity of the α-helical globin fold, Structure 10 (2002) 725–735.
[162] F. Germani, A. Pesce, A. Venturini, L. Moens, M. Bolognesi, S. Dewilde, M. Nardini, High resolution crystal structures of the *Cerebratulus lacteus* mini-Hb in the unligated and carbomonoxy states, Int. J. Mol. Sci. 13 (2012) 8025–8037.
[163] M.A. Marti, D.E. Bikiel, A. Crespo, M. Nardini, M. Bolognesi, D.A. Estrin, Two distinct heme distal site states define *Cerebratulus lacteus* mini-hemoglobin oxygen affinity, Proteins 62 (2006) 641–648.
[164] A. Pesce, M. Nardini, P. Ascenzi, E. Geuens, S. Dewilde, L. Moens, M. Bolognesi, A.F. Riggs, A. Hale, P. Deng, G.U. Nienhaus, J.S. Olson, K. Nienhaus, Thr-E11 regulates O_2 affinity in *Cerebratulus lacteus* mini-hemoglobin, J. Biol. Chem. 279 (2004) 33662–33672.

[165] M.A. Marti, A. Crespo, L. Capece, L. Boechi, D.E. Bikiel, D.A. Scherlis, D.A. Estrin, Dioxygen affinity in heme proteins investigated by computer simulation, J. Inorg. Biochem. 100 (2006) 761–770.
[166] T.K. Das, R.E. Weber, S. Dewilde, J.B. Wittenberg, B.A. Wittenberg, K. Yamauchi, M.L. Van Hauwaert, L. Moens, D.L. Rousseau, Ligand binding in the ferric and ferrous states of *Paramecium* hemoglobin, Biochemistry 39 (2000) 14330–14340.
[167] M.A. Marti, L. Capece, D.E. Bikiel, B. Falcone, D.A. Estrin, Oxygen affinity controlled by dynamical distal conformations: the soybean leghemoglobin and the *Paramecium caudatum* hemoglobin cases, Proteins 68 (2007) 480–487.
[168] G.N. Phillips, M.L. Teodoro, T. Li, B. Smith, J.S. Olson, Bound CO is a molecular probe of electrostatic potential in the distal pocket of myoglobin, J. Phys. Chem. B 103 (1999) 8817–8829.
[169] S. Kundu, G.C. Blouin, S.A. Premer, G. Sarath, J.S. Olson, M.S. Hargrove, Tyrosine B10 inhibits stabilization of bound carbon monoxide and oxygen in soybean leghemoglobin, Biochemistry 43 (2004) 6241–6252.
[170] M. Tarnawski, T.R. Barends, I. Schlichting, Structural analysis of an oxygen-regulated diguanylate cyclase, Acta Crystallogr. D Biol. Crystallogr. 71 (2015) 2158–2177.
[171] A. Pesce, L. Thijs, M. Nardini, F. Desmet, L. Sisinni, L. Gourlay, A. Bolli, M. Coletta, S. Van Doorslaer, X. Wan, M. Alam, P. Ascenzi, L. Moens, M. Bolognesi, S. Dewilde, HisE11 and HisF8 provide bis-histidyl heme hexa-coordination in the globin domain of *Geobacter sulfurreducens* globin-coupled sensor, J. Mol. Biol. 386 (2009) 246–260.
[172] L. Tilleman, S. Abbruzzetti, C. Ciaccio, G. De Sanctis, M. Nardini, A. Pesce, F. Desmet, L. Moens, S. Van Doorslaer, S. Bruno, M. Bolognesi, P. Ascenzi, M. Coletta, C. Viappiani, S. Dewilde, Structural basis for the regulation of CO binding in the archaeal protoglobin from *Methanosarcina acetivorans*, PLoS One 10 (2015) e0125959.
[173] A. Pesce, L. Tilleman, J. Donne, E. Aste, P. Ascenzi, C. Ciaccio, M. Coletta, L. Moens, C. Viappiani, S. Dewilde, M. Bolognesi, M. Nardini, Structure and haem-distal site plasticity in *Methanosarcina acetivorans* protoglobin, PLoS One 8 (2013) e66144.
[174] J. Igarashi, K. Kobayashi, A. Matsuoka, A hydrogen-bonding network formed by the B10-E7-E11 residues of a truncated hemoglobin from *Tetrahymena pyriformis* is critical for stability of bound oxygen and nitric oxide detoxification, J. Biol. Inorg. Chem. 16 (2011) 599–609.
[175] M. Couture, S.R. Yeh, B.A. Wittenberg, J.B. Wittenberg, Y. Ouellet, D.L. Rousseau, M. Guertin, A cooperative oxygen-binding hemoglobin from *Mycobacterium tuberculosis*, Proc. Natl. Acad. Sci. U. S. A. 96 (1999) 11223–11228.
[176] S.R. Yeh, M. Couture, Y. Ouellet, M. Guertin, D.L. Rousseau, A cooperative oxygen binding hemoglobin from *Mycobacterium tuberculosis*. Stabilization of heme ligands by a distal tyrosine residue, J. Biol. Chem. 275 (2000) 1679–1684.
[177] H. Ouellet, M. Milani, M. LaBarre, M. Bolognesi, M. Couture, M. Guertin, The roles of Tyr(CD1) and Trp(G8) in *Mycobacterium tuberculosis* truncated hemoglobin O in ligand binding and on the heme distal site architecture, Biochemistry 46 (2007) 11440–11450.
[178] M. Milani, P.Y. Savard, H. Ouellet, P. Ascenzi, M. Guertin, M. Bolognesi, A TyrCD1/TrpG8 hydrogen bond network and a TyrB10TyrCD1 covalent link shape the heme distal site of *Mycobacterium tuberculosis* hemoglobin O, Proc. Natl. Acad. Sci. U. S. A. 100 (2003) 5766–5771.
[179] M. Mukai, P.Y. Savard, H. Ouellet, M. Guertin, S.R. Yeh, Unique ligand-protein interactions in a new truncated hemoglobin from *Mycobacterium tuberculosis*, Biochemistry 41 (2002) 3897–3905.
[180] M. Nardini, A. Pesce, M. Labarre, C. Richard, A. Bolli, P. Ascenzi, M. Guertin, M. Bolognesi, Structural determinants in the group III truncated hemoglobin from *Campylobacter jejuni*, J. Biol. Chem. 281 (2006) 37803–37812.
[181] C. Lu, T. Egawa, L.M. Wainwright, R.K. Poole, S.R. Yeh, Structural and functional properties of a truncated hemoglobin from a food-borne pathogen *Campylobacter jejuni*, J. Biol. Chem. 282 (2007) 13627–13636.
[182] P. Arroyo Manez, C. Lu, L. Boechi, M.A. Marti, M. Shepherd, J.L. Wilson, R.K. Poole, F.J. Luque, S.R. Yeh, D.A. Estrin, Role of the distal hydrogen-bonding network in regulating oxygen affinity in the truncated hemoglobin III from *Campylobacter jejuni*, Biochemistry 50 (2011) 3946–3956.
[183] B. Stec, G.N. Phillips Jr., How the CO in myoglobin acquired its bend: lessons in interpretation of crystallographic data, Acta Crystallogr. Sect. D 57 (2001) 751–754.
[184] J. Vojtechovsky, K. Chu, J. Berendzen, R.M. Sweet, I. Schlichting, Crystal structures of myoglobin-ligand complexes at near-atomic resolution, Biophys. J. 77 (1999) 2153–2174.
[185] G.S. Kachalova, A.N. Popov, H.D. Bartunik, A steric mechanism for inhibition of CO binding to heme proteins, Science 284 (1999) 473–476.
[186] T.E. Carver, R.E. Brantley Jr., E.W. Singleton, R.M. Arduini, M.L. Quillin, G.N. Phillips Jr., J.S. Olson, A novel site-directed mutant of myoglobin with an unusually high O_2 affinity and low autooxidation rate, J. Biol. Chem. 267 (1992) 14443–14450.
[187] M.L. Quillin, T. Li, J.S. Olson, G.N. Phillips Jr., Y. Dou, M. Ikeda-Saito, R. Regan, M. Carlson, Q.H. Gibson, H. Li, et al., Structural and functional effects of apolar mutations of the distal valine in myoglobin, J. Mol. Biol. 245 (1995) 416–436.
[188] D.G. Lambright, S. Balasubramanian, S.M. Decatur, S.G. Boxer, Anatomy and dynamics of a ligand-binding pathway in myoglobin: the roles of residues 45, 60, 64, and 68, Biochemistry 33 (1994) 5518–5525.
[189] Q.H. Gibson, R. Regan, R. Elber, J.S. Olson, T.E. Carver, Distal pocket residues affect picosecond ligand recombination in myoglobin. An experimental and molecular dynamics study of position 29 mutants, J. Biol. Chem. 267 (1992) 22022–22034.
[190] F. Schotte, J. Soman, J.S. Olson, M. Wulff, P.A. Anfinrud, Picosecond time-resolved X-ray crystallography: probing protein function in real time, J. Struct. Biol. 147 (2004) 235–246.
[191] I. Birukou, D.H. Maillett, A. Birukova, J.S. Olson, Modulating distal cavities in the α and β subunits of human HbA reveals the primary ligand migration pathway, Biochemistry 50 (2011) 7361–7374.
[192] H.H. Lai, T. Li, D.S. Lyons, G.N. Phillips Jr., J.S. Olson, Q.H. Gibson, Phe-46(CD4) orients the distal histidine for hydrogen bonding to bound ligands in sperm whale myoglobin, Proteins 22 (1995) 322–339.
[193] L. Boechi, M. Arrar, M.A. Marti, J.S. Olson, A.E. Roitberg, D.A. Estrin, Hydrophobic effect drives oxygen uptake in myoglobin via histidine E7, J. Biol. Chem. 288 (2013) 6754–6762.
[194] M.F. Perutz, F.S. Mathews, An x-ray study of azide methaemoglobin, J. Mol. Biol. 21 (1966) 199–202.
[195] M.F. Perutz, Myoglobin and haemoglobin: role of distal residues in reactions with haem ligands, Trends Biochem. Sci. 14 (1989) 42–44.
[196] M. Bolognesi, E. Cannillo, P. Ascenzi, G.M. Giacometti, A. Merli, M. Brunori, Reactivity of ferric *Aplysia* and sperm whale myoglobins towards imidazole: X-ray and binding study, J. Mol. Biol. 158 (1982) 305–315.
[197] K.A. Johnson, J.S. Olson, G.N. Phillips Jr., Structure of myoglobin-ethyl isocyanide. Histidine as a swinging door for ligand entry, J. Mol. Biol. 207 (1989) 459–463.
[198] D. Ringe, G.A. Petsko, D.E. Kerr, P.R. Ortiz de Montellano, Reaction of myoglobin with phenylhydrazine: a molecular doorstop, Biochemistry 23 (1984) 2–4.
[199] F. Yang, G.N. Phillips Jr., Crystal structures of CO-, deoxy- and met-myoglobins at various pH values, J. Mol. Biol. 256 (1996) 762–774.
[200] P. Jewsbury, T. Kitagawa, The distal residue-CO interaction in carbonmonoxy myoglobins: a molecular dynamics study of two distal histidine tautomers, Biophys. J. 67 (1994) 2236–2250.
[201] B.P. Schoenborn, H.C. Watson, J.C. Kendrew, Binding of xenon to sperm whale myoglobin, Nature 207 (1965) 28–30.
[202] R.F. Tilton Jr., I.D. Kuntz Jr., G.A. Petsko, Cavities in proteins: structure of a metmyoglobin-xenon complex solved to 1.9 A, Biochemistry 23 (1984) 2849–2857.
[203] J. Cohen, A. Arkhipov, R. Braun, K. Schulten, Imaging the migration pathways for O_2, CO, NO, and Xe inside myoglobin, Biophys. J. 91 (2006) 1844–1857.
[204] E.E. Scott, Q.H. Gibson, Ligand migration in sperm whale myoglobin, Biochemistry 36 (1997) 11909–11917.
[205] A. Ostermann, R. Waschipky, F.G. Parak, G.U. Nienhaus, Ligand binding and conformational motions in myoglobin, Nature 404 (2000) 205–208.
[206] I. Birukou, J. Soman, J.S. Olson, Blocking the gate to ligand entry in human hemoglobin, J. Biol. Chem. 286 (2011) 10515–10529.
[207] J.E. Knapp, R. Pahl, J. Cohen, J.C. Nichols, K. Schulten, Q.H. Gibson, V. Srajer, W.E. Royer Jr., Ligand migration and cavities within scapharca dimeric HbI: studies by time-resolved crystallo-graphy, Xe binding, and computational analysis, Structure 17 (2009) 1494–1504.
[208] K. Nienhaus, J.E. Knapp, P. Palladino, W.E. Royer Jr., G.U. Nienhaus, Ligand migration and binding in the dimeric hemoglobin of *Scapharca inaequivalvis*, Biochemistry 46 (2007) 14018–14031.
[209] M. Bringas, A.A. Petruk, D.A. Estrin, L. Capece, M.A. Marti, Tertiary and quaternary structural basis of oxygen affinity in human hemoglobin as revealed by multiscale simulations, Sci Rep 7 (2017) 10926.
[210] M. Milani, A. Pesce, Y. Ouellet, S. Dewilde, J. Friedman, P. Ascenzi, M. Guertin, M. Bolognesi, Heme-ligand tunneling in group I truncated hemoglobins, J. Biol. Chem. 279 (2004) 21520–21525.
[211] M. Milani, Y. Ouellet, H. Ouellet, M. Guertin, A. Boffi, G. Antonini, A. Bocedi, M. Mattu, M. Bolognesi, P. Ascenzi, Cyanide binding to truncated hemoglobins: a crystallographic and kinetic study, Biochemistry 43 (2004) 5213–5221.
[212] M. Milani, A. Pesce, Y. Ouellet, P. Ascenzi, M. Guertin, M. Bolognesi, *Mycobacterium tuberculosis* hemoglobin N displays a protein tunnel suited for O_2 diffusion to the heme, EMBO J. 20 (2001) 3902–3909.
[213] L. Boechi, M.A. Marti, M. Milani, M. Bolognesi, F.J. Luque, D.A. Estrin, Structural determinants of ligand migration in *Mycobacterium tuberculosis* truncated hemoglobin O, Proteins 73 (2008) 372–379.
[214] V. Guallar, C. Lu, K. Borrelli, T. Egawa, S.R. Yeh, Ligand migration in the truncated hemoglobin-II from *Mycobacterium tuberculosis*: the role of G8 tryptophan, J. Biol. Chem. 284 (2009) 3106–3116.
[215] A. Marcelli, S. Abbruzzetti, J.P. Bustamante, A. Feis, A. Bonamore, A. Boffi, C. Gellini, P.R. Salvi, D.A. Estrin, S. Bruno, C. Viappiani, P. Foggi, Following ligand migration pathways from picoseconds to milliseconds in type II truncated hemoglobin from *Thermobifida fusca*, PLoS One 7 (2012) e39884.
[216] A. Bonamore, A. Ilari, L. Giangiacomo, A. Bellelli, V. Morea, A. Boffi, A novel thermostable hemoglobin from the actinobacterium *Thermobifida fusca*, FEBS J. 272 (2005) 4189–4201.
[217] M.D. Salter, K. Nienhaus, G.U. Nienhaus, S. Dewilde, L. Moens, A. Pesce, M. Nardini, M. Bolognesi, J.S. Olson, The apolar channel in *Cerebratulus lacteus* hemoglobin is the route for O_2 entry and exit, J. Biol. Chem. 283 (2008) 35689–35702.
[218] A. Pesce, M. Nardini, S. Dewilde, L. Capece, M.A. Marti, S. Congia, M.D. Salter, G.C. Blouin, D.A. Estrin, P. Ascenzi, L. Moens, M. Bolognesi, J.S. Olson, Ligand migration in the apolar tunnel of *Cerebratulus lacteus* mini-hemoglobin, J. Biol. Chem. 286 (2011) 5347–5358.
[219] J.P. Bustamante, M.E. Szretter, M. Sued, M.A. Marti, D.A. Estrin, L. Boechi, A quantitative model for oxygen uptake and release in a family of hemeproteins, Bioinformatics 32 (2016) 1805–1813.
[220] Y.H. Ouellet, R. Daigle, P. Lague, D. Dantsker, M. Milani, M. Bolognesi, J.M. Friedman, M. Guertin, Ligand binding to truncated hemoglobin N from

Mycobacterium tuberculosis is strongly modulated by the interplay between the distal heme pocket residues and internal water, J. Biol. Chem. 283 (2008) 27270–27278.
[221] A. Jasaitis, H. Ouellet, J.-C. Lambry, J.-L. Martin, J.M. Friedman, M. Guertin, M.H. Vos, Ultrafast heme-ligand recombination in truncated hemoglobin HbO from *Mycobacterium tuberculosis*: a ligand cage, Chem. Phys. 396 (2012) 10–16.
[222] M. Rougee, D. Brault, Influence of trans weak or strong field ligands upon the affinity of deuteroheme for carbon monoxide. Monoimidazoleheme as a reference for unconstrained five-coordinate hemoproteins, Biochemistry 14 (1975) 4100–4106.
[223] V.L. Robinson, B.B. Smith, A. Arnone, A pH-dependent aquomet-to-hemichrome transition in crystalline horse methemoglobin, Biochemistry 42 (2003) 10113–10125.
[224] D.A. Svistunenko, M.A. Sharpe, P. Nicholls, C. Blenkinsop, N.A. Davies, J. Dunne, M.T. Wilson, C.E. Cooper, The pH dependence of naturally occurring low-spin forms of methaemoglobin and metmyoglobin: an EPR study, Biochem. J. 351 (2000) 595–605.
[225] J.M. Rifkind, O. Abugo, A. Levy, J. Heim, Detection, formation, and relevance of hemichromes and hemochromes, Methods Enzymol. 231 (1994) 449–480.
[226] S. Kakar, F.G. Hoffman, J.F. Storz, M. Fabian, M.S. Hargrove, Structure and reactivity of hexacoordinate hemoglobins, Biophys. Chem. 152 (2010) 1–14.
[227] B.J. Smagghe, J.A. Hoy, R. Percifield, S. Kundu, M.S. Hargrove, G. Sarath, J.L. Hilbert, R.A. Watts, E.S. Dennis, W.J. Peacock, S. Dewilde, L. Moens, G.C. Blouin, J.S. Olson, C.A. Appleby, Review: correlations between oxygen affinity and sequence classifications of plant hemoglobins, Biopolymers 91 (2009) 1083–1096.
[228] T. Burmester, B. Weich, S. Reinhardt, T. Hankeln, A vertebrate globin expressed in the brain, Nature 407 (2000) 520–523.
[229] M. Couture, T. Burmester, T. Hankeln, D.L. Rousseau, The heme environment of mouse neuroglobin. Evidence for the presence of two conformations of the heme pocket, J. Biol. Chem. 276 (2001) 36377–36382.
[230] S. Dewilde, L. Kiger, T. Burmester, T. Hankeln, V. Baudin-Creuza, T. Aerts, M.C. Marden, R. Caubergs, L. Moens, Biochemical characterization and ligand binding properties of neuroglobin, a novel member of the globin family, J. Biol. Chem. 276 (2001) 38949–38955.
[231] J.T. Trent 3rd, R.A. Watts, M.S. Hargrove, Human neuroglobin, a hexacoordinate hemoglobin that reversibly binds oxygen, J. Biol. Chem. 276 (2001) 30106–30110.
[232] H. Sawai, N. Kawada, K. Yoshizato, H. Nakajima, S. Aono, Y. Shiro, Characterization of the heme environmental structure of cytoglobin, a fourth globin in humans, Biochemistry 42 (2003) 5133–5142.
[233] N. Kawada, D.B. Kristensen, K. Asahina, K. Nakatani, Y. Minamiyama, S. Seki, K. Yoshizato, Characterization of a stellate cell activation-associated protein (STAP) with peroxidase activity found in rat hepatic stellate cells, J. Biol. Chem. 276 (2001) 25318–25323.
[234] P. Corti, J. Xue, J. Tejero, N. Wajih, M. Sun, D.B. Stolz, M. Tsang, D.B. Kim-Shapiro, M.T. Gladwin, Globin X is a six-coordinate globin that reduces nitrite to nitric oxide in fish red blood cells, Proc. Natl. Acad. Sci. U. S. A. 113 (2016) 8538–8543.
[235] A. Roesner, C. Fuchs, T. Hankeln, T. Burmester, A globin gene of ancient evolutionary origin in lower vertebrates: evidence for two distinct globin families in animals, Mol. Biol. Evol. 22 (2005) 12–20.
[236] D. de Sanctis, S. Dewilde, C. Vonrhein, A. Pesce, L. Moens, P. Ascenzi, T. Hankeln, T. Burmester, M. Ponassi, M. Nardini, M. Bolognesi, Bishistidyl heme hexacoordination, a key structural property in *Drosophila melanogaster* hemoglobin, J. Biol. Chem. 280 (2005) 27222–27229.
[237] S. Dewilde, B. Ebner, E. Vinck, K. Gilany, T. Hankeln, T. Burmester, J. Kreiling, C. Reinisch, J.R. Vanfleteren, L. Kiger, M.C. Marden, C. Hundahl, A. Fago, S. Van Doorslaer, L. Moens, The nerve hemoglobin of the bivalve mollusc *Spisula solidissima*: molecular cloning, ligand binding studies, and phylogenetic analysis, J. Biol. Chem. 281 (2006) 5364–5372.
[238] C.J. Falzone, B. Christie Vu, N.L. Scott, J.T.J. Lecomte, The solution structure of the recombinant hemoglobin from the cyanobacterium *Synechocystis* sp. PCC 6803 in its hemichrome state, J. Mol. Biol. 324 (2002) 1015–1029.
[239] S.L. Rice, L.E. Boucher, J.L. Schlessman, M.R. Preimesberger, J. Bosch, J.T. Lecomte, Structure of *Chlamydomonas reinhardtii* THB1, a group 1 truncated hemoglobin with a rare histidine-lysine heme ligation, Acta Crystallogr. Sect. F: Struct. Biol. Cryst. Commun. 71 (2015) 718–725.
[240] B.J. Reeder, M.A. Hough, The structure of a class 3 nonsymbiotic plant haemoglobin from *Arabidopsis thaliana* reveals a novel N-terminal helical extension, Acta Crystallogr. D Biol. Crystallogr. 70 (2014) 1411–1418.
[241] B.D. Howes, D. Giordano, L. Boechi, R. Russo, S. Mucciacciaro, C. Ciaccio, F. Sinibaldi, M. Fittipaldi, M.A. Marti, D.A. Estrin, G. di Prisco, M. Coletta, C. Verde, G. Smulevich, The peculiar heme pocket of the 2/2 hemoglobin of cold-adapted *Pseudoalteromonas haloplanktis* TAC125, J. Biol. Inorg. Chem. 13 (2010).
[242] L. Kiger, J. Uzan, S. Dewilde, T. Burmester, T. Hankeln, L. Moens, D. Hamdane, V. Baudin-Creuza, M. Marden, Neuroglobin ligand binding kinetics, IUBMB Life 56 (2004) 709–719.
[243] T. Hankeln, V. Jaenicke, L. Kiger, S. Dewilde, G. Ungerechts, M. Schmidt, J. Urban, M.C. Marden, L. Moens, T. Burmester, Characterization of *Drosophila* hemoglobin. Evidence for hemoglobin-mediated respiration in insects, J. Biol. Chem. 277 (2002) 29012–29017.
[244] E. Gleixner, F. Ripp, T.A. Gorr, R. Schuh, C. Wolf, T. Burmester, T. Hankeln, Knockdown of *Drosophila* hemoglobin suggests a role in O_2 homeostasis, Insect Biochem. Mol. Biol. 72 (2016) 20–30.
[245] C. Hundahl, A. Fago, S. Dewilde, L. Moens, T. Hankeln, T. Burmester, R.E. Weber, Oxygen binding properties of non-mammalian nerve globins, FEBS J. 273 (2006) 1323–1329.
[246] P. Ascenzi, S. Gustincich, M. Marino, Mammalian nerve globins in search of functions, IUBMB Life 66 (2014) 268–276.
[247] X. Liu, M.A. El-Mahdy, J. Boslett, S. Varadharaj, C. Hemann, T.M. Abdelghany, R.S. Ismail, S.C. Little, D. Zhou, L.T. Thuy, N. Kawada, J.L. Zweier, Cytoglobin regulates blood pressure and vascular tone through nitric oxide metabolism in the vascular wall, Nat. Commun. 8 (2017) 14807.
[248] M.B. Amdahl, C.E. Sparacino-Watkins, P. Corti, M.T. Gladwin, J. Tejero, Efficient reduction of vertebrate cytoglobins by the cytochrome b5/cytochrome b5 reductase/NADH system, Biochemistry 56 (2017) 3993–4004.
[249] D.A. Greenberg, K. Jin, A.A. Khan, Neuroglobin: an endogenous neuroprotectant, Curr. Opin. Pharmacol. 8 (2008) 20–24.
[250] T.R. Weiland, S. Kundu, J.T. Trent 3rd, J.A. Hoy, M.S. Hargrove, Bis-histidyl hexacoordination in hemoglobins facilitates heme reduction kinetics, J. Am. Chem. Soc. 126 (2004) 11930–11935.
[251] B.J. Smagghe, J.T. Trent 3rd, M.S. Hargrove, NO dioxygenase activity in hemoglobins is ubiquitous in vitro, but limited by reduction in vivo, PLoS One 3 (2008) e2039.
[252] A.J. Kihm, Y. Kong, W. Hong, J.E. Russell, S. Rouda, K. Adachi, M.C. Simon, G.A. Blobel, M.J. Weiss, An abundant erythroid protein that stabilizes free α-haemoglobin, Nature 417 (2002) 758–763.
[253] Y. Kong, S. Zhou, A.J. Kihm, A.M. Katein, X. Yu, D.A. Gell, J.P. Mackay, K. Adachi, L. Foster-Brown, C.S. Louden, A.J. Gow, M.J. Weiss, Loss of α-hemoglobin-stabilizing protein impairs erythropoiesis and exacerbates β-thalassemia, J. Clin. Invest. 114 (2004) 1457–1466.
[254] X. Yu, Y. Kong, L.C. Dore, O. Abdulmalik, A.M. Katein, S. Zhou, J.K. Choi, D. Gell, J.P. Mackay, A.J. Gow, M.J. Weiss, An erythroid chaperone that facilitates folding of α-globin subunits for hemoglobin synthesis, J. Clin. Invest. 117 (2007) 1856–1865.
[255] D. Gell, Y. Kong, S.A. Eaton, M.J. Weiss, J.P. Mackay, Biophysical characterization of the α-globin binding protein α-hemoglobin stabilizing protein, J. Biol. Chem. 277 (2002) 40602–40609.
[256] D.A. Gell, L. Feng, S. Zhou, P.D. Jeffrey, K. Bendak, A. Gow, M.J. Weiss, Y. Shi, J.P. Mackay, A *cis*-proline in α-hemoglobin stabilizing protein directs the structural reorganization of α-hemoglobin, J. Biol. Chem. 284 (2009) 29462–29469.
[257] T.L. Mollan, E. Khandros, M.J. Weiss, J.S. Olson, The kinetics of α-globin binding to α hemoglobin stabilizing protein (AHSP) indicate preferential stabilization of a hemichrome folding intermediate, J. Biol. Chem. 287 (2012) 11338–11350.
[258] L. Feng, D.A. Gell, S. Zhou, L. Gu, Y. Kong, J. Li, M. Hu, N. Yan, C. Lee, A.M. Rich, R.S. Armstrong, P.A. Lay, A.J. Gow, M.J. Weiss, J.P. Mackay, Y. Shi, Molecular mechanism of AHSP-mediated stabilization of α-hemoglobin, Cell 119 (2004) 629–640.
[259] L. Feng, S. Zhou, L. Gu, D.A. Gell, J.P. Mackay, M.J. Weiss, A.J. Gow, Y. Shi, Structure of oxidized α-haemoglobin bound to AHSP reveals a protective mechanism for haem, Nature 435 (2005) 697–701.
[260] D. Hamdane, C. Vasseur-Godbillon, V. Baudin-Creuza, G.H. Hoa, M.C. Marden, Reversible hexacoordination of α-hemoglobin-stabilizing protein (AHSP)/α-hemoglobin versus pressure. Evidence for protection of the α-chains by their chaperone, J. Biol. Chem. 282 (2007) 6398–6404.
[261] C. Vasseur-Godbillon, D. Hamdane, M.C. Marden, V. Baudin-Creuza, High-yield expression in *Escherichia coli* of soluble human α-hemoglobin complexed with its molecular chaperone, Protein Eng. Des. Sel. 19 (2006) 91–97.
[262] S. Zhou, J.S. Olson, M. Fabian, M.J. Weiss, A.J. Gow, Biochemical fates of α hemoglobin bound to α hemoglobin-stabilizing protein AHSP, J. Biol. Chem. 281 (2006) 32611–32618.
[263] C.M. Santiveri, J.M. Perez-Canadillas, M.K. Vadivelu, M.D. Allen, T.J. Rutherford, N.A. Watkins, M. Bycroft, NMR structure of the α-hemoglobin stabilizing protein: insights into conformational heterogeneity and binding, J. Biol. Chem. 279 (2004) 34963–34970.
[264] V. Baudin-Creuza, C. Vasseur-Godbillon, C. Pato, C. Prehu, H. Wajcman, M.C. Marden, Transfer of human α- to β-hemoglobin via its chaperone protein: evidence for a new state, J. Biol. Chem. 279 (2004) 36530–36533.
[265] C.F. Dickson, A.M. Rich, W.M. D'Avigdor, D.A. Collins, J.A. Lowry, T.L. Mollan, E. Khandros, J.S. Olson, M.J. Weiss, J.P. Mackay, P.A. Lay, D.A. Gell, α-Hemoglobin-stabilizing protein (ahsp) perturbs the proximal heme pocket of oxy-α-hemoglobin and weakens the iron-oxygen bond, J. Biol. Chem. 288 (2013) 19986–20001.
[266] T.L. Mollan, S. Banerjee, G. Wu, C.J. Parker Siburt, A.L. Tsai, J.S. Olson, M.J. Weiss, A.L. Crumbliss, A.I. Alayash, α-Hemoglobin stabilizing protein (AHSP) markedly decreases the redox potential and reactivity of α subunits of human HbA with hydrogen peroxide, J. Biol. Chem. 288 (2013) 4288–4298.
[267] J.T. Lecomte, N.L. Scott, B.C. Vu, C.J. Falzone, Binding of ferric heme by the recombinant globin from the cyanobacterium *Synechocystis* sp. PCC 6803, Biochemistry 40 (2001) 6541–6552.
[268] P. Halder, J.T. Trent 3rd, M.S. Hargrove, Influence of the protein matrix on intramolecular histidine ligation in ferric and ferrous hexacoordinate hemoglobins, Proteins 66 (2007) 172–182.
[269] B.R. Van Dyke, P. Saltman, F.A. Armstrong, Control of myoglobin electron-transfer rates by the distal (nonbound) histidine residue, J. Am. Chem. Soc. 118 (1996) 3490–3492.
[270] Y. Dou, S.J. Admiraal, M. Ikeda-Saito, S. Krzywda, A.J. Wilkinson, T. Li, J.S. Olson, R.C. Prince, I.J. Pickering, G.N. George, Alteration of axial coordination by protein engineering in myoglobin. Bisimidazole ligation in the His64 → Val/Val68 → His double mutant, J. Biol. Chem. 270 (1995) 15993–16001.
[271] E. Khandros, T.L. Mollan, X. Yu, X. Wang, Y. Yao, J. D'Souza, D.A. Gell, J.S. Olson,

M.J. Weiss, Insights into hemoglobin assembly through in vivo mutagenesis of α-hemoglobin stabilizing protein, J. Biol. Chem. 287 (2012) 11325–11337.
[272] K. Krishna Kumar, C.F. Dickson, M.J. Weiss, J.P. Mackay, D.A. Gell, AHSP (α-haemoglobin stabilizing protein) stabilizes apo-α-haemoglobin in a partially folded state, Biochem. J. 432 (2010) 275–282.
[273] L. Astudillo, S. Bernad, V. Derrien, P. Sebban, J. Miksovska, Reduction of the internal disulfide bond between Cys 38 and 83 switches the ligand migration pathway in cytoglobin, J. Inorg. Biochem. 129 (2013) 23–29.
[274] D. Hamdane, L. Kiger, S. Dewilde, B.N. Green, A. Pesce, J. Uzan, T. Burmester, T. Hankeln, M. Bolognesi, L. Moens, M.C. Marden, The redox state of the cell regulates the ligand binding affinity of human neuroglobin and cytoglobin, J. Biol. Chem. 278 (2003) 51713–51721.
[275] P. Ascenzi, M. Marino, F. Polticelli, M. Coletta, M. Gioia, S. Marini, A. Pesce, M. Nardini, M. Bolognesi, B.J. Reeder, M.T. Wilson, Non-covalent and covalent modifications modulate the reactivity of monomeric mammalian globins, Biochim. Biophys. Acta 1834 (2013) 1750–1756.
[276] C. Lechauve, C. Chauvierre, S. Dewilde, L. Moens, B.N. Green, M.C. Marden, C. Celier, L. Kiger, Cytoglobin conformations and disulfide bond formation, FEBS J. 277 (2010) 2696–2704.
[277] A. Fago, C. Hundahl, S. Dewilde, K. Gilany, L. Moens, R.E. Weber, Allosteric regulation and temperature dependence of oxygen binding in human neuroglobin and cytoglobin. Molecular mechanisms and physiological significance, J. Biol. Chem. 279 (2004) 44417–44426.
[278] G. Avella, C. Ardiccioni, A. Scaglione, T. Moschetti, C. Rondinelli, L.C. Montemiglio, C. Savino, A. Giuffre, M. Brunori, B. Vallone, Engineering the internal cavity of neuroglobin demonstrates the role of the haem-sliding mechanism, Acta Crystallogr. D Biol. Crystallogr. 70 (2014) 1640–1648.
[279] B. Vallone, K. Nienhaus, A. Matthes, M. Brunori, G.U. Nienhaus, The structure of carbonmonoxy neuroglobin reveals a heme-sliding mechanism for control of ligand affinity, Proc. Natl. Acad. Sci. U. S. A. 101 (2004) 17351–17356.
[280] D. Hamdane, L. Kiger, G.H. Hoa, S. Dewilde, J. Uzan, T. Burmester, T. Hankeln, L. Moens, M.C. Marden, High pressure enhances hexacoordination in neuroglobin and other globins, J. Biol. Chem. 280 (2005) 36809–36814.
[281] L. Capece, M.A. Marti, A. Bidon-Chanal, A. Nadra, F.J. Luque, D.A. Estrin, High pressure reveals structural determinants for globin hexacoordination: neuroglobin and myoglobin cases, Proteins 75 (2009) 885–894.
[282] A.N. Morozov, J.P. Roach, M. Kotzer, D.C. Chatfield, A possible mechanism for redox control of human neuroglobin activity, J. Chem. Inf. Model. 54 (2014) 1997–2003.
[283] B.G. Guimaraes, D. Hamdane, C. Lechauve, M.C. Marden, B. Golinelli-Pimpaneau, The crystal structure of wild-type human brain neuroglobin reveals flexibility of the disulfide bond that regulates oxygen affinity, Acta Crystallogr. D Biol. Crystallogr. 70 (2014) 1005–1014.
[284] A. Pesce, S. Dewilde, M. Nardini, L. Moens, P. Ascenzi, T. Hankeln, T. Burmester, M. Bolognesi, Human brain neuroglobin structure reveals a distinct mode of controlling oxygen affinity, Structure 11 (2003) 1087–1095.
[285] T. Jayaraman, J. Tejero, B.B. Chen, A.B. Blood, S. Frizzell, C. Shapiro, M. Tiso, B.L. Hood, X. Wang, X. Zhao, T.P. Conrads, R.K. Mallampalli, M.T. Gladwin, 14-3-3 binding and phosphorylation of neuroglobin during hypoxia modulate six-to-five heme pocket coordination and rate of nitrite reduction to nitric oxide, J. Biol. Chem. 286 (2011) 42679–42689.
[286] B.J. Reeder, D.A. Svistunenko, M.T. Wilson, Lipid binding to cytoglobin leads to a change in haem co-ordination: a role for cytoglobin in lipid signalling of oxidative stress, Biochem. J. 434 (2011) 483–492.
[287] A.G. Tennyson, S.J. Lippard, Generation, translocation, and action of nitric oxide in living systems, Chem. Biol. 18 (2011) 1211–1220.
[288] A.L. Ducluzeau, R. van Lis, S. Duval, B. Schoepp-Cothenet, M.J. Russell, W. Nitschke, Was nitric oxide the first deep electron sink? Trends Biochem. Sci. 34 (2009) 9–15.
[289] W.G. Zumft, Cell biology and molecular basis of denitrification, Microbiol. Mol. Biol. Rev. 61 (1997) 533–616.
[290] H. Shoun, S. Fushinobu, L. Jiang, S.W. Kim, T. Wakagi, Fungal denitrification and nitric oxide reductase cytochrome P450nor, Philos. Trans. R. Soc. Lond. Ser. B Biol. Sci. 367 (2012) 1186–1194.
[291] A.U. Igamberdiev, R.D. Hill, Nitrate, NO and haemoglobin in plant adaptation to hypoxia: an alternative to classic fermentation pathways, J. Exp. Bot. 55 (2004) 2473–2482.
[292] J. Simon, Enzymology and bioenergetics of respiratory nitrite ammonification, FEMS Microbiol. Rev. 26 (2002) 285–309.
[293] C. Bogdan, Nitric oxide and the immune response, Nat. Immunol. 2 (2001) 907–916.
[294] J. Green, M.D. Rolfe, L.J. Smith, Transcriptional regulation of bacterial virulence gene expression by molecular oxygen and nitric oxide, Virulence 5 (2014) 794–809.
[295] L.A. del Rio, F.J. Corpas, J.B. Barroso, Nitric oxide and nitric oxide synthase activity in plants, Phytochemistry 65 (2004) 783–792.
[296] M. Brunori, A. Giuffre, E. Forte, D. Mastronicola, M.C. Barone, P. Sarti, Control of cytochrome c oxidase activity by nitric oxide, Biochim. Biophys. Acta 1655 (2004) 365–371.
[297] W.H. Gibson, F.J. Roughton, The kinetics and equilibria of the reactions of nitric oxide with sheep haemoglobin, J. Physiol. 136 (1957) 507–524.
[298] Q.H. Gibson, F.J. Roughton, Further studies on the kinetics and equilibria of the reaction of nitric oxide with haemoproteins, Proc. R. Soc. Lond. B Biol. Sci. 163 (1965) 197–205.
[299] E.V. Arnold, D.S. Bohle, Isolation and oxygenation reactions of nitrosylmyoglobins, Methods Enzymol. 269 (1996) 41–55.
[300] E.G. Moore, Q.H. Gibson, Cooperativity in the dissociation of nitric oxide from hemoglobin, J. Biol. Chem. 251 (1976) 2788–2794.
[301] S. Herold, G. Rock, Mechanistic studies of the oxygen-mediated oxidation of nitrosylhemoglobin, Biochemistry 44 (2005) 6223–6231.
[302] R.F. Eich, T. Li, D.D. Lemon, D.H. Doherty, S.R. Curry, J.F. Aitken, A.J. Mathews, K.A. Johnson, R.D. Smith, G.N. Phillips Jr., J.S. Olson, Mechanism of NO-induced oxidation of myoglobin and hemoglobin, Biochemistry 35 (1996) 6976–6983.
[303] M.P. Doyle, J.W. Hoekstra, Oxidation of nitrogen oxides by bound dioxygen in hemoproteins, J. Inorg. Biochem. 14 (1981) 351–358.
[304] A.J. Gow, B.P. Luchsinger, J.R. Pawloski, D.J. Singel, J.S. Stamler, The oxyhemoglobin reaction of nitric oxide, Proc. Natl. Acad. Sci. U. S. A. 96 (1999) 9027–9032.
[305] M.S. Joshi, T.B. Ferguson Jr., T.H. Han, D.R. Hyduke, J.C. Liao, T. Rassaf, N. Bryan, M. Feelisch, J.R. Lancaster Jr., Nitric oxide is consumed, rather than conserved, by reaction with oxyhemoglobin under physiological conditions, Proc. Natl. Acad. Sci. U. S. A. 99 (2002) 10341–10346.
[306] Y. Zhang, N. Hogg, Mixing artifacts from the bolus addition of nitric oxide to oxymyoglobin: implications for S-nitrosothiol formation, Free Radic. Biol. Med. 32 (2002) 1212–1219.
[307] P.R. Gardner, A.M. Gardner, L.A. Martin, A.L. Salzman, Nitric oxide dioxygenase: an enzymic function for flavohemoglobin, Proc. Natl. Acad. Sci. U. S. A. 95 (1998) 10378–10383.
[308] E.T. Yukl, S. de Vries, P. Moenne-Loccoz, The millisecond intermediate in the reaction of nitric oxide with oxymyoglobin is an iron(III)–nitrato complex, not a peroxynitrite, J. Am. Chem. Soc. 131 (2009) 7234–7235.
[309] J.S. Olson, E.W. Foley, C. Rogge, A.L. Tsai, M.P. Doyle, D.D. Lemon, No scavenging and the hypertensive effect of hemoglobin-based blood substitutes, Free Radic. Biol. Med. 36 (2004) 685–697.
[310] S. Herold, M. Exner, T. Nauser, Kinetic and mechanistic studies of the NO*-mediated oxidation of oxymyoglobin and oxyhemoglobin, Biochemistry 40 (2001) 3385–3395.
[311] P.R. Gardner, A.M. Gardner, W.T. Brashear, T. Suzuki, A.N. Hvitved, K.D. Setchell, J.S. Olson, Hemoglobins dioxygenate nitric oxide with high fidelity, J. Inorg. Biochem. 100 (2006) 542–550.
[312] A. Hausladen, A.J. Gow, J.S. Stamler, Nitrosative stress: metabolic pathway involving the flavohemoglobin, Proc. Natl. Acad. Sci. U. S. A. 95 (1998) 14100–14105.
[313] N. Carrillo, E.A. Ceccarelli, Open questions in ferredoxin-NADP + reductase catalytic mechanism, Eur. J. Biochem. 270 (2003) 1900–1915.
[314] M. Hoshino, K. Ozawa, H. Seki, P.C. Ford, Photochemistry of nitric oxide adducts of water-soluble iron (III) porphyrin and ferrihemoproteins studied by nanosecond laser photolysis, J. Am. Chem. Soc. 115 (1993) 9568–9575.
[315] P.C. Ford, B.O. Fernandez, M.D. Lim, Mechanisms of reductive nitrosylation in iron and copper models relevant to biological systems, Chem. Rev. 105 (2005) 2439–2456.
[316] M. Hoshino, M. Maeda, R. Konishi, H. Seki, P.C. Ford, Studies on the reaction mechanism for reductive nitrosylation of ferrihemoproteins in buffer solutions, J. Am. Chem. Soc. 118 (1996) 5702–5707.
[317] F. Cutruzzola, K. Brown, E.K. Wilson, A. Bellelli, M. Arese, M. Tegoni, C. Cambillau, M. Brunori, The nitrite reductase from *Pseudomonas aeruginosa*: essential role of two active-site histidines in the catalytic and structural properties, Proc. Natl. Acad. Sci. U. S. A. 98 (2001) 2232–2237.
[318] M.P. Doyle, R.A. Pickering, T.M. DeWeert, J.W. Hoekstra, D. Pater, Kinetics and mechanism of the oxidation of human deoxyhemoglobin by nitrites, J. Biol. Chem. 256 (1981) 12393–12398.
[319] R. Sturms, A.A. DiSpirito, M.S. Hargrove, Plant and cyanobacterial hemoglobins reduce nitrite to nitric oxide under anoxic conditions, Biochemistry 50 (2011) 3873–3878.
[320] C.H. Switzer, W. Flores-Santana, D. Mancardi, S. Donzelli, D. Basudhar, L.A. Ridnour, K.M. Miranda, J.M. Fukuto, N. Paolocci, D.A. Wink, The emergence of nitroxyl (HNO) as a pharmacological agent, Biochim. Biophys. Acta 1787 (2009) 835–840.
[321] J.M. Fukuto, C.C. J., R.L. Kinkade, A comparison of the chemistry associated with the biological signaling and actions of nitroxyl (HNO) and nitric oxide (NO), J. Inorg. Biochem. 118 (2012) 201–208.
[322] B.B. Rios-Gonzalez, E.M. Roman-Morales, R. Pietri, J. Lopez-Garriga, Hydrogen sulfide activation in hemeproteins: the sulfheme scenario, J. Inorg. Biochem. 133 (2014) 78–86.
[323] D.W. Kraus, J.B. Wittenberg, Hemoglobins of the *Lucina pectinata*/bacteria symbiosis. I. Molecular properties, kinetics and equilibria of reactions with ligands, J. Biol. Chem. 265 (1990) 16043–16053.
[324] S.N. Vinogradov, D.A. Walz, B. Pohajdak, L. Moens, O.H. Kapp, T. Suzuki, C.N. Trotman, Adventitious variability? The amino acid sequences of non-vertebrate globins, Comp. Biochem. Physiol. B 106 (1993) 1–26.
[325] C. Khosla, J.E. Bailey, The *Vitreoscilla* hemoglobin gene: molecular cloning, nucleotide sequence and genetic expression in *Escherichia coli*, Mol Gen Genet 214 (1988) 158–161.
[326] A. Bonamore, A. Boffi, Flavohemoglobin: structure and reactivity, IUBMB Life 60 (2008) 19–28.
[327] S.G. Vasudevan, W.L. Armarego, D.C. Shaw, P.E. Lilley, N.E. Dixon, R.K. Poole, Isolation and nucleotide sequence of the hmp gene that encodes a haemoglobin-like protein in *Escherichia coli* K-12, Mol Gen Genet 226 (1991) 49–58.
[328] S. McLean, L.A. Bowman, R.K. Poole, Peroxynitrite stress is exacerbated by flavohaemoglobin-derived oxidative stress in *Salmonella typhimurium* and is relieved by nitric oxide, Microbiology 156 (1099) (2010) 3556–3565.
[329] I.S. Bang, L. Liu, A. Vazquez-Torres, M.L. Crouch, J.S. Stamler, F.C. Fang,

Maintenance of nitric oxide and redox homeostasis by the salmonella flavohemoglobin hmp, J. Biol. Chem. 281 (2006) 28039–28047.
[330] R. Cramm, R.A. Siddiqui, B. Friedrich, Primary sequence and evidence for a physiological function of the flavohemoprotein of *Alcaligenes eutrophus*, J. Biol. Chem. 269 (1994) 7349–7354.
[331] A.R. Richardson, P.M. Dunman, F.C. Fang, The nitrosative stress response of *Staphylococcus aureus* is required for resistance to innate immunity, Mol. Microbiol. 61 (2006) 927–939.
[332] M.M. Nakano, Essential role of flavohemoglobin in long-term anaerobic survival of *Bacillus subtilis*, J. Bacteriol. 188 (2006) 6415–6418.
[333] A. Lewinska, G. Bartosz, Yeast flavohemoglobin protects against nitrosative stress and controls ferric reductase activity, Redox Rep. 11 (2006) 231–239.
[334] L. Liu, M. Zeng, A. Hausladen, J. Heitman, J.S. Stamler, Protection from nitrosative stress by yeast flavohemoglobin, Proc. Natl. Acad. Sci. U. S. A. 97 (2000) 4672–4676.
[335] R.K. Poole, M.F. Anjum, J. Membrillo-Hernandez, S.O. Kim, M.N. Hughes, V. Stewart, Nitric oxide, nitrite, and Fnr regulation of hmp (flavohemoglobin) gene expression in *Escherichia coli* K-12, J. Bacteriol. 178 (1996) 5487–5492.
[336] L. Svensson, B.I. Marklund, M. Poljakovic, K. Persson, Uropathogenic *Escherichia coli* and tolerance to nitric oxide: the role of flavohemoglobin, J. Urol. 175 (2006) 749–753.
[337] G. Ollesch, A. Kaunzinger, D. Juchelka, M. Schubert-Zsilavecz, U. Ermler, Phospholipid bound to the flavohemoprotein from *Alcaligenes eutrophus*, Eur. J. Biochem. 262 (1999) 396–405.
[338] A. Bonamore, A. Farina, M. Gattoni, M.E. Schinina, A. Bellelli, A. Boffi, Interaction with membrane lipids and heme ligand binding properties of *Escherichia coli* flavohemoglobin, Biochemistry 42 (2003) 5792–5801.
[339] P. D'Angelo, D. Lucarelli, S. della Longa, M. Benfatto, J.L. Hazemann, A. Feis, G. Smulevich, A. Ilari, A. Bonamore, A. Boffi, Unusual heme iron-lipid acyl chain coordination in *Escherichia coli* flavohemoglobin, Biophys. J. 86 (2004) 3882–3892.
[340] A. Bonamore, P. Gentili, A. Ilari, M.E. Schinina, A. Boffi, *Escherichia coli* flavohemoglobin is an efficient alkylhydroperoxide reductase, J. Biol. Chem. 278 (2003) 22272–22277.
[341] R.A. Helmick, A.E. Fletcher, A.M. Gardner, C.R. Gessner, A.N. Hvitved, M.C. Gustin, P.R. Gardner, Imidazole antibiotics inhibit the nitric oxide dioxygenase function of microbial flavohemoglobin, Antimicrob. Agents Chemother. 49 (2005) 1837–1843.
[342] K.T. Elvers, G. Wu, N.J. Gilberthorpe, R.K. Poole, S.F. Park, Role of an inducible single-domain hemoglobin in mediating resistance to nitric oxide and nitrosative stress in *Campylobacter jejuni* and *Campylobacter coli*, J. Bacteriol. 186 (2004) 5332–5341.
[343] C.E. Monk, B.M. Pearson, F. Mulholland, H.K. Smith, R.K. Poole, Oxygen- and NssR-dependent globin expression and enhanced iron acquisition in the response of campylobacter to nitrosative stress, J. Biol. Chem. 283 (2008) 28413–28425.
[344] A.D. Frey, P.T. Kallio, Nitric oxide detoxification–a new era for bacterial globins in biotechnology? Trends Biotechnol. 23 (2005) 69–73.
[345] R. Kaur, R. Pathania, V. Sharma, S.C. Mande, K.L. Dikshit, Chimeric *Vitreoscilla* hemoglobin (VHb) carrying a flavoreductase domain relieves nitrosative stress in *Escherichia coli*: new insight into the functional role of VHb, Appl. Environ. Microbiol. 68 (2002) 152–160.
[346] M. Milani, A. Pesce, H. Ouellet, M. Guertin, M. Bolognesi, Truncated hemoglobins and nitric oxide action, IUBMB Life 55 (2003) 623–627.
[347] N.L. Scott, Y. Xu, G. Shen, D.A. Vuletich, C.J. Falzone, Z. Li, M. Ludwig, M.P. Pond, M.R. Preimesberger, D.A. Bryant, J.T. Lecomte, Functional and structural characterization of the 2/2 hemoglobin from *Synechococcus* sp. PCC 7002, Biochemistry 49 (2010) 7000–7011.
[348] E.A. Johnson, S.L. Rice, M.R. Preimesberger, D.B. Nye, L. Gilevicius, B.B. Wenke, J.M. Brown, G.B. Witman, J.T. Lecomte, Characterization of THB1, a *Chlamydomonas reinhardtii* truncated hemoglobin: linkage to nitrogen metabolism and identification of lysine as the distal heme ligand, Biochemistry 53 (2014) 4573–4589.
[349] A. Hemschemeier, M. Duner, D. Casero, S.S. Merchant, M. Winkler, T. Happe, Hypoxic survival requires a 2-on-2 hemoglobin in a process involving nitric oxide, Proc. Natl. Acad. Sci. U. S. A. 110 (2013) 10854–10859.
[350] H. Ouellet, Y. Ouellet, C. Richard, M. Labarre, B. Wittenberg, J. Wittenberg, M. Guertin, Truncated hemoglobin HbN protects *Mycobacterium bovis* from nitric oxide, Proc. Natl. Acad. Sci. U. S. A. 99 (2002) 5902–5907.
[351] S. Arya, D. Sethi, S. Singh, M.D. Hade, V. Singh, P. Raju, S.B. Chodisetti, D. Verma, G.C. Varshney, J.N. Agrewala, K.L. Dikshit, Truncated hemoglobin, HbN, is post-translationally modified in *Mycobacterium tuberculosis* and modulates host-pathogen interactions during intracellular infection, J. Biol. Chem. 288 (2013) 29987–29999.
[352] E. Parrilli, M. Giuliani, D. Giordano, R. Russo, G. Marino, C. Verde, M.L. Tutino, The role of a 2-on-2 haemoglobin in oxidative and nitrosative stress resistance of Antarctic *Pseudoalteromonas haloplanktis* TAC125, Biochimie 92 (2010) 1003–1009.
[353] L.J. Ignarro, G.M. Byrns Re Fau-Buga, K.S. Buga Gm Fau-Wood, K.S. Wood, Endothelium-derived relaxing factor from pulmonary artery and vein possesses pharmacologic and chemical properties identical to those of nitric oxide radical, Circ. Res. 61 (1987) 866–879.
[354] J.H. Crawford, B.K. Chacko, C.G. Kevil, R.P. Patel, The red blood cell and vascular function in health and disease, Antioxid. Redox Signal. 6 (2004) 992–999.
[355] D.B. Kim-Shapiro, A.N. Schechter, M.T. Gladwin, Unraveling the reactions of nitric oxide, nitrite, and hemoglobin in physiology and therapeutics, Arterioscler. Thromb. Vasc. Biol. 26 (2006) 697–705.
[356] R.P. Rother, L. Bell, P. Hillmen, M.T. Gladwin, The clinical sequelae of intravascular hemolysis and extracellular plasma hemoglobin: a novel mechanism of human disease, JAMA 293 (2005) 1653–1662.
[357] M.T. Gladwin, F.P. Ognibene, L.K. Pannell, J.S. Nichols, M.E. Pease-Fye, J.H. Shelhamer, A.N. Schechter, Relative role of heme nitrosylation and beta-cysteine 93 nitrosation in the transport and metabolism of nitric oxide by hemoglobin in the human circulation, Proc. Natl. Acad. Sci. U. S. A. 97 (2000) 9943–9948.
[358] J.O. Lundberg, M.T. Weitzberg E Fau-Gladwin, M.T. Gladwin, The nitrate-nitrite-nitric oxide pathway in physiology and therapeutics, Nat. Rev. Drug Discov. 7 (2008) 156–167 (LID - 10 1038/nrd2466 [doi]).
[359] M.T. Gladwin, J.H. Shelhamer, A.N. Schechter, M.E. Pease-Fye, M.A. Waclawiw, J.A. Panza, F.P. Ognibene, R.O. Cannon III, Role of circulating nitrite and S-nitrosohemoglobin in the regulation of regional blood flow in humans, Proc. Natl. Acad. Sci. U. S. A. 97 (2000) 11482–11487.
[360] K. Cosby, J.H. Partovi Ks Fau-Crawford, R.P. Crawford Jh Fau-Patel, C.D. Patel Rp Fau-Reiter, S. Reiter Cd Fau-Martyr, B.K. Martyr S Fau-Yang, M.A. Yang Bk Fau-Waclawiw, G. Waclawiw Ma Fau-Zalos, X. Zalos G Fau-Xu, K.T. Xu X Fau-Huang, H. Huang Kt Fau-Shields, D.B. Shields H Fau-Kim-Shapiro, A.N. Kim-Shapiro Db Fau-Schechter, R.O. Schechter An Fau-Cannon III, M.T. Cannon Ro Fau-Gladwin III, M.T. Gladwin, Nitrite reduction to nitric oxide by deoxyhemoglobin vasodilates the human circulation, Nat. Med. 9 (2003) 1498–1505.
[361] K.T. Huang, N. Keszler A Fau-Patel, R.P. Patel N Fau-Patel, M.T. Patel Rp Fau-Gladwin, D.B. Gladwin Mt Fau-Kim-Shapiro, N. Kim-Shapiro Db Fau-Hogg, N. Hogg, The reaction between nitrite and deoxyhemoglobin. Reassessment of reaction kinetics and stoichiometry, J. Biol. Chem. 280 (2005) 31126–31131.
[362] Z. Huang, S. Shiva, D.B. Kim-Shapiro, R.P. Patel, L.A. Ringwood, C.E. Irby, K.T. Huang, C. Ho, N. Hogg, A.N. Schechter, M.T. Gladwin, Enzymatic function of hemoglobin as a nitrite reductase that produces NO under allosteric control, J. Clin. Invest. 115 (2005) 2099–2107.
[363] K.H. Hopmann, B. Cardey, M.T. Gladwin, D.B. Kim-Shapiro, A. Ghosh, Hemoglobin as a nitrite anhydrase: modeling methemoglobin-mediated N_2O_3 formation, Chemistry 17 (2011) 6348–6358.
[364] E. Nagababu, S. Ramasamy, J.M. Rifkind, S-nitrosohemoglobin: a mechanism for its formation in conjunction with nitrite reduction by deoxyhemoglobin, Nitric Oxide 15 (2006) 20–29.
[365] J. Tejero, S. Basu, C. Helms, N. Hogg, S.B. King, D.B. Kim-Shapiro, M.T. Gladwin, Low NO concentration dependence of reductive nitrosylation reaction of hemoglobin, J. Biol. Chem. 287 (2012) 18262–18274.
[366] S. Basu, R. Grubina, J. Huang, J. Conradie, Z. Huang, A. Jeffers, A. Jiang, X. He, I. Azarov, R. Seibert, A. Mehta, R. Patel, S.B. King, N. Hogg, A. Ghosh, M.T. Gladwin, D.B. Kim-Shapiro, Catalytic generation of N_2O_3 by the concerted nitrite reductase and anhydrase activity of hemoglobin, Nat. Chem. Biol. 3 (2007) 785–794.
[367] D.B. Kim-Shapiro, M.T. Gladwin, Mechanisms of nitrite bioactivation, Nitric Oxide 38 (2014) 58–68.
[368] Q.K. Timerghazin, G.H. Peslherbe, A.M. English, Resonance description of S-nitrosothiols: insights into reactivity, Org. Lett. 9 (2007) 3049–3052.
[369] L. Jia, C. Bonaventura, J. Bonaventura, J.S. Stamler, S-nitrosohaemoglobin: a dynamic activity of blood involved in vascular control, Nature 380 (1996) 221–226.
[370] J.S. Stamler, L. Jia, J.P. Eu, T.J. McMahon, I.T. Demchenko, J. Bonaventura, K. Gernert, C.A. Piantadosi, Blood flow regulation by S-nitrosohemoglobin in the physiological oxygen gradient, Science 276 (1997) 2034–20347.
[371] A.J. Gow, J.S. Stamler, Reactions between nitric oxide and haemoglobin under physiological conditions, Nature 391 (1998) 169–173.
[372] T.J. McMahon, R.E. Moon, B.P. Luschinger, M.S. Carraway, A.E. Stone, B.W. Stolp, A.J. Gow, J.R. Pawloski, P. Watke, D.J. Singel, C.A. Piantadosi, J.S. Stamler, Nitric oxide in the human respiratory cycle, Nat. Med. 8 (2002) 711–717.
[373] A. Doctor, R. Platt, M.L. Sheram, A. Eischeid, T. McMahon, T. Maxey, J. Doherty, M. Axelrod, J. Kline, M. Gurka, A. Gow, B. Gaston, Hemoglobin conformation couples erythrocyte S-nitrosothiol content to O_2 gradients, Proc. Natl. Acad. Sci. U. S. A. 102 (2005) 5709–5714.
[374] J.R. Pawloski, D.T. Hess, J.S. Stamler, Export by red blood cells of nitric oxide bioactivity, Nature 409 (2001) 622–626.
[375] X. Xu, M. Cho, N.Y. Spencer, N. Patel, Z. Huang, H. Shields, S.B. King, M.T. Gladwin, N. Hogg, D.B. Kim-Shapiro, Measurements of nitric oxide on the heme iron and beta-93 thiol of human hemoglobin during cycles of oxygenation and deoxygenation, Proc. Natl. Acad. Sci. U. S. A. 100 (2003) 11303–11308.
[376] K.T. Huang, I. Azarov, S. Basu, J. Huang, D.B. Kim-Shapiro, Lack of allosterically controlled intramolecular transfer of nitric oxide from the heme to cysteine in the beta subunit of hemoglobin, Blood 107 (2006) 2602–2604.
[377] A. Doctor, B. Gaston, D.B. Kim-Shapiro, Detecting physiologic fluctuations in the S-nitrosohemoglobin micropopulation: triiodide versus 3C, Blood 108 (2006) 3225–3227.
[378] B.C. Smith, M.A. Marletta, Mechanisms of S-nitrosothiol formation and selectivity in nitric oxide signaling, Curr. Opin. Chem. Biol. 16 (2012) 498–506.
[379] K.A. Broniowska, N. Hogg, The chemical biology of S-nitrosothiols, Antioxid. Redox Signal. 17 (2012) 969–980.
[380] D.A. Wink, R.W. Nims, J.F. Darbyshire, D. Christodoulou, I. Hanbauer, G.W. Cox, F. Laval, J. Laval, J.A. Cook, M.C. Krishna, et al., Reaction kinetics for nitrosation of cysteine and glutathione in aerobic nitric oxide solutions at neutral pH. Insights into the fate and physiological effects of intermediates generated in the NO/O_2 reaction, Chem. Res. Toxicol. 7 (1994) 519–525.
[381] V.G. Kharitonov, A.R. Sundquist, V.S. Sharma, Kinetics of nitrosation of thiols by nitric oxide in the presence of oxygen, J. Biol. Chem. 270 (1995) 28158–28164.

[382] S. Goldstein, G. Czapski, Mechanism of the nitrosation of thiols and amines by oxygenated NO solutions: the nature of the nitrosating intermediates, J. Am. Chem. Soc. 118 (1996) 3419–3425.
[383] M. Angelo, J.S. Singel Dj Fau-Stamler, J.S. Stamler, An S-nitrosothiol (SNO) synthase function of hemoglobin that utilizes nitrite as a substrate, Proc. Natl. Acad. Sci. U. S. A. 103 (2006) 8366–8371.
[384] B.P. Luchsinger, A.J. Rich En Fau-Gow, E.M. Gow Aj Fau-Williams, J.S. Williams Em Fau-Stamler, D.J. Stamler Js Fau-Singel, D.J. Singel, Routes to S-nitroso-hemoglobin formation with heme redox and preferential reactivity in the beta subunits, Proc. Natl. Acad. Sci. U. S. A. 100 (2003) 461–466.
[385] T.S. Isbell, C.W. Sun, L.C. Wu, X. Teng, D.A. Vitturi, B.G. Branch, C.G. Kevil, N. Peng, J.M. Wyss, N. Ambalavanan, L. Schwiebert, J. Ren, K.M. Pawlik, M.B. Renfrow, R.P. Patel, T.M. Townes, SNO-hemoglobin is not essential for red blood cell-dependent hypoxic vasodilation, Nat. Med. 14 (2008) 773–777.
[386] R. Zhang, D.T. Hess, Z. Qian, A. Hausladen, F. Fonseca, R. Chaube, J.D. Reynolds, J.S. Stamler, Hemoglobin betaCys93 is essential for cardiovascular function and integrated response to hypoxia, Proc. Natl. Acad. Sci. U. S. A. 112 (2015) 6425–6430.
[387] R. Zhang, D.T. Hess, J.D. Reynolds, J.S. Stamler, Hemoglobin S-nitrosylation plays an essential role in cardioprotection, J. Clin. Invest. 126 (2016) 4654–4658.
[388] F. Richter, B.H. Meurers, C. Zhu, V.P. Medvedeva, M.F. Chesselet, Neurons express hemoglobin α- and β-chains in rat and human brains, J. Comp. Neurol. 515 (2009) 538–547.
[389] A.C. Straub, A.W. Lohman, M. Billaud, S.R. Johnstone, S.T. Dwyer, M.Y. Lee, P.S. Bortz, A.K. Best, L. Columbus, B. Gaston, B.E. Isakson, Endothelial cell expression of haemoglobin α regulates nitric oxide signalling, Nature 491 (2012) 473–477.
[390] L.A. Biwer, E.P. Taddeo, B.M. Kenwood, K.L. Hoehn, A.C. Straub, B.E. Isakson, Two functionally distinct pools of eNOS in endothelium are facilitated by myoendothelial junction lipid composition, Biochim. Biophys. Acta 1861 (2016) 671–679.
[391] N. Brown, K. Alkhayer, R. Clements, N. Singhal, R. Gregory, S. Azzam, S. Li, E. Freeman, J. McDonough, Neuronal hemoglobin expression and its relevance to multiple sclerosis neuropathology, J. Mol. Neurosci. 59 (2016) 1–17.
[392] T.C.T. Keller, J.T. Butcher, G.B. Broseghini-Filho, C. Marziano, L.J. DeLalio, S. Rogers, B. Ning, J.N. Martin, S. Chechova, M. Cabot, X. Shu, A.K. Best, M.E. Good, A. Simao Padilha, M. Purdy, M. Yeager, S.M. Peirce, S. Hu, A. Doctor, E. Barrett, T.H. Le, L. Columbus, B.E. Isakson, Modulating vascular hemodynamics with an alpha globin mimetic peptide (HbαX), Hypertension 68 (2016) 1494–1503.
[393] X. Liu, J. Tong, J.R. Zweier, D. Follmer, C. Hemann, R.S. Ismail, J.L. Zweier, Differences in oxygen-dependent nitric oxide metabolism by cytoglobin and myoglobin account for their differing functional roles, FEBS J. 280 (2013) 3621–3631.
[394] S.N. Vinogradov, L. Moens, Diversity of globin function: enzymatic, transport, storage, and sensing, J. Biol. Chem. 283 (2008) 8773–8777.
[395] S. Hou, R.W. Larsen, D. Boudko, C.W. Riley, E. Karatan, M. Zimmer, G.W. Ordal, M. Alam, Myoglobin-like aerotaxis transducers in archaea and bacteria, Nature 403 (2000) 540–544.
[396] S. Hou, T. Freitas, R.W. Larsen, M. Piatibratov, V. Sivozhelezov, A. Yamamoto, E.A. Meleshkevitch, M. Zimmer, G.W. Ordal, M. Alam, Globin-coupled sensors: a class of heme-containing sensors in archaea and bacteria, Proc. Natl. Acad. Sci. U. S. A. 98 (2001) 9353–9358.
[397] W. Zhang, G.N. Phillips Jr., Structure of the oxygen sensor in *Bacillus subtilis*: signal transduction of chemotaxis by control of symmetry, Structure 11 (2003) 1097–1110.
[398] S. Aono, T. Kato, M. Matsuki, H. Nakajima, T. Ohta, T. Uchida, T. Kitagawa, Resonance Raman and ligand binding studies of the oxygen-sensing signal transducer protein HemAT from *Bacillus subtilis*, J. Biol. Chem. 277 (2002) 13528–13538.
[399] K. Kitanishi, K. Kobayashi, T. Uchida, K. Ishimori, J. Igarashi, T. Shimizu, Identification and functional and spectral characterization of a globin-coupled histidine kinase from *Anaeromyxobacter* sp. Fw109-5, J. Biol. Chem. 286 (2011) 35522–35534.
[400] X. Wan, J.R. Tuckerman, J.A. Saito, T.A. Freitas, J.S. Newhouse, J.R. Denery, M.Y. Galperin, G. Gonzalez, M.A. Gilles-Gonzalez, M. Alam, Globins synthesize the second messenger bis-(3′-5′)-cyclic diguanosine monophosphate in bacteria, J. Mol. Biol. 388 (2009) 262–270.
[401] J.R. Tuckerman, G. Gonzalez, E.H. Sousa, X. Wan, J.A. Saito, M. Alam, M.A. Gilles-Gonzalez, An oxygen-sensing diguanylate cyclase and phosphodiesterase couple for c-di-GMP control, Biochemistry 48 (2009) 9764–9774.
[402] S. Sen Santara, J. Roy, S. Mukherjee, M. Bose, R. Saha, S. Adak, Globin-coupled heme containing oxygen sensor soluble adenylate cyclase in *Leishmania* prevents cell death during hypoxia, Proc. Natl. Acad. Sci. U. S. A. 110 (2013) 16790–16795.
[403] X. Jia, J.B. Wang, S. Rivera, D. Duong, E.E. Weinert, An O_2-sensing stressosome from a Gram-negative bacterium, Nat. Commun. 7 (2016) 12381.
[404] L. Pauling, H.A. Itano, et al., Sickle cell anemia a molecular disease, Science 110 (1949) 543–548.
[405] B. Giardine, J. Borg, D.R. Higgs, K.R. Peterson, S. Philipsen, D. Maglott, B.K. Singleton, D.J. Anstee, A.N. Basak, B. Clark, F.C. Costa, P. Faustino, H. Fedosyuk, A.E. Felice, A. Francina, R. Galanello, M.V. Gallivan, M. Georgitsi, R.J. Gibbons, P.C. Giordano, C.L. Harteveld, J.D. Hoyer, M. Jarvis, P. Joly, E. Kanavakis, P. Kollia, S. Menzel, W. Miller, K. Moradkhani, J. Old, A. Papachatzopoulou, M.N. Papadakis, P. Papadopoulos, S. Pavlovic, L. Perseu, M. Radmilovic, C. Riemer, S. Satta, I. Schrijver, M. Stojiljkovic, S.L. Thein, J. Traeger-Synodinos, R. Tully, T. Wada, J.S. Waye, C. Wiemann, B. Zukic, D.H. Chui, H. Wajcman, R.C. Hardison, G.P. Patrinos, Systematic documentation and analysis of human genetic variation in hemoglobinopathies using the microattribution approach, Nat. Genet. 43 (2011) 295–301.
[406] R.C. Hardison, D.H. Chui, B. Giardine, C. Riemer, G.P. Patrinos, N. Anagnou, W. Miller, H. Wajcman, HbVar: a relational database of human hemoglobin variants and thalassemia mutations at the globin gene server, Hum. Mutat. 19 (2002) 225–233.
[407] D.C. Rees, T.N. Williams, M.T. Gladwin, Sickle-cell disease, Lancet 376 (2010) 2018–2031.
[408] F.A. Ferrone, Polymerization and sickle cell disease: a molecular view, Microcirculation 11 (2004) 115–128.
[409] C. Bohr, K. Hasselbalch, A. Krogh, Uber einen in biologischer Beziehung wichtigen Einfluss, den die Kohlensaurespannung des Blutes auf dessen Sauerstoffbindung ubt, Acta Physiol. 16 (1904) 402–412.
[410] A.V. Hill, Proceedings of the physiological society: January 22, 1910, J. Physiol. 40 (1910) iv–vii.
[411] G.S. Adair, A critical study of the direct method of measuring osmotic pressure of hemoglobin, Proc. R. Soc. London, Ser. A 108A (1925) 627–637.
[412] G.S. Adair, The hemoglobin system: VI. The oxygen disssociation curve of hemoglobin, J. Biol. Chem. 63 (1925) 529–545.
[413] D.E. Koshland Jr., G. Nemethy, D. Filmer, Comparison of experimental binding data and theoretical models in proteins containing subunits, Biochemistry 5 (1966) 365–385.
[414] Q. Cui, M. Karplus, Allostery and cooperativity revisited, Protein Sci. 17 (2008) 1295–1307.
[415] W.A. Eaton, E.R. Henry, J. Hofrichter, S. Bettati, C. Viappiani, A. Mozzarelli, Evolution of allosteric models for hemoglobin, IUBMB Life 59 (2007) 586–599.
[416] W.A. Eaton, E.R. Henry, J. Hofrichter, A. Mozzarelli, Is cooperative oxygen binding by hemoglobin really understood? Nat. Struct. Biol. 6 (1999) 351–358.
[417] E.R. Henry, A. Mozzarelli, C. Viappiani, S. Abbruzzetti, S. Bettati, L. Ronda, S. Bruno, W.A. Eaton, Experiments on hemoglobin in single crystals and silica gels distinguish among allosteric models, Biophys. J. 109 (2015) 1264–1272.
[418] J. Monod, J. Wyman, J.P. Changeux, On the nature of allosteric transitions: a plausible model, J. Mol. Biol. 12 (1965) 88–118.
[419] J. Monod, F. Jacob, Teleonomic mechanisms in cellular metabolism, growth, and differentiation, Cold Spring Harb. Symp. Quant. Biol. 26 (1961) 389–401.
[420] K. Imai, Precision determination and Adair scheme analysis of oxygen equilibrium curves of concentrated hemoglobin solution. A strict examination of Adair constant evaluation methods, Biophys. Chem. 37 (1990) 197–210.
[421] M.C. Marden, B. Bohn, J. Kister, C. Poyart, Effectors of hemoglobin. Separation of allosteric and affinity factors, Biophys. J. 57 (1990) 397–403.
[422] K. Imai, The Monod-Wyman-Changeux allosteric model describes haemoglobin oxygenation with only one adjustable parameter, J. Mol. Biol. 167 (1983) 741–749.
[423] M.L. Doyle, J.M. Holt, G.K. Ackers, Effects of NaCl on the linkages between O_2 binding and subunit assembly in human hemoglobin: titration of the quaternary enhancement effect, Biophys. Chem. 64 (1997) 271–287.
[424] E.R. Henry, C.M. Jones, J. Hofrichter, W.A. Eaton, Can a two-state MWC allosteric model explain hemoglobin kinetics? Biochemistry 36 (1997) 6511–6528.
[425] E.R. Henry, S. Bettati, J. Hofrichter, W.A. Eaton, A tertiary two-state allosteric model for hemoglobin, Biophys. Chem. 98 (2002) 149–164.
[426] C. Bauer, E. Schroder, Carbamino compounds of haemoglobin in human adult and foetal blood, J. Physiol. 227 (1972) 457–471.
[427] J.V. Kilmartin, L. Rossi-Bernardi, Inhibition of CO_2 combination and reduction of the Bohr effect in haemoglobin chemically modified at its α-amino groups, Nature 222 (1969) 1243–1246.
[428] T.C. Lee, Q.H. Gibson, Allosteric properties of carbamylated hemoglobins, J. Biol. Chem. 256 (1981) 4570–4577.
[429] F.B. Jensen, Red blood cell pH, the Bohr effect, and other oxygenation-linked phenomena in blood O_2 and CO_2 transport, Acta Physiol. Scand. 182 (2004) 215–227.
[430] M.F. Perutz, A.J. Wilkinson, M. Paoli, G.G. Dodson, The stereochemical mechanism of the cooperative effects in hemoglobin revisited, Annu. Rev. Biophys. Biomol. Struct. 27 (1998) 1–34.
[431] Y. Yuan, M.F. Tam, V. Simplaceanu, C. Ho, New look at hemoglobin allostery, Chem. Rev. 115 (2015) 1702–1724.
[432] J.A. Lukin, C. Ho, The structure–function relationship of hemoglobin in solution at atomic resolution, Chem. Rev. 104 (2004) 1219–1230.
[433] M.F. Perutz, The Bohr effect and combination with organic phosphates, Nature 228 (1970) 734–739.
[434] J.V. Kilmartin, J.F. Wootton, Inhibition of Bohr effect after removal of C-terminal histidines from haemoglobin beta-chains, Nature 228 (1970) 766–767.
[435] R.W. Root, The respiratory function of the blood of marine fishes, Biol. Bull. 61 (1931).
[436] E. Dodson, G. Dodson, Movements at the hemoglobin A-hemes and their role in ligand binding, analyzed by X-ray crystallography, Biopolymers 91 (2009) 1056–1063.
[437] R. Benesch, R.E. Benesch, The effect of organic phosphates from the human erythrocyte on the allosteric properties of hemoglobin, Biochem. Biophys. Res. Commun. 26 (1967) 162–167.
[438] R. Benesch, R.E. Benesch, Intracellular organic phosphates as regulators of oxygen release by haemoglobin, Nature 221 (1969) 618–622.
[439] M.F. Perutz, K. Imai, Regulation of oxygen affinity of mammalian haemoglobins, J. Mol. Biol. 136 (1980) 183–191.
[440] I. Tyuma, K. Shimizu, Different response to organic phosphates of human fetal and adult hemoglobins, Arch. Biochem. Biophys. 129 (1969) 404–405.

[441] H. Muirhead, M.F. Perutz, Structure of haemoglobin. A three-dimensional fourier synthesis of reduced human haemoglobin at 5.5 A resolution, Nature 199 (1963) 633–638.
[442] M.M. Silva, P.H. Rogers, A. Arnone, A third quaternary structure of human hemoglobin A at 1.7-A resolution, J. Biol. Chem. 267 (1992) 17248–17256.
[443] M.K. Safo, D.J. Abraham, The enigma of the liganded hemoglobin end state: a novel quaternary structure of human carbonmonoxy hemoglobin, Biochemistry 44 (2005) 8347–8359.
[444] S. Dey, P. Chakrabarti, J. Janin, A survey of hemoglobin quaternary structures, Proteins 79 (2011) 2861–2870.
[445] R. Srinivasan, G.D. Rose, The T-to-R transformation in hemoglobin: a reevaluation, Proc. Natl. Acad. Sci. U. S. A. 91 (1994) 11113–11117.
[446] N. Shibayama, K. Sugiyama, S.Y. Park, Structures and oxygen affinities of crystalline human hemoglobin C (beta6 Glu- > Lys) in the R and R2 quaternary structures, J. Biol. Chem. 286 (2011) 33661–33668.
[447] J.S. Fan, Y. Zheng, W.Y. Choy, V. Simplaceanu, N.T. Ho, C. Ho, D. Yang, Solution structure and dynamics of human hemoglobin in the carbonmonoxy form, Biochemistry 52 (2013) 5809–5820.
[448] Q. Gong, V. Simplaceanu, J.A. Lukin, J.L. Giovannelli, N.T. Ho, C. Ho, Quaternary structure of carbonmonoxyhemoglobins in solution: structural changes induced by the allosteric effector inositol hexaphosphate, Biochemistry 45 (2006) 5140–5148.
[449] J.A. Lukin, G. Kontaxis, V. Simplaceanu, Y. Yuan, A. Bax, C. Ho, Quaternary structure of hemoglobin in solution, Proc. Natl. Acad. Sci. U. S. A. 100 (2003) 517–520.
[450] S.C. Sahu, V. Simplaceanu, Q. Gong, N.T. Ho, F. Tian, J.H. Prestegard, C. Ho, Insights into the solution structure of human deoxyhemoglobin in the absence and presence of an allosteric effector, Biochemistry 46 (2007) 9973–9980.
[451] X.J. Song, V. Simplaceanu, N.T. Ho, C. Ho, Effector-induced structural fluctuation regulates the ligand affinity of an allosteric protein: binding of inositol hexaphosphate has distinct dynamic consequences for the T and R states of hemoglobin, Biochemistry 47 (2008) 4907–4915.
[452] J.A. Lukin, G. Kontaxis, V. Simplaceanu, Y. Yuan, A. Bax, C. Ho, Backbone resonance assignments of human adult hemoglobin in the carbonmonoxy form, J. Biomol. NMR 28 (2004) 203–204.
[453] Y. Xu, Y. Zheng, J.S. Fan, D. Yang, A new strategy for structure determination of large proteins in solution without deuteration, Nat. Methods 3 (2006) 931–937.
[454] L. Makowski, J. Bardhan, D. Gore, J. Lal, S. Mandava, S. Park, D.J. Rodi, N.T. Ho, C. Ho, R.F. Fischetti, WAXS studies of the structural diversity of hemoglobin in solution, J. Mol. Biol. 408 (2011) 909–921.
[455] M. Khoshouei, M. Radjainia, W. Baumeister, R. Danev, Cryo-EM structure of haemoglobin at 3.2 Å determined with the Volta phase plate, Nat. Commun. 8 (2017).
[456] N. Shibayama, K. Sugiyama, J.R. Tame, S.Y. Park, Capturing the hemoglobin allosteric transition in a single crystal form, J. Am. Chem. Soc. 136 (2014) 5097–5105.
[457] S.Y. Park, T. Yokoyama, N. Shibayama, Y. Shiro, J.R. Tame, 1.25 A resolution crystal structures of human haemoglobin in the oxy, deoxy and carbonmonoxy forms, J. Mol. Biol. 360 (2006) 690–701.
[458] M.F. Perutz, Stereochemistry of cooperative effects in haemoglobin, Nature 228 (1970) 726–739.
[459] J. Baldwin, C. Chothia, Haemoglobin: the structural changes related to ligand binding and its allosteric mechanism, J. Mol. Biol. 129 (1979) 175–220.
[460] T.C. Mueser, P.H. Rogers, A. Arnone, Interface sliding as illustrated by the multiple quaternary structures of liganded hemoglobin, Biochemistry 39 (2000) 15353–15364.
[461] M. Brunori, R.W. Noble, E. Antonini, J. Wyman, The reactions of the isolated α and β chains of human hemoglobin with oxygen and carbon monoxide, J. Biol. Chem. 241 (1966) 5238–5243.
[462] J.A. Hewitt, J.V. Kilmartin, L.F. Eyck, M.F. Perutz, Noncooperativity of the dimer in the reaction of hemoglobin with oxygen, Proc. Natl. Acad. Sci. U. S. A. 69 (1972) 203–207.
[463] J. Wyman Jr., Linked functions and reciprocal effects in hemoglobin: a second look, Adv. Protein Chem. 19 (1964) 223–286.
[464] G.K. Ackers, Energetics of subunit assembly and ligand binding in human hemoglobin, Biophys. J. 32 (1980) 331–346.
[465] G.K. Ackers, Deciphering the molecular code of hemoglobin allostery, Adv. Protein Chem. 51 (1998) 185–253.
[466] G.K. Ackers, M.L. Doyle, D. Myers, M.A. Daugherty, Molecular code for cooperativity in hemoglobin, Science 255 (1992) 54–63.
[467] J.M. Holt, G.K. Ackers, The Hill coefficient: inadequate resolution of cooperativity in human hemoglobin, Methods Enzymol. 455 (2009) 193–212.
[468] F.C. Mills, M.L. Johnson, G.K. Ackers, Oxygenation-linked subunit interactions in human hemoglobin: experimental studies on the concentration dependence of oxygenation curves, Biochemistry 15 (1976) 5350–5362.
[469] A.H. Chu, G.K. Ackers, Mutual effects of protons, NaCl, and oxygen on the dimer-tetramer assembly of human hemoglobin. The dimer Bohr effect, J. Biol. Chem. 256 (1981) 1199–1205.
[470] S.H. Ip, G.K. Ackers, Thermodynamic studies on subunit assembly in human hemoglobin. Temperature dependence of the dimer-tetramer association constants for oxygenated and unliganded hemoglobins, J. Biol. Chem. 252 (1977) 82–87.
[471] R. Valdes Jr., G.K. Ackers, Thermodynamic studies on subunit assembly in human hemoglobin. Calorimetric measurements on the reconstitution of oxyhemoglobin from isolated chains, J. Biol. Chem. 252 (1977) 88–91.
[472] H.A. Saroff, A.P. Minton, The Hill plot and the energy of interaction in hemoglobin, Science 175 (1972) 1253–1255.
[473] M.F. Perutz, H. Muirhead, J.M. Cox, L.C. Goaman, Three-dimensional Fourier synthesis of horse oxyhaemoglobin at 2.8 A resolution: the atomic model, Nature 219 (1968) 131–139.
[474] M.F. Perutz, H. Miurhead, J.M. Cox, L.C. Goaman, F.S. Mathews, E.L. McGandy, L.E. Webb, Three-dimensional Fourier synthesis of horse oxyhaemoglobin at 2.8 A resolution: (1) x-ray analysis, Nature 219 (1968) 29–32.
[475] W. Bolton, M.F. Perutz, Three dimensional fourier synthesis of horse deoxyhaemoglobin at 2.8 Angstrom units resolution, Nature 228 (1970) 551–552.
[476] G. Fermi, M.F. Perutz, B. Shaanan, R. Fourme, The crystal structure of human deoxyhaemoglobin at 1.74 A resolution, J. Mol. Biol. 175 (1984) 159–174.
[477] B. Shaanan, Structure of human oxyhaemoglobin at 2.1 A resolution, J. Mol. Biol. 171 (1983) 31–59.
[478] B.R. Gelin, A.W. Lee, M. Karplus, Hemoglobin tertiary structural change on ligand binding. Its role in the co-operative mechanism, J. Mol. Biol. 171 (1983) 489–559.
[479] J. Janin, S.J. Wodak, Reaction pathway for the quaternary structure change in hemoglobin, Biopolymers 24 (1985) 509–526.
[480] B.R. Gelin, M. Karplus, Mechanism of tertiary structural change in hemoglobin, Proc. Natl. Acad. Sci. U. S. A. 74 (1977) 801–805.
[481] D.J. Abraham, R.A. Peascoe, R.S. Randad, J. Panikker, X-ray diffraction study of di and tetra-ligated T-state hemoglobin from high salt crystals, J. Mol. Biol. 227 (1992) 480–492.
[482] M.F. Perutz, Nature of haem-haem interaction, Nature 237 (1972) 495–499.
[483] J.L. Hoard, K.M. Smith (Ed.), Porphyrins and Metalloporphyrins, Elsevier, Amsterdam, 1985, pp. 317–380.
[484] M.F. Perutz, S.S. Hasnain, P.J. Duke, J.L. Sessler, J.E. Hahn, Stereochemistry of iron in deoxyhaemoglobin, Nature 295 (1982) 535–538.
[485] P. Eisenberger, R.G. Shulman, B.M. Kincaid, G.S. Brown, S. Ogawa, Extended X-ray absorption fine structure determination of iron nitrogen distances in haemoglobin, Nature 274 (1978) 30–34.
[486] K. Spartalian, G. Lang, J.P. Collman, R.R. Gagne, C.A. Reed, Mössbauer spectroscopy of hemoglobin model compounds: evidence for conformational excitation, J. Chem. Phys. 63 (1975) 5375–5382.
[487] R.G. Shulman, Spectroscopic contributions to the understanding of hemoglobin function: implications for structural biology, IUBMB Life 51 (2001) 351–357.
[488] C. Viappiani, S. Abbruzzetti, L. Ronda, S. Bettati, E.R. Henry, A. Mozzarelli, W.A. Eaton, Experimental basis for a new allosteric model for multisubunit proteins, Proc. Natl. Acad. Sci. U. S. A. 111 (2014) 12758–12763.
[489] A. Szabo, M. Karplus, A mathematical model for structure-function relations in hemoglobin, J. Mol. Biol. 72 (1972) 163–197.
[490] A. Szabo, M. Karplus, Analysis of cooperativity in hemoglobin. Valency hybrids, oxidation, and methemoglobin replacement reactions, Biochemistry 14 (1975) 931–940.
[491] A.W. Lee, M. Karplus, Structure-specific model of hemoglobin cooperativity, Proc. Natl. Acad. Sci. U. S. A. 80 (1983) 7055–7059.
[492] A.W. Lee, M. Karplus, C. Poyart, E. Bursaux, Analysis of proton release in oxygen binding by hemoglobin: implications for the cooperative mechanism, Biochemistry 27 (1988) 1285–1301.
[493] R.E. Alcantara, C. Xu, T.G. Spiro, V. Guallar, A quantum-chemical picture of hemoglobin affinity, Proc. Natl. Acad. Sci. U. S. A. 104 (2007) 18451–18455.
[494] K. Nagai, T. Kitagawa, H. Morimoto, Quaternary structures and low frequency molecular vibrations of haems of deoxy and oxyhaemoglobin studied by resonance raman scattering, J. Mol. Biol. 136 (1980) 271–289.
[495] S. Matsukawa, K. Mawatari, Y. Yoneyama, T.J. Kitagawa, Correlation between the iron-histidine stretching frequencies and oxygen affinity of hemoglobins. A continuous strain model, J. Am. Chem. Soc. 107 (1985) 1108–1113.
[496] J.M. Friedman, Structure, dynamics, and reactivity in hemoglobin, Science 228 (1985) 1273–1280.
[497] H. Hori, T. Kitagawa, Iron-ligand stretching band in the resonance Raman spectra of ferrous iron porphyrin derivatives. Importance as a probe band for quaternary structure of hemoglobin, J. Am. Chem. Soc. 102 (1980) 3608–3613.
[498] J.P. Collman, J.I. Brauman, T.J. Collins, B.L. Iverson, G. Lang, R.B. Pettman, J.L. Sessler, M.A. Walters, Synthesis and characterization of the “pocket” porphyrins, J. Am. Chem. Soc. 105 (1983) 3038–3052.
[499] M.F. Perutz, Structure and mechanism of haemoglobin, Br. Med. Bull. 32 (1976) 195–208.
[500] R. Hille, J.S. Olson, G. Palmer, Spectral transitions of nitrosyl hemes during ligand binding to hemoglobin, J. Biol. Chem. 254 (1979) 12110–12120.
[501] J.C. Maxwell, W.S. Caughey, An infrared study of NO bonding to heme B and hemoglobin A. Evidence for inositol hexaphosphate induced cleavage of proximal histidine to iron bonds, Biochemistry 15 (1976) 388–396.
[502] A. Szabo, M.F. Perutz, Equilibrium between six- and five-coordinated hemes in nitrosylhemoglobin: interpretation of electron spin resonance spectra, Biochemistry 15 (1976) 4427–4428.
[503] N.L. Chan, J.S. Kavanaugh, P.H. Rogers, A. Arnone, Crystallographic analysis of the interaction of nitric oxide with quaternary-T human hemoglobin, Biochemistry 43 (2004) 118–132.
[504] M. Paoli, G. Dodson, R.C. Liddington, A.J. Wilkinson, Tension in haemoglobin revealed by Fe-His(F8) bond rupture in the fully liganded T-state, J. Mol. Biol. 271 (1997) 161–167.
[505] E.M. Jones, E. Monza, G. Balakrishnan, G.C. Blouin, P.J. Mak, Q. Zhu, J.R. Kincaid, V. Guallar, T.G. Spiro, Differential control of heme reactivity in α and β subunits of hemoglobin: a combined Raman spectroscopic and computational study, J. Am. Chem. Soc. 136 (2014) 10325–10339.
[506] A.J. Mathews, J.S. Olson, J.P. Renaud, J. Tame, K. Nagai, The assignment of carbon monoxide association rate constants to the α and β subunits in native and mutant human deoxyhemoglobin tetramers, J. Biol. Chem. 266 (1991) 21631–21639.

[507] K. Nagai, B. Luisi, D. Shih, G. Miyazaki, K. Imai, C. Poyart, A. De Young, L. Kwiatkowsky, R.W. Noble, S.H. Lin, et al., Distal residues in the oxygen binding site of haemoglobin studied by protein engineering, Nature 329 (1987) 858–860.
[508] J. Tame, D.T. Shih, J. Pagnier, G. Fermi, K. Nagai, Functional role of the distal valine (E11) residue of α subunits in human haemoglobin, J. Mol. Biol. 218 (1991) 761–767.
[509] S. Bruno, S. Bettati, M. Manfredini, A. Mozzarelli, M. Bolognesi, D. Deriu, C. Rosano, A. Tsuneshige, T. Yonetani, E.R. Henry, Oxygen binding by $\alpha(Fe^{2+})_2\beta(Ni^{2+})_2$ hemoglobin crystals, Protein Sci. 9 (2000) 683–692.
[510] S. Unzai, R. Eich, N. Shibayama, J.S. Olson, H. Morimoto, Rate constants for O_2 and CO binding to the α and beta subunits within the R and T states of human hemoglobin, J. Biol. Chem. 273 (1998) 23150–23159.
[511] A. Mozzarelli, C. Rivetti, G.L. Rossi, E.R. Henry, W.A. Eaton, Crystals of haemoglobin with the T quaternary structure bind oxygen noncooperatively with no Bohr effect, Nature 351 (1991) 416–419.
[512] A. Arnone, X-ray diffraction study of binding of 2,3-diphosphoglycerate to human deoxyhaemoglobin, Nature 237 (1972) 146–149.
[513] V. Richard, G.G. Dodson, Y. Mauguen, Human deoxyhaemoglobin-2,3-diphosphoglycerate complex low-salt structure at 2.5 A resolution, J. Mol. Biol. 233 (1993) 270–274.
[514] T. Yonetani, S.I. Park, A. Tsuneshige, K. Imai, K. Kanaori, Global allostery model of hemoglobin. Modulation of O(2) affinity, cooperativity, and Bohr effect by heterotropic allosteric effectors, J. Biol. Chem. 277 (2002) 34508–34520.
[515] J. Kister, C. Poyart, S.J. Edelstein, An expanded two-state allosteric model for interactions of human hemoglobin A with nonsaturating concentrations of 2,3-diphosphoglycerate, J. Biol. Chem. 262 (1987) 12085–12091.
[516] T. Yonetani, M. Laberge, Protein dynamics explain the allosteric behaviors of hemoglobin, Biochim. Biophys. Acta 1784 (2008) 1146–1158.
[517] N. Shibayama, S. Miura, J.R. Tame, T. Yonetani, S.Y. Park, Crystal structure of horse carbonmonoxyhemoglobin-bezafibrate complex at 1.55-A resolution. A novel allosteric binding site in R-state hemoglobin, J. Biol. Chem. 277 (2002) 38791–38796.
[518] T. Yokoyama, S. Neya, A. Tsuneshige, T. Yonetani, S.Y. Park, J.R. Tame, R-state haemoglobin with low oxygen affinity: crystal structures of deoxy human and carbonmonoxy horse haemoglobin bound to the effector molecule L35, J. Mol. Biol. 356 (2006) 790–801.
[519] I. Lalezari, P. Lalezari, C. Poyart, M. Marden, J. Kister, B. Bohn, G. Fermi, M.F. Perutz, New effectors of human hemoglobin: structure and function, Biochemistry 29 (1990) 1515–1523.
[520] A. Tsuneshige, K. Kanaori, U. Samuni, D. Danstker, J.M. Friedman, S. Neya, L. Giangiacomo, T. Yonetani, Semihemoglobins, high oxygen affinity dimeric forms of human hemoglobin respond efficiently to allosteric effectors without forming tetramers, J. Biol. Chem. 279 (2004) 48959–48967.
[521] M.J. Grabowski, A.M. Brzozowski, Z.S. Derewenda, T. Skarznnski, M. Cygler, A. Stepien, A.E. Derewenda, Crystallization of human oxyhaemoglobin from poly (ethylene glycol) solutions, Biochem. J. 171 (1978) 277–279.
[522] K.B. Ward, B.C. Wishner, E.E. Lattman, W.E. Love, Structure of deoxyhemoglobin A crystals grown from polyethylene glycol solutions, J. Mol. Biol. 98 (1975) 161–177.
[523] C. Rivetti, A. Mozzarelli, G.L. Rossi, E.R. Henry, W.A. Eaton, Oxygen binding by single crystals of hemoglobin, Biochemistry 32 (1993) 2888–2906.
[524] A. Mozzarelli, C. Rivetti, G.L. Rossi, W.A. Eaton, E.R. Henry, Allosteric effectors do not alter the oxygen affinity of hemoglobin crystals, Protein Sci. 6 (1997) 484–489.
[525] N. Shibayama, S. Saigo, Fixation of the quaternary structures of human adult haemoglobin by encapsulation in transparent porous silica gels, J. Mol. Biol. 251 (1995) 203–209.
[526] S. Bettati, A. Mozzarelli, T state hemoglobin binds oxygen noncooperatively with allosteric effects of protons, inositol hexaphosphate, and chloride, J. Biol. Chem. 272 (1997) 32050–32055.
[527] S. Bruno, M. Bonaccio, S. Bettati, C. Rivetti, C. Viappiani, S. Abbruzzetti, A. Mozzarelli, High and low oxygen affinity conformations of T state hemoglobin, Protein Sci. 10 (2001) 2401–2407.
[528] Q.H. Gibson, The photochemical formation of a quickly reacting form of haemoglobin, Biochem. J. 71 (1959) 293–303.
[529] R. Cassoly, Q.H. Gibson, S. Ogawa, R.G. Shulman, Effects of phosphate upon CO binding kinetics and NMR spectra of hemoglobin valency hybrids, Biochem. Biophys. Res. Commun. 44 (1971) 1015–1021.
[530] E. Antonini, E. Chiancone, M. Brunori, Studies on the relations between molecular and functional properties of hemoglobin. VI. Observations on the kinetics of hemoglobin reactions in concentrated salt solutions, J. Biol. Chem. 242 (1967) 4360–4366.
[531] J.J. Hopfield, R.G. Shulman, S. Ogawa, An allosteric model of hemoglobin. I. Kinetics, J. Mol. Biol. 61 (1971) 425–443.
[532] C.A. Sawicki, Q.H. Gibson, Quaternary conformational changes in human hemoglobin studied by laser photolysis of carboxyhemoglobin, J. Biol. Chem. 251 (1976) 1533–1542.
[533] J. Hofrichter, J.H. Sommer, E.R. Henry, W.A. Eaton, Nanosecond absorption spectroscopy of hemoglobin: elementary processes in kinetic cooperativity, Proc. Natl. Acad. Sci. U. S. A. 80 (1983) 2235–2239.
[534] S. Fischer, K.W. Olsen, K. Nam, M. Karplus, Unsuspected pathway of the allosteric transition in hemoglobin, Proc. Natl. Acad. Sci. U. S. A. 108 (2011) 5608–5613.
[535] C. Viappiani, S. Bettati, S. Bruno, L. Ronda, S. Abbruzzetti, A. Mozzarelli, W.A. Eaton, New insights into allosteric mechanisms from trapping unstable protein conformations in silica gels, Proc. Natl. Acad. Sci. U. S. A. 101 (2004) 14414–14419.
[536] S. Franzen, B. Bohn, C. Poyart, G. DePillis, S.G. Boxer, J.L. Martin, Functional aspects of ultra-rapid heme doming in hemoglobin, myoglobin, and the myoglobin mutant H93G, J. Biol. Chem. 270 (1995) 1718–1720.
[537] S. Franzen, B. Bohn, C. Poyart, J.L. Martin, Evidence for sub-picosecond heme doming in hemoglobin and myoglobin: a time-resolved resonance Raman comparison of carbonmonoxy and deoxy species, Biochemistry 34 (1995) 1224–1237.
[538] M. Levantino, H.T. Lemke, G. Schiro, M. Glownia, A. Cupane, M. Cammarata, Observing heme doming in myoglobin with femtosecond X-ray absorption spectroscopy, Struct. Dyn. 2 (2015) 041713.
[539] J.L. Martin, A. Migus, C. Poyart, Y. Lecarpentier, R. Astier, A. Antonetti, Femtosecond photolysis of CO-ligated protoheme and hemoproteins: appearance of deoxy species with a 350-fsec time constant, Proc. Natl. Acad. Sci. U. S. A. 80 (1983) 173–177.
[540] J.W. Petrich, C. Poyart, J.L. Martin, Photophysics and reactivity of heme proteins: a femtosecond absorption study of hemoglobin, myoglobin, and protoheme, Biochemistry 27 (1988) 4049–4060.
[541] M. Lim, T.A. Jackson, P.A. Anfinrud, Nonexponential protein relaxation: dynamics of conformational change in myoglobin, Proc. Natl. Acad. Sci. U. S. A. 90 (1993) 5801–5804.
[542] F. Schotte, M. Lim, T.A. Jackson, A.V. Smirnov, J. Soman, J.S. Olson, G.N. Phillips Jr., M. Wulff, P.A. Anfinrud, Watching a protein as it functions with 150-ps time-resolved x-ray crystallography, Science 300 (2003) 1944–1947.
[543] D. Bourgeois, B. Vallone, A. Arcovito, G. Sciara, F. Schotte, P.A. Anfinrud, M. Brunori, Extended subnanosecond structural dynamics of myoglobin revealed by Laue crystallography, Proc. Natl. Acad. Sci. U. S. A. 103 (2006) 4924–4929.
[544] T.R. Barends, L. Foucar, A. Ardevol, K. Nass, A. Aquila, S. Botha, R.B. Doak, K. Falahati, E. Hartmann, M. Hilpert, M. Heinz, M.C. Hoffmann, J. Kofinger, J.E. Koglin, G. Kovacsova, M. Liang, D. Milathianaki, H.T. Lemke, J. Reinstein, C.M. Roome, R.L. Shoeman, G.J. Williams, I. Burghardt, G. Hummer, S. Boutet, I. Schlichting, Direct observation of ultrafast collective motions in CO myoglobin upon ligand dissociation, Science 350 (2015) 445–450.
[545] M. Levantino, G. Schiro, H.T. Lemke, G. Cottone, J.M. Glownia, D. Zhu, M. Chollet, H. Ihee, A. Cupane, M. Cammarata, Ultrafast myoglobin structural dynamics observed with an X-ray free-electron laser, Nat. Commun. 6 (2015) 6772.
[546] R.A. Goldbeck, R.M. Esquerra, D.S. Kliger, Hydrogen bonding to Trp beta37 is the first step in a compound pathway for hemoglobin allostery, J. Am. Chem. Soc. 124 (2002) 7646–7647.
[547] G. Balakrishnan, M.A. Case, A. Pevsner, X. Zhao, C. Tengroth, G.L. McLendon, T.G. Spiro, Time-resolved absorption and UV resonance Raman spectra reveal stepwise formation of T quaternary contacts in the allosteric pathway of hemoglobin, J. Mol. Biol. 340 (2004) 843–856.
[548] M. Cammarata, M. Levantino, M. Wulff, A. Cupane, Unveiling the timescale of the R-T transition in human hemoglobin, J. Mol. Biol. 400 (2010) 951–962.
[549] T.G. Spiro, G. Balakrishnan, Quaternary speeding in hemoglobin, J. Mol. Biol. 400 (2010) 949–950.
[550] E.M. Jones, G. Balakrishnan, T.G. Spiro, Heme reactivity is uncoupled from quaternary structure in gel-encapsulated hemoglobin: a resonance Raman spectroscopic study, J. Am. Chem. Soc. 134 (2012) 3461–3471.
[551] V. Jayaraman, K.R. Rodgers, I. Mukerji, T.G. Spiro, Hemoglobin allostery: resonance Raman spectroscopy of kinetic intermediates, Science 269 (1995) 1843–1848.
[552] J.M. Friedman, D.L. Rousseau, M.R. Ondrias, R.A. Stepnoski, Transient Raman study of hemoglobin: structural dependence of the iron-histidine linkage, Science 218 (1982) 1244–1246.
[553] G.I. Berglund, G.H. Carlsson, A.T. Smith, H. Szoke, A. Henriksen, J. Hajdu, The catalytic pathway of horseradish peroxidase at high resolution, Nature 417 (2002) 463–468.
[554] C.A. Bonagura, B. Bhaskar, H. Shimizu, H. Li, M. Sundaramoorthy, D.E. McRee, D.B. Goodin, T.L. Poulos, High-resolution crystal structures and spectroscopy of native and compound I cytochrome c peroxidase, Biochemistry 42 (2003) 5600–5608.
[555] T. Chatake, N. Shibayama, S.Y. Park, K. Kurihara, T. Tamada, I. Tanaka, N. Niimura, R. Kuroki, Y. Morimoto, Protonation states of buried histidine residues in human deoxyhemoglobin revealed by neutron crystallography, J. Am. Chem. Soc. 129 (2007) 14840–14841.
[556] R.M. Winslow, M.L. Swenberg, R.L. Berger, R.I. Shrager, M. Luzzana, M. Samaja, L. Rossi-Bernardi, Oxygen equilibrium curve of normal human blood and its evaluation by Adair's equation, J. Biol. Chem. 252 (1977) 2331–2337.